Recognition of Selenocysteyl-tRNA^{Sec} by Elongation Factor SelB

Inaugural-Dissertation

zur Erlangung des Grades eines

Doktors der Naturwissenschaften

an der

Fakultät für Medizin

der

uni**versität**
Witten/Herdecke

vorlegt von

Alena Paleskava

aus Minsk

Witten 2009

Mentor

(Erstgutachter):   Prof. Dr. Marina V. Rodnina

Fakultatsreferent

(Zweitgutachter):   Prof. Dr. Wolfgang Wintermeyer

Tag der Disputation: 20.05.2009

Table of Contents

Paper 1 – 4

Curriculum vitae

Acknowledgements

List of Papers

This doctoral thesis is based on the following papers:

Paper 1

Kothe, U., Paleskava, A., Konevega, A.L., and Rodnina, M.V. (2006). Single-step purification of specific tRNAs by hydrophobic tagging. Anal Biochem 356, 148-150.

Paper 2

Fischer, N., Paleskava, A., Gromadski, K.B., Konevega, A.L., Wahl, M.C., Stark, H., and Rodnina, M.V. (2007). Towards understanding selenocysteine incorporation into bacterial proteins. Biol Chem 388, 1061-1067.

Paper 3

Paleskava, A., Konevega, A.L., and Rodnina, M.V. Thermodynamic and Kinetic Framework of Selenocysteinyl-tRNA^{Sec} Recognition by Elongation Factor SelB. Manuscript

Paper 4

Fischer, N., Gromadski, K., Paleskava, A., Stark, H. and Rodnina, M.V. Structure of SelB·GTP·Sec-tRNA^{Sec} bound to the ribosome. Manuscript

Summary

In prokaryotes, UGA stop codons can be recoded to direct the incorporation of selenocysteine (Sec) into protein on the ribosome. Recoding requires a Sec incorporation sequence (SECIS) downstream of the UGA codon, a specialized translation factor SelB, and a non-canonical Sec-tRNA^{Sec}. The aim of the present work was elucidation of the mechanism of Sec insertion machinery in bacteria.

Sec-tRNA^{Sec} can bind to SelB in the GTP-, GDP-bound or nucleotide-free (apo) form. However, selenocysteine insertion into peptides is strongly impaired in the presence of GDP or GDPNP, suggesting that GTP binding and hydrolysis were required for SelB function on the ribosome. The affinity of Sec-tRNA^{Sec} binding to SelB·GTP (K_d = 0.3 pM) is more than a million-fold higher than that to the GDP-bound or the apo form of the factor (K_d = 0.4-0.5 µM). The high selectivity for SelB·GTP is restricted to Sec-tRNA^{Sec}, whereas Ser-tRNA^{Sec} and deacylated tRNA^{Sec} bind to all forms of SelB with the same affinity. The tight binding of Sec-tRNA^{Sec} to SelB·GTP correlates with the net formation of four ion pairs, three of which seem to involve Sec. The SelB·GTP·Sec-tRNA^{Sec} complex is also kinetically very stable, with the half-life time in the hours range (k_{off} = 10^{-3} s^{-1}). GTP hydrolysis increases the dissociation rate constant by several orders of magnitude (k_{off} = 230 s^{-1}), which explains why GTP hydrolysis is required for the delivery of Sec-tRNA^{Sec} to the ribosome.

A rapid-kinetics approach was developed to study mechanistic details of SelB function on the ribosome. To isolate individual fully modified tRNA^{Sec}, a new purification strategy was established based on hydrophobic tagging of the aminoacyl moiety. Labeling of SelB, Sec-tRNA^{Sec}, and other components of the translational machinery allows for the direct observation of the formation or dissociation of complexes by monitoring changes in the fluorescence of single dyes or fluorescence resonance energy transfer between two fluorophores. These observables were used to study rapid kinetics of interactions between those components of the Sec insertion machinery.

Review

Protein synthesis

The steps of protein synthesis

Protein synthesis is one of the fundamental processes in the living cell. The sequence of a polypeptide is determined by the codons in mRNA. Amino acids are esterified to the acceptor end of the transfer RNAs (tRNAs), adaptor molecules which translate codons of mRNA into amino acid sequence. The delivery of the correct amino acid is based on the complementary interaction between the codon of mRNA and anticodon of tRNA. Protein synthesis is brought about by a large ribonucleoprotein complex, the ribosome, with the help of a number of translation factors.

Protein synthesis comprises four major steps (Fig. 1). The initiation starts with the help of the initiation factors (IFs), IF1, IF2, and IF3. IF2 facilitates binding of initiator fMet-tRNA^{fMet} to the start codon of mRNA, AUG, which is positioned in the peptidyl (P) site of the small ribosomal subunit (the 30S subunit). Subsequently, the large ribosomal subunit (50S) binds resulting in a 70S initiation complex with the initiator tRNA in the P site and the second mRNA codon positioned in the aminoacyl (A) site ready for binding the next aminoacyl-tRNA (aa-tRNA). After the formation of the ribosome initiation complex, protein synthesis proceeds to the cyclic elongation step. At the beginning, a complex of elongation factor Tu (EF-Tu), GTP, and aa-tRNA binds to the A site in a codon-dependent manner. The hydrolysis of GTP by the elongation factor is crucial for the selection of the correct tRNA and rejection of incorrect tRNAs which are not complementary to the mRNA codon. After GTP hydrolysis, EF-Tu is released from aa-tRNA and the ribosome, allowing for the accommodation of aa-tRNA in the peptidyl transferase center. The peptidyl moiety is then transferred from the P-site bound peptidyl-tRNA to the aa-tRNA in the A site, resulting in an extension of the peptide chain by one amino acid. Subsequently, two tRNAs and mRNA move relative to the ribosome in a process called translocation, which is catalyzed by elongation factor G (EF-G). As a result, the peptidyl-tRNA
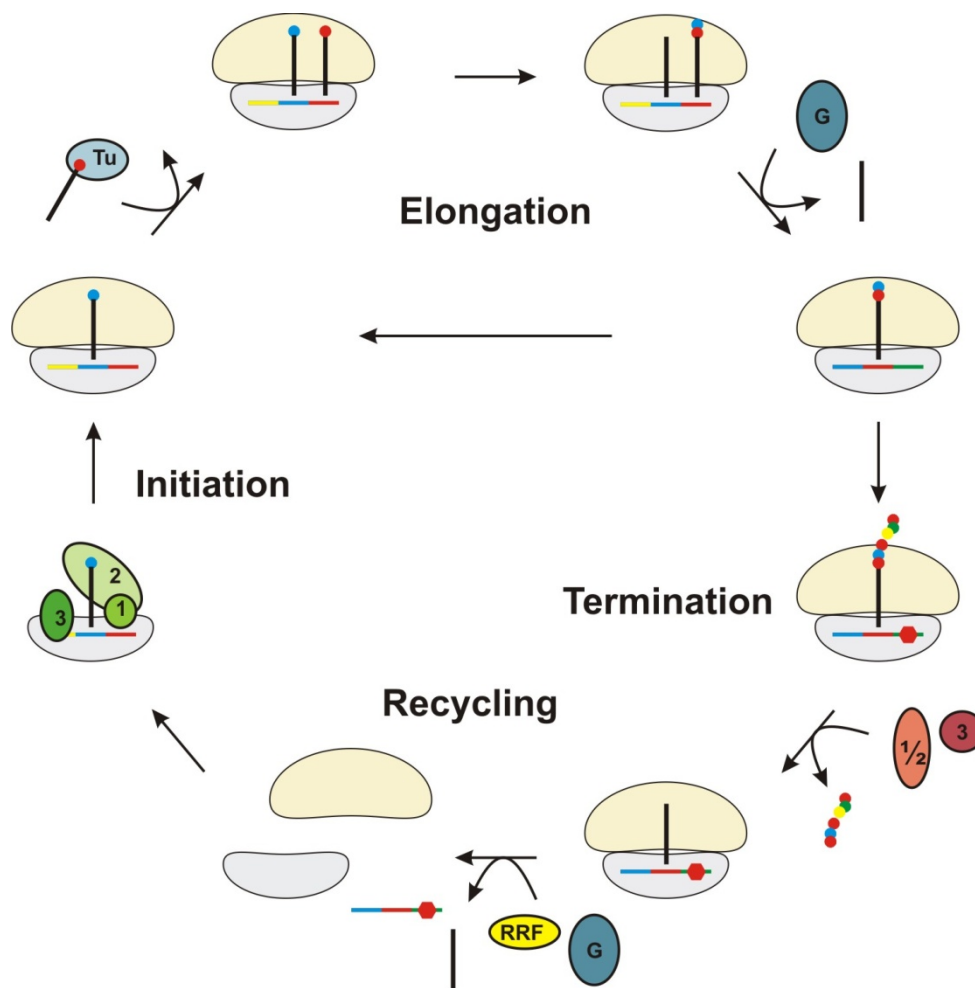
Fig. 1. The prokaryotic translation cycle. Initiation, mediated by initiation factors 1, 2, and 3 (green circles), culminates in the joining of 30S (gray) and 50S (beige) subunits on the mRNA with initiator tRNA (black line with blue circle) in the P site. This complex, aided by the elongation factors Tu and G (blue circles), subsequently undergoes multiple rounds of elongation. Termination, under the control of release factors 1, 2, and 3 (red circles), frees the newly synthesized polypeptide upon recognition of the stop codon. Ribosomal recycling factor (yellow circle) and elongation factor G than prepare the translational machinery for subsequent initiation events.

together with the mRNA is displaced from the A to the P site, while deacylated tRNA moves from the P to the exit (E) site and finally dissociates from the ribosome, and the next codon is exposed in the empty A site. The third step occurs when the complete peptide has been synthesized, the termination of translation. A stop codon presented in the A site of the ribosome is recognized by the class I release factors (RFs). RF1 can read UAA and UAG codons, whereas RF2 is specific for UAA and UGA codons. Release factors trigger hydrolysis of the polypeptide chain from the P-site tRNA. The class II RF, RF3 catalyzes the dissociation of RF1 or RF2, and

subsequently the ribosome proceeds to the final, recycling step. The ribosomal subunits dissociate, tRNA and mRNA are released from the ribosome with the help of ribosomal recycling factor, EF-G, and IF3. The resulting ribosomal subunits are ready to assemble on another mRNA to give rise to a new protein.

GTPases in translation

Proteins that belong to the GTPase superfamily have regulatory roles in all processes of life. GTPases cycle between their active GTP-bound and inactive GDP-bound conformations. In the GTP-bound state, GTPases interact with their effectors and take part in cellular signaling. GTP hydrolysis serves as a switch to terminate signaling, while the exchange of bound GDP with GTP activates signaling. For many GTPases, GTP hydrolysis and GDP release are catalyzed by further regulatory proteins. Bacterial translational GTPases, including IF2, EF-Tu, EF-G, and RF3, belong to the family of ribosome-associated GTPases that act at different stages of prokaryotic protein synthesis. Their guanine nucleotide-binding domains (G-domains) share a structural design common among all GTPases. Cryo-EM reconstructions revealed a common interaction site of the translational GTPases on the ribosome (Allen et al., 2005; Frank and Agrawal, 2000; Klaholz et al., 2004; Myasnikov et al., 2005; Stark et al., 2000; Stark et al., 2002; Valle et al., 2003). Although the significance of the ribosome in stimulating GTP hydrolysis by translational GTPases is well established, the detailed mechanism of GTPase activation as well as the exact role of GTP hydrolysis for the function of different G proteins is not entirely clear.

IF2 plays a central role during the initiation stage of protein synthesis. In the first phase of initiation, IF2, together with IF1 and IF3, facilitates the formation of the 30S initiation complex with mRNA and fMet-tRNA[fMet]. During the second phase, the 50S subunit joins the 30S initiation complex, IF1 and IF3 are ejected, IF2 hydrolyzes GTP and dissociates, and fMet-tRNA[fMet] becomes properly positioned in the ribosomal P site (Gualerzi, 2000). A recent structural study of the 30S initiation complex with IF2 in the GTP-bound state suggests that IF2 positions the acceptor end of fMet-tRNA[fMet] for insertion into the 50S subunit (Simonetti et al., 2008). A large part of IF2 in the complex is complementary in shape to the 50S surface, which explains how IF2 and fMet-tRNA[fMet] favor subunit association. Rapid GTP hydrolysis by IF2 takes place immediately upon binding of the 50S subunit to the 30S initiation

complex and IF2 is retained on the ribosome in the GDP·P$_i$ form for a considerable time (Tomsic et al., 2000). The immediate GTPase activation occurs because the GTP-binding domain of IF2 directly faces the GTPase activating center of the 50S subunit (Simonetti et al., 2008). The structure of the 70S initiation complex stabilized by GDPNP mimics the state of the initiation complex just after the binding of the 50S subunit, but preceding GTP hydrolysis on IF2, which is still bound to fMet-tRNA^{fMet} (Allen et al., 2005). The structure of the 70S ribosome complexed with the initiator tRNA and GDP-bound IF2 represents the state following GTP hydrolysis, when IF1 and IF3 are ejected and no interaction between IF2 and fMet-tRNA^{fMet} can be seen (Myasnikov et al., 2005). The precise role of the IF2 GTPase is not completely understood, but it appears that GTP hydrolysis does not terminate the interaction of the IF2 with its effector, the ribosome, because IF2·GDP also binds to the ribosome (Myasnikov et al., 2005) and delivers fMet-tRNA^{fMet} to the P site (Tomsic et al., 2000). There is no guanine nucleotide exchange factor (GEF) for IF2. The similarly low affinities for GTP and GDP (Pon et al., 1985), low kinetic lability of the complex (Milon et al., 2006), and the high cellular concentration of GTP are sufficient to rapidly exchange GDP for GTP and to restore the GTP-bound state of IF2.

In its active GTP-bound form, EF-Tu tightly binds aa-tRNA (Abrahamson et al., 1985; Ott et al., 1989) and delivers it to the A site of the ribosome. The unusually high rate of ternary complex binding to the ribosome (Pape et al., 1998) suggested an active mechanism for initial binding of the ternary complex to the ribosome. The L7/L12 stalk region of the ribosome recruits the ternary complex and facilitates its positioning on the ribosome (Diaconu et al., 2005). The intrinsically very slow GTP hydrolysis in the ternary complex is strongly stimulated and controlled by the codon-anticodon interaction, ensuring selection of cognate aa-tRNA (Rodnina et al., 1995). The decoding center in the 30S subunit recognizes the geometry of the matched codon-anticodon helix (Ogle et al., 2001; Selmer et al., 2006). The conserved bases A1492 and A1493 form A-minor interactions that are restricted to Watson-Crick base pairs at the first two positions. Additional contributions to monitoring of the second and third codon positions are made by C518, G530, and residues of ribosomal protein S12. The movement of these conserved bases has a key impact to the global structural changes in the 30S subunit in response to the binding of the cognate anticodon (Ogle et al., 2002). The path of communication that leads from structural changes in the 30S subunit to the 50S subunit to activate the GTPase of EF-Tu is not

fully resolved. The signal may be transmitted to the 50S subunit through the subunit interface, where several connections between the subunits are found (Cate et al., 1999). Another possible way of signaling is through the tRNA molecule which is in contact with both the codon and EF-Tu (Cochella and Green, 2005; Piepenburg et al., 2000; Valle et al., 2003), as described in detail below. GTP hydrolysis occurs by an attack on the γ-phosphate by a water molecule, which is resolved in crystal structures of EF-Tu·GTP (Berchtold et al., 1993). Rapid kinetic measurements revealed an essential role of histidine 84 in the chemical step of GTP hydrolysis (Daviter et al., 2003). A recent cryo-EM study supported the biochemical results by showing that the hydrophobic gate, which shields histidine 84 in the ground state of EF-Tu, opens to allow for the movement of histidine 84 toward the nucleotide (Villa et al., 2009). Release of inorganic phosphate triggers the fast conformational change of EF-Tu toward its inactive GDP conformation (Kothe and Rodnina, 2006), which has a lowered affinity to aa-tRNA and the ribosome. The nucleotide exchange factor, EF-Ts, binds to EF-Tu·GDP to restore its GTP-bound form. EF-Ts accelerates the dissociation of GDP (Gromadski et al., 2002) and thereby promotes the formation of the ternary complex under conditions of sufficient concentration of GTP and aa-tRNAs.

Upon peptide bond formation, EF-G catalyzes translocation, that is the simultaneous movement of two tRNAs bound to the mRNA within the ribosome. As soon as EF-G binds to the ribosome, the ratcheted conformation of the ribosome with tRNAs in their hybrid states is induced or stabilized (Agirrezabala et al., 2008; Frank and Agrawal, 2000; Julian et al., 2008; Spiegel et al., 2007). Upon GTP hydrolysis, EF-G undergoes a conformational change followed by a ribosome rearrangement, called "unlocking". The latter conformational rearrangement precedes both tRNA-mRNA translocation and phosphate release from EF-G (Savelsbergh et al., 2003). GTP hydrolysis does not trigger dissociation of the factor, suggesting that phosphate release, rather than GTP hydrolysis, is crucial for the dissociation of EF-G from the ribosome (Savelsbergh et al., 2005). EF-G utilizes the energy of GTP hydrolysis to induce a rearrangement of the ribosome and, subsequently, biases forward movement of mRNA·tRNAs, which itself seems to happen spontaneously (Wintermeyer et al., 2004). Similarly to IF2, EF-G does not require GEF to recycle to the GTP form, as the affinities for GTP and GDP are comparable and the dissociation rate constants are high (Wilden et al., 2006).

The role of RF3, a GTPase involved in the termination step of protein synthesis, is becoming increasingly understood. The recent high-resolution structures of post-termination ribosomal complexes with either RF1 of RF2 bound to the A site and deacylated tRNA in the P site reveal that the stop codon is recognized in a pocket formed by conserved elements of the class I RFs and the 16S ribosomal RNA (Korostelev et al., 2008; Laurberg et al., 2008; Weixlbaumer et al., 2008). Despite the obvious overlap in the binding sites of the tRNAs and RF1/RF2 on the ribosome, the biochemical results clearly indicate that the ribosome decoding center must function in fundamentally different ways for these two seemingly related processes (Youngman et al., 2007). The recognition of stop codons by class I RFs induces specific structural rearrangements in the decoding center, which trigger hydrolysis of the ester bond in peptidyl-tRNA, presumably through the contact between the universally conserved GGQ motif and the peptidyl-transferase center of the ribosomal 50S subunit (Zaher and Green, 2009). RF3 binds to the ribosome in the GDP-bound form, because the affinity of RF3 for GDP is three orders of magnitude higher than that for GTP (Zavialov et al., 2001). RF1/RF2 prebound to the ribosome catalyze the dissociation of GDP from RF3. Subsequent GTP binding to RF3 induces conformational changes both in RF3, forming a more extended structure, and the ribosome, characterized by the ratchet-like movement of the small relative to the large subunit that is accompanied by the movement of the deacylated tRNA from the P into the hybrid P/E state (Gao et al., 2007). Structural rearrangements break the interaction between the ribosome and RF1/RF2, which may cause the dissociation of the factors. Finally, GTP hydrolysis causes RF3 to switch back to its low-affinity GDP-bound form, which triggers its rapid dissociation from the ribosome (Noble and Song, 2008).

tRNA as an active player in translation

During protein synthesis, tRNA molecules interact with aminoacyl-tRNA synthetases (ARSs), elongation factors, mRNAs, and the ribosome. All aa-tRNAs share the same overall tertiary structure which is L-shaped with the anticodon and the aminoacylated 3' terminus forming the two ends. The tertiary structure is based on the common secondary cloverleaf structure with the acceptor stem, the D arm, the anticodon arm, the variable arm, and the TΨC arm. Typically, tRNAs contain several

base modifications such as the universally occurring pseudouridine (Ψ) and dihydrouridine (D). Additionally, tRNAs are specifically modified at various nucleosides with a large variety of functional groups (Agris, 2004).

Studies on translation require large amounts of purified individual tRNAs. However, few purified tRNAs are commercially available. Individual tRNAs can be easily produced by *in vitro* transcription, but the lack of modifications of the tRNA transcripts may influence or impair their function (Agris, 2004; Konevega et al., 2004). The overall similarity of tRNAs makes it difficult to purify specific tRNAs from total tRNA. Recently, a simple method has been developed to allow the rapid isolation of individual tRNAs (Kothe et al., 2006) (Paper 1). This method is based on selective tagging of the amino group of specifically charged aa-tRNAs with the hydrophobic 9-fluorenylmethylsuccinimidylcarbonat (FmocOSu), followed by a single chromatographic purification step using reversed-phase HPLC or low-pressure hydrophobic interaction chromatography. The idea of the method is to add a large aromatic group to the aminoacylated tRNA, thereby increasing its hydrophobicity and retention time on the column, allowing for separation of Fmoc-aa-tRNA complex from the bulk of deacylated tRNA. Subsequent deacylation of the complex results in pure tRNA of the desired specificity. The current method is generally applicable for all tRNAs, because it relies solely on the selective aminoacylation by highly specific ARSs and the subsequent modification of the amino group. In contrast to a previously published method (Gillam et al., 1968), the ester used in the present work (FmocOSu) is readily available at low cost and is stable. Compared to other methods, such as affinity chromatography with immobilized EF-Tu (Ribeiro et al., 1995) or streptavidin binding of N-biotinylated aa-tRNAs (Putz et al., 1997), the present method utilizes chromatographic materials that are significantly less expensive and allows for the purification in one chromatographic step of tRNAs in large preparative amounts.

Due to the redundancy of the genetic code, most amino acids are encoded by two or more codons and are delivered by different tRNAs. For example, *Escherichia coli* cells express 46 different tRNAs (Komine et al., 1990) to incorporate 21 amino acids, encoded by 62 codons. The smaller number of tRNAs compared to codons is due to the ability of certain tRNAs to interact with more than one codon corresponding to one amino acid. There is a different degree of precision which is allowed at diverse codon-anticodon positions. At the first two positions of codon-

anticodon interactions only Watson-Crick base pairs are allowed, whereas at the third position both Watson-Crick and wobble base pairing are possible (Crick, 1966). In addition, some tRNAs with modified nucleosides in the wobble position have decoding capacities that are more extensive than the wobble hypothesis would allow for (Mitra et al., 1979; Nasvall et al., 2004). In such cases, the tRNAs have a broader reading spectrum than envisaged in the classic codon reading scheme.

To ensure the fidelity of gene expression, amino acids should be attached to their cognate tRNA by an specific ARSs. The error rate of aminoacylation is on the order of 10^{-6}, which is nearly 100-1000 times more precise than the overall protein synthesis (Ibba and Soll, 2000). To secure such a high accuracy of aminoacylation, ARSs must make extremely fine distinctions between amino acid substrates that may differ by no more than a single methyl group and between tRNA molecules possessing an overall similar structure. The selection of the correct amino acid by ARS involves the use of induced fit to enhance binding specificity, the imposition of fidelity at the level of chemistry, and the application of postsynthetic editing mechanism to hydrolyze incorrect products in a discrete editing domain. The discrimination of tRNAs by ARSs relies both on direct contact between synthetases and functional groups of the tRNAs, as well as the modulation of the RNA-protein binding affinity by global features of tRNA structure (Francklyn, 2008; Giege et al., 1998). An additional role is played by EF-Tu which by ternary complex formation effectively prevents aa-tRNAs from competing with uncharged tRNAs for their cognate ARSs, which bind charged and uncharged tRNAs with similar affinities (Pingoud et al., 1973).

For a long time the elaborate mechanism of tRNA and amino acid recognition by ARSs was believed to be absolutely crucial for the correct protein synthesis, as both EF-Tu and the ribosome were considered to lack specificity for different amino acids, once they are esterified onto tRNA. However, a small number of aa-tRNAs (Asn-tRNA^{Asn}, Gln-tRNA^{Gln}, Cys-tRNA^{Cys}, and Sec-tRNA^{Sec}) are made by synthesizing the amino acid on the tRNA by first attaching a non-cognate amino acid (the precursor of the final amino acid) to the tRNA, which is then converted to the cognate one by tRNA-dependent modifying enzymes. Because organisms using these pathways do not show misincorporation it appears that intermediates are not incorporated into the peptide. Thus, in these cases relaxed-specificity of ARSs that

form misacylated aa-tRNA species is compensated by other components of the translation machinery.

All correctly acylated elongator tRNAs, except for Sec-tRNA^{Sec} which is discussed in detail below, bind EF-Tu with approximately the same affinity (Abrahamson et al., 1985; Louie and Jurnak, 1985; Louie et al., 1984; Rudinger et al., 1996), but several thousand-fold differences in the dissociation constants were observed for misacylated tRNAs (Asahara and Uhlenbeck, 2002; Dale et al., 2004; LaRiviere et al., 2001). These data suggest that EF-Tu possesses a considerable specificity for both the amino acid side chain and the tRNA body. The thermodynamic contributions of the amino acid and the tRNA to the overall binding affinity are independent of each other and compensate for one another when the tRNA is esterified with the cognate amino acid. The lack of thermodynamic compensation for misacylated tRNAs leads to a much wider range of affinities for EF-Tu and tRNAs. Although misacylated tRNAs with low affinity for EF-Tu could not incorporate the amino acid into the growing peptide, several misacylated tRNAs stably bind to EF-Tu and are delivered to the ribosome. This notion is in accordance with previous observations that some misacylated suppressor tRNAs are active in translation (Giege et al., 1998; Saks et al., 1994) and explains why alanine could be successfully incorporated instead of cysteine (Cys) after reduction of Cys-tRNA^{Cys} to Ala-tRNA^{Cys} in the classic Chapeville experiment.

Different aa-tRNAs exhibit similar kinetic and thermodynamic properties in decoding cognate codons on the ribosomes (Daviter et al., 2006; Kothe and Rodnina, 2007; Ledoux and Uhlenbeck, 2008), ensuring that all amino acids are incorporated into protein with similar efficiencies and rates, despite their significant differences in size, charge, and hydrophobicity. The esterified amino acid makes a contribution to the affinity of the tRNA for the A site, as dissociation rates of deacylated tRNAs are quite different from those of aa-tRNAs (Fahlman et al., 2004). Although misacylated tRNAs have similar affinities for the ribosomal A site as their correctly acylated counterparts, several misacylated tRNAs could read mismatched codons (Ledoux, 2008). This implies that the identity of the esterified amino acid is an important contributor to the accurate decoding of aa-tRNAs on the ribosome. The uniformity of aa-tRNA binding to the ribosome depends on a unique combination of structural elements, suggesting that each tRNA sequence has coevolved with its anticodon and

set of posttranscriptional modifications to tune ribosome affinity to a value that is the same for all tRNAs (Fahlman et al., 2004; Olejniczak et al., 2005).

During tRNA selection on the ribosome, a cognate codon-anticodon interaction triggers a series of events that results in the acceptance of that tRNA for peptide bond formation. There is evidence showing that codon recognition is coupled to conformational changes of both the tRNA (Rodnina et al., 1994) and the G domain of EF-Tu (Rodnina et al., 1995), which presumably represents the transition to the GTPase state. The structural rearrangements of aa-tRNA in the GTPase-activated state of the ternary complex on the ribosome were visualized by cryo-EM (Schuette et al., 2009; Stark et al., 2002; Valle et al., 2003; Villa et al., 2009). The opening of the tRNA at the junction between the partially disordered D stem-loop and T-acceptor arm and a kink between the D and anticodon stems reorient the anticodon domain of aa-tRNA to reach into the decoding center, the acceptor arm of the tRNA contacts ribosomal protein S12, the T loop at the elbow region interacts with the 23S rRNA where ribosomal protein L11 is bound and the acceptor stem is attached to EF-Tu. Aa-tRNA in the A/T site is significantly distorted in comparison to its structure in the ternary complex: the region around the anticodon loop is in nearly the accommodated orientation, while the bend allows the rest of the tRNA to remain in the orientation presented by EF-Tu. The bending of aa-tRNA might be part of a signal transmission through the tRNA molecule between the decoding center and the G domain of EF-Tu. This is supported by the finding that there was no GTPase activation when two RNA fragments were used instead of intact tRNA (Piepenburg et al., 2000). Further evidence for the contribution of tRNA to decoding was obtained by kinetic analysis of the Hirsh suppressor, a Trp-tRNA[Trp] that carries a G24A substitution in the D arm and recognizes both tryptophan (UGG) and stop (UGA) codons (Cochella and Green, 2005). The miscoding is achieved by acceleration of forward selection rates independent of correct codon-anticodon pairing. The D-arm substitution likely has a direct effect on tRNA deformability, affecting the capacity of the tRNA to assume a bent conformation without additional energy from the cognate codon-anticodon interaction in the decoding center (Daviter et al., 2006). Taking together, tRNAs should be considered as active participants in translation, rather than static "adaptors", as more specific roles for tRNAs are uncovered.

The selenocysteine incorporation machinery

Selenoproteins

Selenium was discovered in 1817 by a Swedish chemist J.J. Berzelius while he investigated a disease found among workers at a sulfuric acid plant. The element was named after the Greek goddess of the moon, Selene, in analogy to the naming of the previously discovered and closely related element tellurium (Latin: *tellus* – earth). Selenium belongs to the same group of elements in the periodic table as oxygen and sulfur; these elements form important functional groups of amino acids. The abundance of selenium in the Earth's crust is about four magnitudes lower than that of sulfur, which is also reflected in the natural abundance of these elements in biological systems.

Selenium has long been considered as a potentially toxic substance, especially to grazing animals, when eating selenium-accumulating plants during the periods of droughts in western USA and China. The significance of selenium for biological processes was shown for the first time in the mid-1950s, when it was identified as an essential trace element for bacteria, birds, and mammals (Pinsent, 1954; Schwarz and Foltz, 1957). Since that time, the efforts were focused on understanding the biochemical role of selenium, rather than the mechanisms of its toxicity and excretion. In 1973, two independent groups found that selenium is a component of glutathione peroxidase (Flohe et al., 1973; Rotruck et al., 1973). This discovery marked the first example of a natural selenium-containing protein and provided the foundation for the rapid development of the molecular biology of selenium. In subsequent years, the list of selenoproteins has been steadily growing, and selenoproteins were identified in bacteria, archaea, and eukaryotes. Although in several bacterial molybdenum-containing enzymes selenium was present as a dissociable cofactor (Wagner and Andreesen, 1979), the major biological form of selenium in proteins of all three domains of life was shown to be selenocysteine (Sec). Sec was first recognized as an internal component of glycine reductase selenoprotein A (Cone et al., 1976) and later was shown to be encoded by UGA (Chambers et al., 1986; Zinoni et al., 1986). Selenoproteins can be found in all three kingdoms of life, but not in all species of eukarya, archaea, and eubacteria (Xu et al., 2007). For example, neither fungi nor higher plants can incorporate Sec at specific

locations. Moreover, about half of the completely sequenced genomes in each of the three domains of life appear to lack selenoprotein genes. In these genomes, neither genes that are conserved among organisms that contain the Sec insertion system, nor known selenoproteins can be found (Gladyshev, 2001).

The majority of the proteins included in the current list of bacterial selenoproteins appear to be involved in catabolic processes and utilize Sec to catalyze various redox reactions (Stadtman, 1996). In several of these enzymes, Sec is coordinated to metals. For instance, formate dehydrogenases (FDH) are examples of a molybdopterin-selenoproteins, in which the Sec residue is coordinated, through its selenium atom, to a molybdenum atom (Gladyshev et al., 1994). In the group of hydrogenases, Sec is coordinated to a nickel atom (Garcin et al., 1999). In these enzymes, Sec is located in the active center, and a replacement of Sec with Cys leads to dramatic loss in biologic activity. Substitution of Sec by Cys in *E. coli* FDH resulted in an almost 1000-fold activity decrease, while the Sec to Ser mutant was completely inactive (Axley et al., 1991). Selenoproteins A and B are components of the glycine, sarcosine, and betaine reductase complexes in *Eubacterium acidaminophilum* (Wagner et al., 1999). The three complexes contain the same selenoprotein A polypeptide and distinct substrate-specific selenoprotein B polypeptides. There is a number of selenoproteins with functions that are unusual for bacterial selenoenzymes. One of them, the Sec-containing selenophosphate synthetase (SPS or SelD in *E. coli*), participates in Sec synthesis and therefore may be considered as an autoregulatory enzyme (Stadtman, 1996). Moreover, this protein is a singular example of an overlap between prokaryotic and eukaryotic selenoproteins. An unexpected addition to the list of bacterial selenoproteins, peroxiredoxin, is found in *E. acidaminophilum* (Andreesen et al., 1999). This antioxidant protein is involved in the detoxification of peroxides, a function that appears to be more common among eukaryotic selenoproteins (see below).

Sec-containing proteins in archaea resemble bacterial selenoproteins and include FDH, hydrogenase, heterodisulfide reductase, formylmethanofuran dehydrogenase, and SPS. Only a few of these selenoproteins were characterized biochemically (Gladyshev, 2001). In spite of the similarity between bacterial and archaeal selenoproteins, the mechanism for Sec incorporation appears to be different in these organisms, as described below.

The largest number of selenoproteins is found in vertebrate genomes, and the list of known eukaryotic selenoproteins is growing rapidly. In contrast to prokaryotes and archaea, eukaryotic selenoproteins of known functions participate in redox pathways linked to anabolic and regulatory processes (Gladyshev, 2001). The function of selenoproteins is essential in the development of eukaryotic organisms, as the disruption of the murine Sec-tRNA^{Sec} gene leads to embryonic lethality (Bosl et al., 1997). One of the essential selenoprotein genes could be the thioredoxin reductase gene. The protein expressed by this gene is present in all living organisms, but its Sec-containing form occurs only in animals. Moreover, disruption of the thioredoxin gene is lethal in mice (Matsui et al., 1996).

Although eukaryotic selenoproteins do not share sequence homologies, similar structures, or related functions, they may be divided into two groups, based on the location of Sec in the sequence (Hatfield and Gladyshev, 2002). The first group is the most abundant and includes proteins in which Sec is located in the N-terminal part of a relatively short functional domain. This location is similar to that of the CxxC motif (two Cys residues separated by two other amino acids), which is involved in redox reactions catalyzed by thiol-disulfide oxidoreductases. In fact, several selenoproteins, such as SelW, SelP, SelT, SelM, and BthD, exhibit a similar redox motif, except that one of the Cys residues is replaced by Sec (Kryukov et al., 1999). Three deiodinase isozymes, SelN, SPS, and a 15 kDa-selenoprotein contain a modified motif in which Sec is separated from Cys by a single amino acid residue (Gladyshev and Kryukov, 2001). The members of a subgroup of glutathione peroxidase homologs contain a single Sec residue, suggesting that Sec is either oxidized during catalysis to selenenic acid or forms intermolecular selenosulfide bonds (Brigelius-Flohe, 1999).

The second group of eukaryotic selenoproteins is characterized by the presence of Sec in C-terminal sequences. In these proteins, the location of Sec in conformationally flexible C-terminal sequences ensures its accessibility (Sun et al., 1999). This situation is functionally similar to the fusion of a low-molecular-weight redox compound to the C terminus of a functional domain (Sun et al., 2001). In thioredoxin reductases belonging to this group, the function of the Sec-containing motif is to transfer reducing equivalents from the buried disulfide active site to the active center of a protein substrate. The function of the G-rich protein, another member of the group, is not known. Independently of the location of Sec in

functionally characterized selenoproteins, the Sec residue appears to participate in redox reactions.

Selenocysteine biosynthesis

When the genetic code was deciphered in the 1960s, 20 amino acids were assigned to the 61 sense codons out of the 64 possible within the triplet code, and three codons were found to serve as terminators of protein synthesis. At that time it was believed that only one code word, AUG, had a dual role. It function was both the initiation of protein synthesis with methionine and the insertion of methionine at internal positions. However, in 1989 it became clear that also UGA has a dual function, encoding for both termination and Sec insertion. The fact that Sec is transferred to the ribosome by a specific tRNA^{Sec} provided the strongest evidence that Sec is indeed the 21st amino acid in the genetic code.

The primary and secondary structure of tRNA^{Sec} differ from those of the other tRNAs in having a longer acceptor stem, a long variable arm, and substitutions at several base positions which are conserved among other elongator tRNAs (Baron and Bock, 1991; Baron et al., 1990; Carlson et al., 2001; Schon et al., 1989) (Fig. 2).

Sec does not readily occur as a free amino acid; instead, its synthesis takes place on tRNA^{Sec}. tRNA^{Sec} is initially charged with serine by seryl-tRNA synthetase (SerRS). In bacteria, the tRNA-bound seryl residue is directly converted to a selenocysteinyl residue by the pyridoxal phosphate-containing enzyme selenocysteine synthase (SecS or SelA in *E. coli*), using selenomonophosphate as the selenium donor substrate (Fig. 3). The latter is synthesized from selenite and ATP by SPS, or SelD in *E. coli*. Finally, the resulting Sec-tRNA^{Sec} binds to a specific translational elongation factor, SelB. To deliver Sec-tRNA^{Sec} to ribosomes translating mRNAs coding for selenoproteins, SelB interacts with a specific mRNA sequence forming a stem-loop (selenocysteine insertion sequence, SECIS). The presence of SECIS element downstream of the UGA codon ensures its recognition as the codon for selenocysteine incorporation, rather than as a stop codon ((Böck, 2001) and references cited therein).
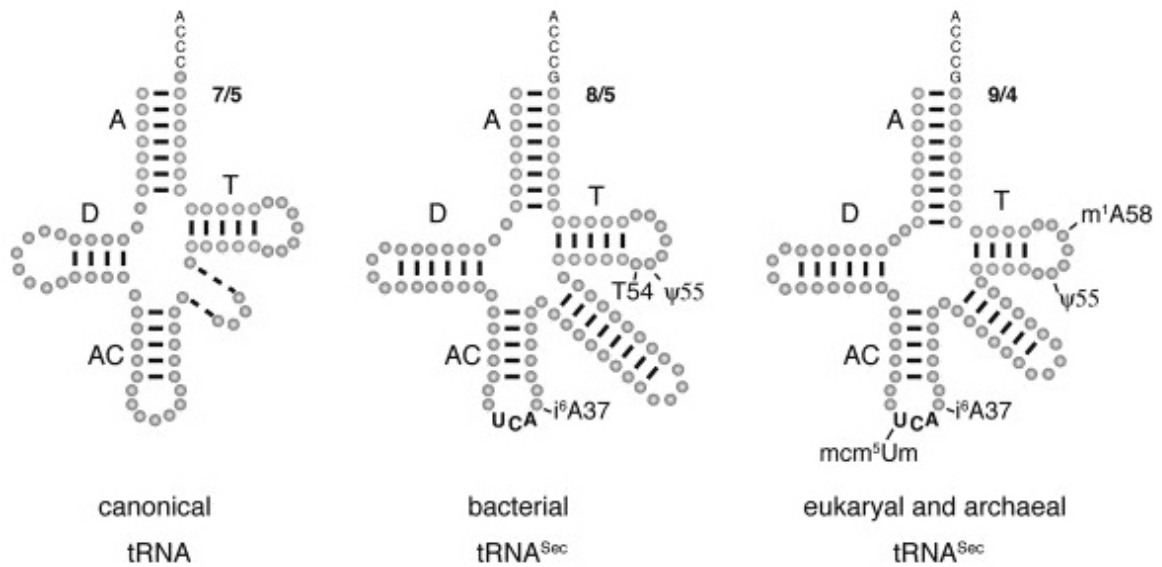
Fig. 2. Comparison of secondary structures of canonical tRNAs and selenocysteine tRNAs^Sec. The various secondary structure elements are indicated: A, D, AC, and T stand for the amino acid, D, anticodon and T stems, respectively. 7/5, 8/5, 9/4 indicate the number of base pairs forming the coaxial A-T arm in the tRNAs shown. Dashes in the canonical tRNA structure signify that the extra arm is of variable length in different tRNAs. Modified bases are indicated where identified in the bacterial and eukaryal tRNA^Sec and were omitted in the canonical tRNA. The archaeal tRNA^Sec was not investigated for its base modification content (Allmang and Krol, 2006).
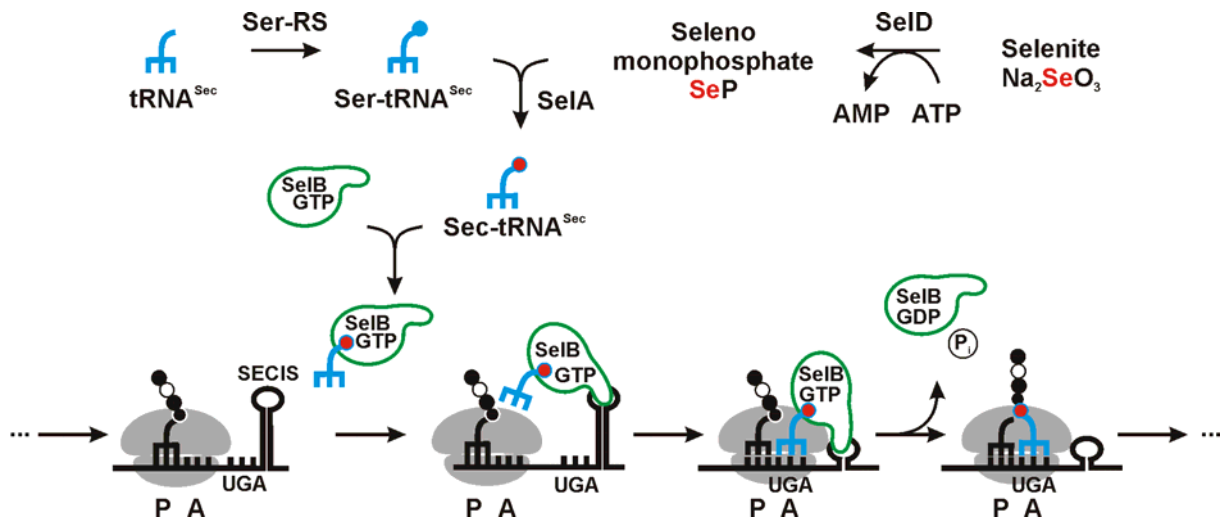

Fig. 3. Sec incorporation into proteins in bacteria.

Sec biosynthesis in bacteria was studied in detail. SelA is a homo-oligomer with a molecular mass of about 500 kD, consisting of ten monomers of 50 kD each (Forchhammer et al., 1991). In line with the conservation of sequence and reaction

mechanism (Tormay et al., 1998), SelA proteins from *E. coli* and *Moorella thermoacetica* are very similar in shape and size (Engelhardt et al., 1992; Fischer et al., 2007) (Paper 2). SelA has a crown-like ring structure with five bilobed wings. The density distribution in the cryo-EM map shows a clear dissection into five subunits, each subunit containing a dimer of SelA monomers. One Ser-tRNA^{Sec} molecule binds near each margin of the dimeric subunit (Engelhardt et al., 1992). Binding experiments also gave a stoichiometry of one tRNA molecule per two protein monomers (Forchhammer and Bock, 1991). Mutated tRNA^{Sec} variants, when charged with serine, are able to interact with SecS. tRNA^{Sec} with the variable arm of tRNA^{Ser} was as efficient as wild-type tRNA^{Sec}, whereas a mutant with a shortened acceptor stem exhibited a reduced rate of selenylation (Baron and Bock, 1991). It appears that once the tRNA is charged with serine it is immediately bound to SelA and stays until selenophosphate is available as the substrate molecule. To convert Ser-tRNA^{Sec} to selenocysteyl-tRNA^{Sec}, the amino group of the seryl residue forms a Schiff base with the carbonyl of the pyridoxal 5-phosphate cofactor of the SecS. Following dehydration to an aminoacrylyl intermediate, selenocysteyl-tRNA^{Sec} is formed and dissociates from the factor (Forchhammer and Bock, 1991).

Selenophosphate is not only used in selenoprotein synthesis but also serves as a donor for the synthesis of 5-methylaminomethyl-2-selenouridine in the anticodons of tRNA^{Glu}, tRNA^{Gln}, and tRNA^{Lys} isoacceptors (Ching et al., 1985; Wittwer and Stadtman, 1986). The first step in SelD-catalyzed synthesis of monoselenophosphate involves the nucleophilic attack presumably by the Cys17 residue of SelD (Kim et al., 1992) on the γ-phosphate group of ATP, which results in the formation of an enzyme-phosphoryl intermediate. The latter reacts with selenite to form selenophosphate. Bound ADP is then hydrolyzed to release orthophosphate and AMP as products. *E. coli* can also use Sec as an alternative to the selenite source of selenium. NifS-like protein, selenocysteine lyase, catalyzes the pyridoxal 5'-phosphate-dependent decomposition of L-Sec to L-alanine and elemental selenium, which can be used as a substrate for selenophosphate synthethase (Lacourciere et al., 2000; Mihara et al., 2002). Although the sequence of SPS is highly conserved, *Haemophilus influenzae* (bacteria), *Methanococcus jannaschii* (archaea), mice, and humans contain a Sec residue which aligns with Cys17 in the *E. coli* enzyme (Bult et al., 1996; Fleischmann et al., 1995; Guimaraes et al., 1996). As described above, the SPS provides selenophosphate for SecS, thus generating Sec-

tRNA^{Sec}. This raises the question of how incorporation of Sec within the SPS is achieved, as selenophosphate has to be generated first in order to translate the gene of SPS. Some amount of SPS molecules can be inherited through cell division; alternatively, a low level of UGA suppression independent of Sec incorporation (e.g., by cysteinyl-tRNA^{Cys}) might occur, resulting in a partly active SPS enzyme (Hüttenhofer and Böck, 1998). The reason for the presence of Sec in enzymes involved in the Sec-incorporating pathway might thus be a way of fine-tuning this system, allowing a slow upregulation of the selenophosphate production.

In archea and eukarya, Sec synthesis follows a different pathway. Ser-tRNA^{Sec} is phosphorylated by O-phosphoseryl-tRNA^{Sec} kinase (PSTK) (Fig. 4A). Surprisingly, this enzyme can efficiently phosphorylate a chimeric Thr-tRNA^{Sec} and the affinity of PSTK for tRNA^{Sec} is similar to that for Ser-tRNA^{Sec}, indicating that the aminoacyl residue attached to tRNA^{Sec} is not involved in recognition. The conversion of O-phosphoseryl-tRNA^{Sec} to Sec-tRNA^{Sec} is carried out by the pyridoxal phosphate-containing enzyme SecS. SPS1 and SPS2 were described to catalyze the formation of selenomonophosphate. However, recent data established that only SPS2 is essential for selenoprotein synthesis and that SPS1 functions in a pathway that is not related to Sec biosynthesis. In eukarya and archaea, SelB function is shared by two proteins, elongation factor EFSec which binds Sec-tRNA^{Sec} and SECIS-binding protein 2 (SBP2) which interacts with the SECIS element. Protein SECp43 facilitates the interaction between Sec-tRNA^{Sec}, EFSec, and SBP2 *in vivo* and redistributes the nucleocytoplasmic localization of SecS and SPS1. SECp43 was also shown to participate in the 2'-O-methylation of the tRNA^{Sec} at position U34, thus being a candidate for the Um34 methylase. According to the current model, SBP2 binds the SECIS, which usually resides in the 3' untranslated region, and serves as a platform to recruit the EFSec/Sec-tRNA^{Sec} complex, prior to UGA decoding (Fig. 4B). Upon ribosome binding, ribosomal protein L30 was suggested to displace SBP2, thereby inducing a more closed conformation of the SECIS. This movement may trigger GTP hydrolysis by EFSec and the release of the Sec-tRNA^{Sec} to the A site of the ribosome. It remains to be understood why Sec-tRNA^{Sec} shuttles between the cytoplasm and the nucleus and what is the role of SPS1, since it is now clear that SPS1 does not participate in Sec biosynthesis ((Allmang and Krol, 2006; Allmang et al., 2009) and references cited therein).
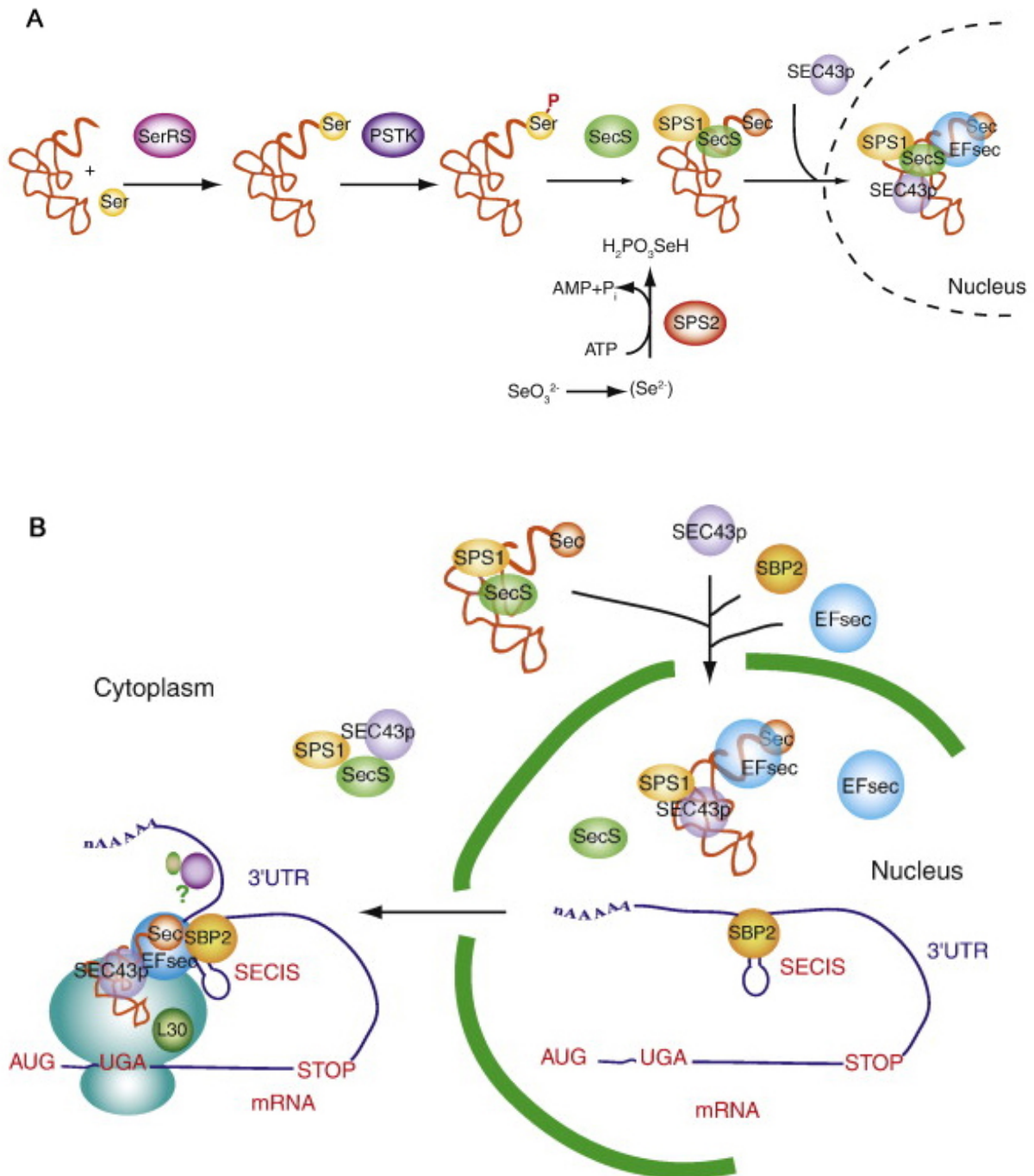
Fig. 4. Sec incorporation into proteins in eukaryotes. (A) Sec biosynthesis. (B) Model for selenoprotein synthesis. Shuttling of the SPS1/SECp43/EFSec/Sec-tRNA^{Sec} complex into the nucleus and the association with SBP2 and the SECIS element are depicted. Cytoplasmic export of the SECIS-bound complex is shown on the left (Allmang et al., 2009).

Selenocysteine-inserting tRNA

tRNA^{Sec} is the only known tRNA that governs the expression of an entire class of proteins, the selenoproteins. This tRNA can therefore be called the key molecule and the central component in selenoprotein biosynthesis (Hatfield and Gladyshev, 2002). Bacterial tRNA^{Sec} molecules are considerably longer than most other canonical tRNAs. The longest tRNA known to date is tRNA^{Sec} from *Clostridium thermoaceticum*, exhibiting a length of 100 bases (Tormay et al., 1994). This is due to the extended variable arm as well as to the extended acceptor stem, unique features present in all Sec-inserting tRNAs. The tertiary structure of *E. coli* tRNA^{Sec} resembles the overall L-shape of canonical tRNAs, with comparable distances between the CCA-end and the anticodon (~76 Å) (Baron et al., 1993). Thus, the extra base pair (A5a-U67a) in the amino acid acceptor stem does not cause any significant structural distortion that would change the respective orientations of the two extremities of the molecules.

The sequence of tRNA^{Sec} from *E. coli* deviates from the tRNA consensus sequence at several positions: G at position 8, U at position 9, U at position 14, pyrimidine-purine pair at positions 10-25, and purine-pyrimidine pair at positions 11-24, the latter being present in bacterial initiator tRNAs as well. The purine-pyrimidine tertiary base pair between positions 15-48, which is characteristic for canonical tRNAs, is missing in tRNA^{Sec} (Schon et al., 1989). On the basis of chemical and enzymatic probing, a three-dimensional model of tRNA^{Sec} was constructed and revealed a set of unique interactions in the core of the structure (Baron et al., 1993) (Fig. 5). One of them, a base pair between C16 and C59, helps to stabilize the contacts between the D and T loops of the tRNA. In canonical tRNAs, the U8-A14 interaction is universal and links the two arms of the molecule; in tRNA^{Sec} it is replaced by a triple interaction in which G8 forms a Hoogsteen pair with A21, while A21 makes Watson-Crick interactions with U14. For the third suggested unusual pairing C15-G20a-G48, unambiguous experimental evidence is still lacking.

The anticodon of tRNA^{Sec} is UCA, which enables it to decode UGA codons. tRNA^{Sec} contains relatively few modified nucleotides, compared to other tRNAs, which may have up to 17 modifications (Hatfield and Gladyshev, 2002). *E. coli* tRNA^{Sec} contains dihydrouridine (D) at position 20, ribothymidine (T) at position 54, pseudouridine (ψ) at positions 55 and 38, and isopentenyladenosine (i^{6}A) in position 37. As shown for other tRNAs, isopentenylation of position 37 in tRNA appears to be
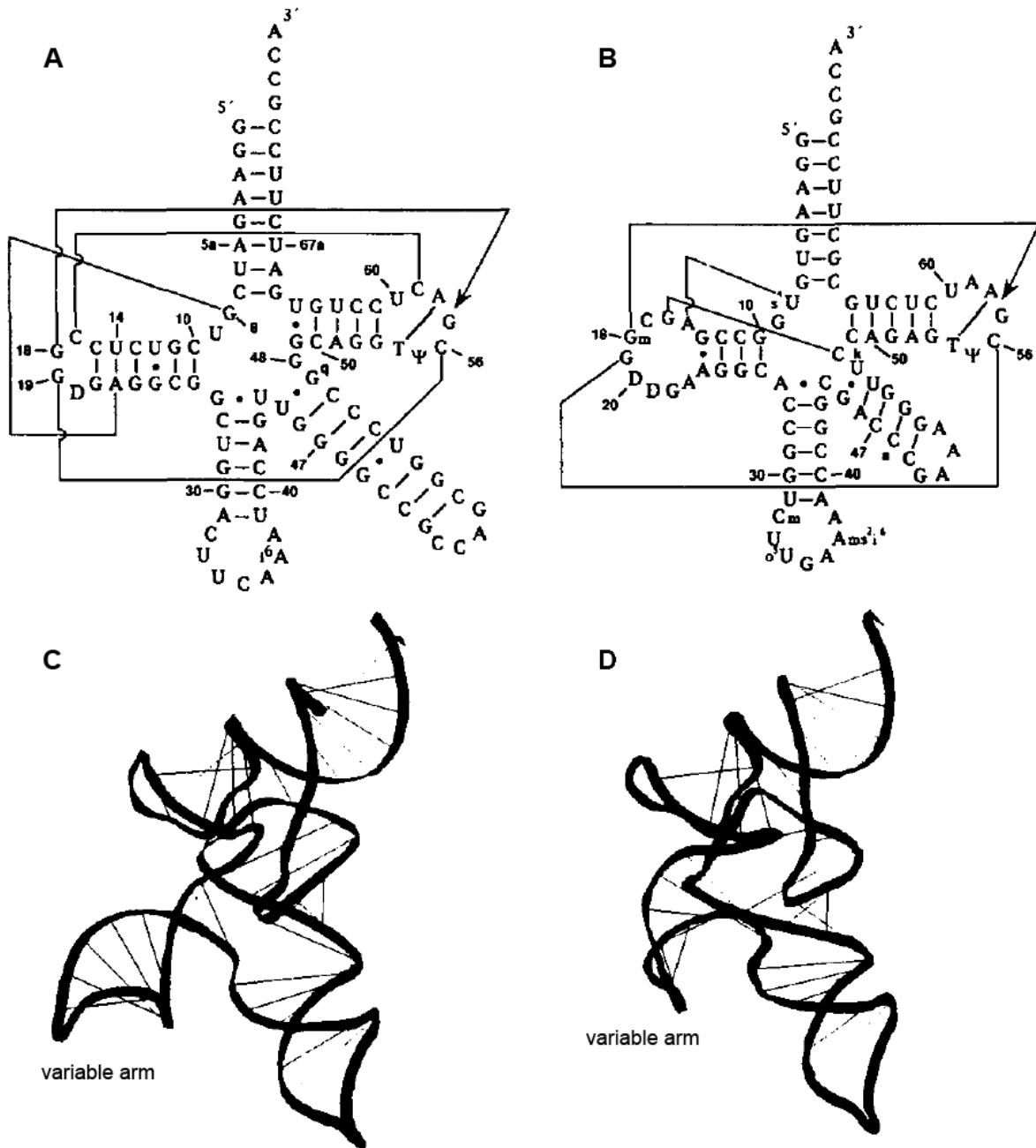
Fig. 5. Comparison of tRNA^{Sec} and tRNA^{Ser} structures. Tertiary interaction networks in tRNA[Sec] (A) and tRNA[Ser] (B). 3-dimensional backbone model of tRNA[Sec] (C) and tRNA[Ser] (D) (Baron et al., 1993).

important for efficient binding of aa-tRNA to ribosomes (Gefter and Russell, 1969; Konevega et al., 2004; Vacher et al., 1984). The modification stabilizes the first base pair of the codon-anticodon complex and thereby assists in preventing misreading of the first codon position (Wilson and Roe, 1989). However, both *in vivo* (Bouadloun et al., 1986) and *in vitro* (Diaz and Ehrenberg, 1991) results indicate that the i^{6}A modification increases third-position misreading due to decreased proofreading.

Indeed, an unusual wobble interaction at the third position of the codon seems to be possible with wild-type tRNA^{Sec} which recognizes the Cys codons UGC and UGU almost as well as the UGA codon (Baron et al., 1990). This is consistent with the presence of an unmodified U at position 34 of tRNA^{Sec} (Schon et al., 1989). Mutants of tRNA^{Sec} containing the anticodons UUA and CUA can decode both UAA and UAG codons, but nucleotide C34 in tRNA$_{CUA}$ restricts wobble base pairing much more than U34 in tRNA$_{UUA}$ (Heider et al., 1992). The fact that U34 in tRNA$_{UUA}$ recognizes G in the third position of the codon suggests that wild-type tRNA^{Sec} could read the tryptophan codon UGG as well. Similar cases of "four-way wobble", when unmodified U34 base pairs with either of four ribonucleotides, are only known for mitochondrial tRNAs (Jukes, 1990).

Seryl-tRNA synthetase-specific identity elements within tRNA^{Sec}

tRNA^{Sec} is aminoacylated with serine; it would be expected therefore that the identity elements for SerRS in tRNA^{Sec} should be the same as in tRNA^{Ser}. However, there is little sequence homology between tRNA^{Sec} and the canonical serine isoacceptors (Baron et al., 1993). Thus, the identity elements in these tRNAs might involve: sequence-specific sites, conformational features, and/or different sites or regions in tRNA^{Sec} and tRNA^{Ser} for interaction with synthetase (Ohama et al., 1994).

Binding of cognate tRNA^{Ser} to SerRS involves the α-helical coiled-coil domain (helical arm) of the synthetase and the long variable arm of the tRNA. The helical arm crosses perpendicularly over the variable arm of the tRNA, making extensive contacts with the backbone between the second and sixth base pairs (Biou et al., 1994). However, no identity elements are found in the variable arm, which would thus appear just as a structural element providing binding energy for complex formation (Normanly et al., 1992). The interaction of SerRS with the variable arm of tRNA^{Ser} is important for the efficient and specific aminoacylation, as replacement of the long variable arm of *E. coli* tRNA^{Ser} by a short type 1 tRNA loop leads to a reduction for k_{cat}/K_m of aminoacylation by a factor of $3.5 \cdot 10^3$ (Sampson and Saks, 1993).

The junction between the variable arm and the coaxially stacked anticodon and D stems is looser in tRNA^{Sec} than in tRNA^{Ser}. This is due to different 26-44 pairs in the two tRNAs and to the lack of tertiary interactions between neighboring nucleotides from the variable arm and residues from the D loop in tRNA^{Sec} (Fig. 5).

As a consequence, the orientation of the variable region relative to the L-plane is different in tRNA^{Sec} and in tRNA^{Ser} (Baron et al., 1993). Several mutants were tested to identify the role of the variable arm of tRNA^{Sec} in the interaction with SerRS (Baron et al., 1990). The replacement of the variable arm with that of tRNA^{Ser} reduced the k_{cat}/K_m value for aminoacylation to about 20% of the wild-type value. Reduction by one base pair caused a suppression of UGA readthrough to about 30% of that observed with wild-type tRNA^{Sec}, whereas an increase by three base pairs had no effect at all. Since structure and orientation of the variable arm of tRNA^{Sec} differ from that of tRNA^{Ser}, it can be anticipated that charging of tRNA^{Sec} requires a conformational adaptation of the variable arm. The missing tertiary interaction between positions 15 and 48 could increase the flexibility of the variable arm relative to the rest of the molecule facilitating this adaptation (Baron et al., 1993). Another feature unique to the serine system which makes it suitable for Sec incorporation is the absence of recognition of the tRNA anticodon, a critical identity element in many other synthetase systems (Saks et al., 1994). Eight nucleotides conferring serine identity to tRNAs in *E. coli* are located at the end of the acceptor stem and in the second base pair of the D stem (Normanly et al., 1992). The six identity elements in the acceptor stem are conserved in tRNA^{Sec} and probably interact with SerRS, as their counterparts in tRNA^{Ser} (Baron et al., 1993). Deletion of the base pair A5a-U67a in the acceptor stem, which results in a canonical seven base pair configuration, improved the aminoacylation rate of tRNA^{Sec} by 2-3 fold (Baron and Bock, 1991).

Thus, an unusually long acceptor stem together with the absence of the C11-G24 identity pair in the tRNA^{Sec} (although it could be mimicked by the neighboring pair C10-G25), as well as the differences in the orientation of the variable arm relative to the body of the two tRNAs probably explain the 100-fold decrease in charging efficiency of tRNA^{Sec} as compared to tRNA^{Ser} (Baron and Bock, 1991). The aminoacylation of tRNA^{Sec} is not as efficient as that of tRNA^{Ser}, which correlates with the much higher demand for the elongator aa-tRNA during translation and the necessity to optimize the structure of tRNA^{Sec} so as to provide the highest specificity for the interaction with SelA and the SelB protein that carries the selenocysteinyl-tRNA^{Sec} to the ribosome.

28

SelB-specific identity elements within tRNA^{Sec}

The unique structural features which distinguish tRNA^{Sec} and all other elongator tRNAs in binding to different elongation factors are located in the acceptor stem and the junction of the D stem and the T stem (Hüttenhofer and Böck, 1998). In particular, tRNA^{Sec} possesses a 13 base pair-long acceptor arm formed of coaxially stacked acceptor and T stems, which is longer than in canonical tRNAs, where it is 12 base pairs long (7 and 5 base pairs). This structural feature is evolutionary conserved; e.g. in bacteria, the acceptor arm is formed by stacking of the 8 base pairs A stem and 5 base pairs T stem, whereas in archaea and eukarya the same length is achieved by stacking of the longer A stem (9 base pairs) and shorter T stem (4 base pairs) (Allmang and Krol, 2006) (Fig. 2).

Removal of the A5a-U67a base pair, which reduced the 8 base pair aminoacyl acceptor stem of tRNA^{Sec} to the canonical length of 7 base pairs, not only improved the aminoacylation rate, but also enabled the interaction with EF-Tu. At the same time, the recognition by SelB was completely abolished (Baron and Bock, 1991). However, the length alone is not sufficient for the recognition of tRNA^{Sec} by SerRS or EF-Tu, as indicated by experiments with minihelices representing amino acid acceptor arms of the canonical tRNAs. Minihelices containing either 12 or 13 base pairs were recognized with the same affinity by EF-Tu from *Thermus thermophilus* (Rudinger et al., 1994), which suggests that other features, for example the combinations of nucleotides unique to tRNA^{Sec}, can be involved in the discrimination against EF-Tu binding.

Mutational analysis of a minihelix derived from the amino acid acceptor arm of *E. coli* tRNA^{Sec} has shown that the presence of C7•G66, G49•U65, and C50•G64 at their 8th, 9th, and 10th positions, which is a unique combination of base pairs among all elongator *E. coli* tRNAs (Steinberg et al., 1993), are the antideterminants responsible for the rejection of the Asp-minihelix^{Sec} by prokaryotic EF-Tu (Rudinger et al., 1996) (Fig. 6). In fact, transplanting this set of nucleotides into a minihelix derived from tRNA^{Asp} abolished its recognition by EF-Tu. Given that the interactions of aa-tRNA with EF-Tu are restricted to the first 10 base pairs of the acceptor arm (Rudinger et al., 1994), it can be expected that this combination of base pairs can also act as an antideterminant in the complete tRNA. The antideterminant properties of the acceptor arm may be enhanced by the rest of the tRNA^{Sec} molecule, as mutations in the D and the variable arm permit the translation of UGA codons,

without a SECIS element (Li and Yarus, 1992). The nature of the nucleotides in the antideterminant box is as important as their precise location in the acceptor stem, since the shift of these base pairs by one position towards the CCA-end renders the shifted variant a substrate of EF-Tu (Rudinger et al., 1996). Thereby, the effect of the A5a-U67a deletion, which resulted in a tRNA^{Sec} that was able to bind to EF-Tu (Baron and Bock, 1991), may be attributed to the shift of the antideterminant box by one base pair with respect to the 3'-end adenosine and not to the decrease in length of the acceptor arm of tRNA^{Sec} (Rudinger et al., 1996).
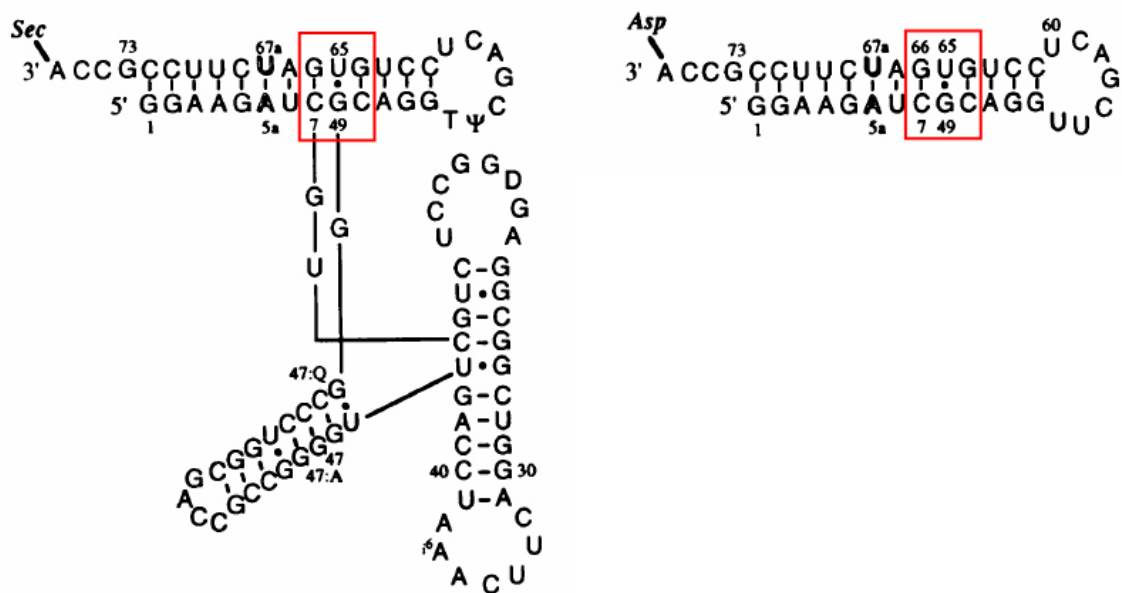

Fig. 6. Structures of *E. coli* tRNA^{Sec} and minihelix^{Sec}, which can be charged with Asp. The antideterminant box that prevents recognition by EF-Tu is indicated in red.

Additional support for the idea that one of the major determinants for tRNA^{Sec} recognition by SelB is the junction region of the T and acceptor stems comes from modeling of the interaction between tRNA^{Sec} and SelB based on the crystal structure of SelB from an archaeon *Methanococcus maripaludis* (Leibundgut et al., 2005) (Fig. 7). A loop between β25 and β26 strands in domain III of SelB (Leu361-Asp-Leu-Pro-Pro-Thr-Thr-Leu368) was found to be considerably longer than its analog in EF-Tu, where it mediates an important unspecific contact with the backbone of the acceptor arm of tRNA (Nissen et al., 1999). The extended loop in SelB is strictly conserved among archaea and is also present in eukaryotes and eubacteria; it may contact the

elbow region of tRNA, presumably at the last two base pairs of the acceptor stem and the first three base pairs of the T stem (Leibundgut et al., 2005).
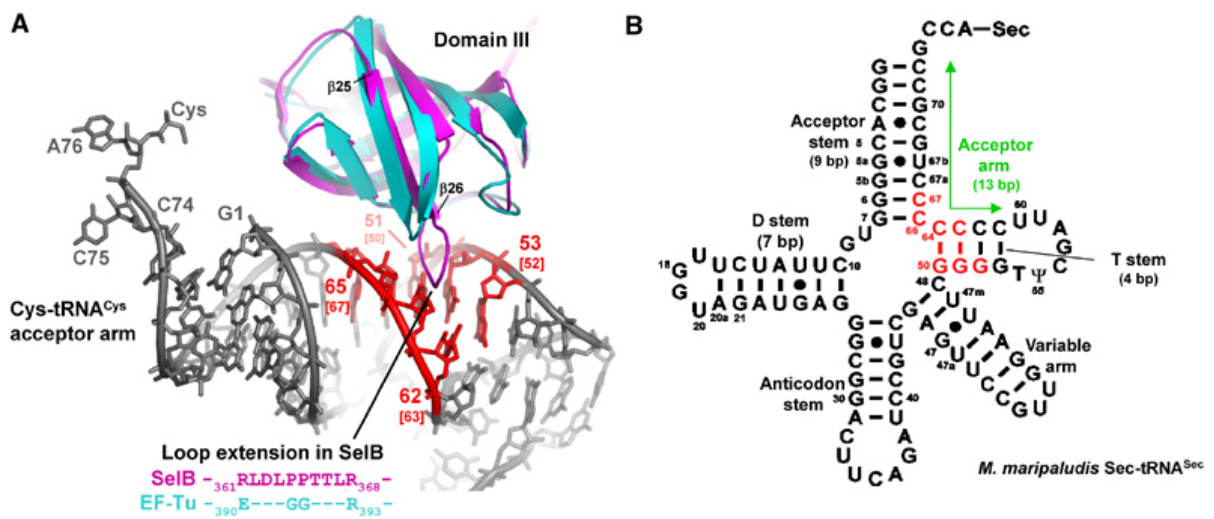

Fig. 7. Superposition of SelB domain III with the corresponding EF-Tu domain which is involved in the tRNA backbone contact. (A) SelB (magenta) contains a loop that is considerably extended in comparison to EF-Tu (cyan), where this region is involved in tRNA (grey) binding. Contacts between SelB and the modelled tRNA[Cys] are colored in red. The base-pair numbering is according to tRNA[Cys]. In addition, the corresponding bases from *M. maripaludis* tRNA[Sec] are shown in brackets. (B) Potential contact sites of SelB with tRNA[Sec] are shown in the secondary structure diagram of *M. maripaludis* Sec-tRNA[Sec] and are colored red. The contact area is derived from the tRNA[Cys]:SelB model (Leibundgut et al., 2005).

SelB - a protein with multiple ligand binding sites

The delivery of elongator aa-tRNAs to the ribosome is carried out by EF-Tu·GTP. However, the affinity of Sec-tRNA[Sec] to EF-Tu is about 100-fold lower than that of other elongator aa-tRNAs, which – given the large excess of canonical aa-tRNA over Sec-tRNA[Sec] in the cell – would preclude efficient binding of Sec-tRNA[Sec] to EF-Tu (Forster et al., 1990). Instead, Sec-tRNA[Sec] requires a specialized elongation factor SelB (Forchhammer et al., 1989).

SelB, with a molecular mass of about 69 kD, consists of four domains and shares homology with EF-Tu within part of the structure (Fig. 8). The crystal structure of SelB from the archaeon *M. maripaludis* (Leibundgut et al., 2005) and the structural model of *E. coli* SelB based on the sequence homology modeling between SelB and EF-Tu (Hilgenfeld et al., 1996) revealed that the N-terminal part of SelB folds into

three domains which presumably have the same functions as in EF-Tu, i.e. bind guanosine nucleotides and Sec-tRNA[Sec] (Hüttenhofer and Böck, 1998). The carboxy-terminal domain IV of SelB, which is not present in EF-Tu, plays a role in the interaction of the enzyme with the mRNA stem-loop structure (SECIS) present immediately downstream of all bacterial Sec-encoding UGA codons (Huttenhofer et al., 1996a; Kromayer et al., 1996).
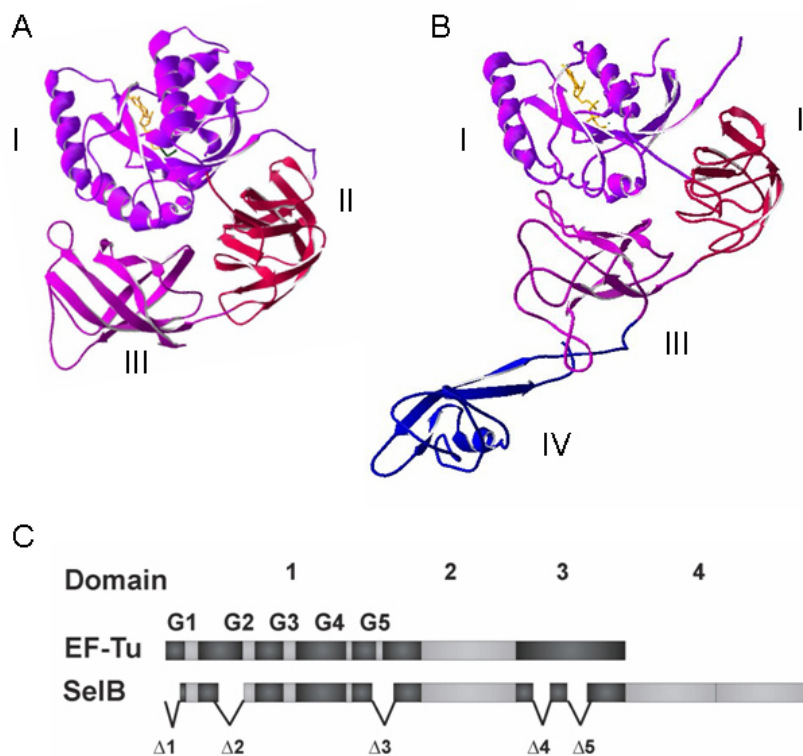

Fig. 8. Comparison of EF-Tu and SelB structures. (A) Structure of EF-Tu·GDPNP from *Thermus aquaticus* (Kjeldgaard et al., 1993). (B) Structure of SelB·GDP from *M. maripaludis* (Leibundgut et al., 2005). Individual domains are denoted I, II, III, and IV. The guanine nucleotide (yellow) is bound to domain I, which carries the GTPase activity. (C) Domain structure of the bacterial SelB in comparison to the three domains of EF-Tu. The G motifs involved in binding of the guanine nucleotides are indicated by G1 to G5. Deletions within the SelB sequence relative to the EF-Tu primary structure are indicated.

Interaction with guanine nucleotides

SelB belongs to the GTPase superfamily of proteins and thus its guanine nucleotide-binding domain comprises many structural and mechanistic features characteristic for e.g. small regulatory GTPases (such as the Ras family) and the α-subunits of heterotrimeric G proteins (Thanbichler and Bock, 2001). In spite of the

same overall fold of the nucleotide-binding domains of SelB and EF-Tu, several deletions were found in SelB (Hilgenfeld et al., 1996) (Fig. 8C). The absence of 11 amino-terminal residues most probably does not influence the structural integrity of the domain, but might destabilize the interaction of domains I and II. Another deletion affects the part of the so-called "effector region", which in EF-Tu forms the entrance of the tRNA-binding cleft. This suggests that the amino acid binding pocket may be more open in SelB, as compared to EF-Tu. EF-Tu requires a guanine nucleotide exchange factor, EF-Ts, to reduce its affinity for guanine nucleotides and accelerate the release of GDP (Gromadski et al., 2002). The crystal structure of EF-Tu in complex with EF-Ts revealed contact sites in domains I and III (Kawashima et al., 1996; Wang et al., 1997). Only a few of these residues in domain I are present in *E. coli* SelB, whereas the contact residues in domain III are absent (Hilgenfeld et al., 1996). This sequence peculiarity supports the notion that SelB does not require a GEF for its activation. The affinity of SelB binding to GTP is about 20-fold higher than to GDP and the rate of spontaneous GDP dissociation from SelB is on the same order of magnitude as the EF-Ts-catalyzed dissociation of GDP from EF-Tu (Forchhammer et al., 1989; Gromadski et al., 2002; Thanbichler et al., 2000), which would allow the spontaneous exchange of GDP by GTP. This behavior is somewhat similar to the situation seen for translational factors IF2 and EF-G which also deviate from typical G proteins by being independent of a GEF activity (Rodnina et al., 2000; Wilden et al., 2006).

The crystal structure of SelB from *M. maripaludis* reveals that the protein adopts a "molecular chalice" arrangement (Leibundgut et al., 2005). The first three domains form the cup of the chalice, whereas its base is formed by domain IV, which is linked to the cup via two long antiparallel β strands. The comparison of the structures of SelB·GDP, SelB·GppNHp, and nucleotide-free SelB revealed that SelB domains II/III retain their GTP-like orientation relative to domain I upon nucleotide exchange and conformational changes are restricted to the switch 2 region in domain I. This is surprising because in EF-Tu the shift of the switch 2 region leads to a large movement of domains II/III relative to the G domain (Abel et al., 1996; Berchtold et al., 1993; Kjeldgaard et al., 1993; Polekhina et al., 1996). Although the GTP-like domain arrangement of SelB is a striking feature, it is not an exception among translation factors. IF2γ, a close structural homologue of SelB for domains I-III, also adopts a GTP-like overall domain arrangement in the apo- and GDP-bound form

(Roll-Mecak et al., 2004; Schmitt et al., 2002). In addition, a GTP-like conformation of domain II relative to domain I has been observed for EF-G (AEvarsson et al., 1994; Czworkowski et al., 1994; Hansson et al., 2005) and IF2/eIF5B (Roll-Mecak et al., 2000). This implicates that the GTP-like domain orientation in SelB is not induced due to crystal packing and reflects the fact that the coupling of the nucleotide exchange with switch 2 and domain II/III movements differs from that in EF-Tu (Leibundgut et al., 2005).

Despite the similarities in the conformations of archaeal SelB in the GTP- and GDP-bound forms, the ribosome is capable of discriminating between SelB·GTP and SelB·GDP. Furthermore, GTP hydrolysis by SelB is required for factor's function on the ribosome as Sec insertion into peptides is strongly impaired or abolished when GTP is replased with GDP or GDPNP (Fischer et al., 2007) (Paper 2). The GTPase activation mechanism of SelB is not known. The low intrinsic GTPase activity of the binary complex SelB·GTP was stimulated very little on either unprogrammed ribosomes or ribosomes containing an mRNA hairpin which promotes Sec incorporation (Huttenhofer and Bock, 1998). Approximately the same small GTPase acceleration upon addition of vacant ribosomes was found earlier for EF-Tu (Rodnina et al., 1996). This fact together with the similarity of the G domains of two proteins (Hilgenfeld et al., 1996) suggests that the mechanism of GTP hydrolysis by SelB is similar to that proposed for EF-Tu (Berchtold et al., 1993; Daviter et al., 2003), and that the correct codon-anticodon interaction is required for the acceleration of GTP hydrolysis (Pape et al., 1998; Rodnina et al., 1995), as described above in detail for EF-Tu.

Interaction with selenocysteyl-tRNA^{Sec}

As described above, the unusual structure of Sec-tRNA^{Sec} enables its interaction with SelB. Apart from the structure of the tRNA, the nature of the aminoacyl residue plays an important role. SelB in the active GTP-bound form efficiently interacts with tRNA^{Sec} when it carries Sec at its 3' end, whereas the affinity for seryl-tRNA^{Sec} and deacylated tRNA^{Sec} is six orders of magnitude lower (Paper 3). This discrimination is crucial, because when the Sec residue in the active site of FDH$_H$ is substituted by serine, the activity of the enzyme is lost (Axley et al., 1991).
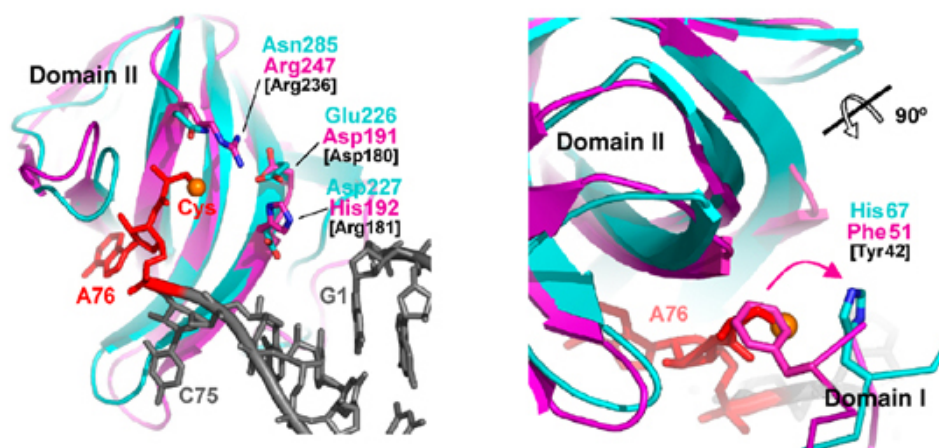
Fig. 9. Aminoacyl-binding pocket of SelB and superposition with the corresponding EF-Tu·GDPNP·Cys-tRNA^Cys region. *M. maripaludis* SelB is shown in magenta, *T. aquaticus* EF-Tu in cyan, the tRNA in grey and its terminal 3'Cys-A76 in red. Amino acids of *E. coli* SelB are labeled in black. As a reference, the sulfur atom of the cysteyl moiety is displayed as an orange sphere. In SelB, Phe51 from domain I protrudes into the aminoacyl-binding pocket, thereby occupying the position of the modeled cysteyl side chain (Leibundgut et al., 2005).

The binding site for the CCA-Phe end on EF-Tu is formed by the cleft between domains I and II and is lined up by the side chains of six amino acid residues (Berchtold et al., 1993). Two of them are conserved among EF-Tu and SelB (Phe229 and Thr239 in EF-Tu, Phe183 and Thr193 in SelB). However, the main part of the aminoacyl-binding pocket from *E. coli* SelB is formed by residues Asp180, Arg181, and Arg236, which are unique to SelB (Hilgenfeld et al., 1996) (Fig. 9). Asp180 and Arg236 are conserved among SelB molecules from all kingdoms, whereas Arg181 is present in bacterial SelBs and is substituted by His in archaeal and eukaryotic SelBs (His192 in *M. maripaludis* (Leibundgut et al., 2005)). Residues Arg181 and Arg236 introduce two positive charges into the aminoacyl-binding pocket and either of them would have the capacity to interact with the negatively charged selenol group. However, it is also possible that both residues together are involved in complexing and stabilizing the reactive Se^- ion. The importance of the above-listed residues for Sec binding was corroborated by mutational analysis which revealed that the presence of at least one positive charge in the aminoacyl-binding pocket of SelB is required for function. Removal of both positive charges, however, does not confer the capacity to accept Ser-tRNA^Sec as a ligand suggesting that recognition may also include structural changes in tRNA or other regions of SelB upon binding of the selenol group (Leibundgut et al., 2005). The determination of the number of ionic

35

interactions involved in SelB-tRNA^{Sec} interaction suggests that binding of SelB·GTP to Sec-tRNA^{Sec} results in the net formation of four ion pairs, whereas binding to Ser-tRNA^{Sec} or deacylated tRNA^{Sec} in only one additional ion pair (Paper 3).

Another important amino acid residue in SelB is Tyr42. It is located in domain I and, in the absence of Sec-tRNA^{Sec}, reaches the aminoacyl-binding pocket of domain II, which might cause a steric clash with the aminoacyl moiety modeled into the binding pocket (Leibundgut et al., 2005). The inherent flexibility of Tyr42 suggests that this hydrophobic residue would have to move out of the pocket when Sec binds and could serve as a lid to protect the highly reactive Se from oxidation. This is different from EF-Tu, where the corresponding His67 residue does not change position upon tRNA binding (Berchtold et al., 1993; Kjeldgaard et al., 1993; Nissen et al., 1999).

Interaction with the SECIS element

SelB differs from EF-Tu in a C-terminal extension of 272 amino acids (domain IV, SelB-C), which does not show any homology to other known proteins and is only slightly conserved among different eubacterial SelB variants (Hilgenfeld et al., 1996). The crystal structure of SelB-C from *M. thermoacetica* revealed that it consists of four winged-helix (WH) domains arranged in tandem (Selmer and Su, 2002). The WH motifs were originally found in many DNA-binding proteins (Clark et al., 1993; Gajiwala and Burley, 2000) and have recently been discovered in RNA-binding proteins including the La protein (Alfano et al., 2004; Dong et al., 2004), eukaryotic initiation factor 3 (eIF3k) (Wei et al., 2004), and proteins involved in RNA metabolism (Savchenko et al., 2005). The four tandem WH motifs of SelB-C create an elongated L-shaped extension. Each arm of the L consists of two globular WH domains. The domains are arranged in a consecutive manner, such that domains WH1/WH2 and domains WH3/WH4 have approximately the same orientation. Although the domains are remarkably similar, consisting of three helices flanked by a three-stranded antiparallel β-sheet, the sequence homology between the domains is low (Selmer and Su, 2002). The low sequence conservation between SelB-C from different bacteria may reflect the same kind of divergence as the low sequence similarity between the four domains suggesting that this is a fold where large sequence diversity can be tolerated. Despite of the significant sequence variety of SelB-C, two

regions containing conserved exposed amino acid residues were identified (Selmer and Su, 2002). The most invariable part among all bacterial SelB-C is domain WH4, where about half of the residues are conserved. Another constant area is a small charged patch next to a small hydrophobic area in the WH2 domain.

Footprinting analysis of the SelB-mRNA complex indicated that bases G23 and U24 in the apical loop in the mRNA hairpin, as well as residue U17 located in a bulge 5' to the loop, are directly involved in binding to SelB (Huttenhofer et al., 1996b) (Fig. 10A, B). The biochemical data were supported by crystal structures of protein-RNA complexes from *M. thermoacetica* and *E. coli* (Soler et al., 2007; Yoshizawa et al., 2005) (Fig. 10C, D). The two terminal tandem WH modules establish specific interactions with the SECIS hairpin. The WH4 module binds the backbone and the loop of the hairpin (Soler et al., 2007). The SECIS element binds to the basic surface of SelB which is complementary to the shape of the RNA and consists of five highly conserved residues that are located on one side of the WH4 domain. Sequence-specific contacts are established with two conserved nucleotides (G23 and U24) at the tip of the RNA hairpin. Upon complex formation, the structure of the WH3/4 domains is not substantially affected. In contrast, the SECIS RNA appears to undergo considerable structural rearrangements (Yoshizawa et al., 2005). In the complex, the RNA hairpin adopts a highly compact structure with only two unstacked nucleotides in the loop, G23 and U26. Nucleotides G22 and C25 form a Watson-Crick base pair which is not found in the free form of the SECIS element (Fourmy et al., 2002). The turn in the sugar phosphate backbone is thus achieved with only two nucleotides and nonstandard values for torsion angles in the loop. The bulged U17 is present in most of the known SECIS RNA sequences. Substitution of U17 with C completely abolishes selenocystein incorporation *in vivo* (Liu et al., 1998), indicating the importance of U at this position. The absence of this nucleotide in *M. thermoacetica* SECIS element gives an opportunity to compare the mode of SelB interaction with RNA structures with and without the conserved base (Fig. 10E). The bulged U17 is inserted between aromatic and aliphatic side chains of conserved amino acids, which form a binding pocket in *E. coli* WH3 that discriminates a uracil from other bases (Soler et al., 2007) (Fig. 10D). In the co-crystal structure of WH3/4-SECIS from *M. thermoacetica* the third WH motif is too distant to establish any contacts with RNA, lacking the bulged U17 (Yoshizawa et al., 2005) (Fig. 10C). The additional contacts between *E. coli* WH3/4 and the SECIS hairpin involve nucleotide
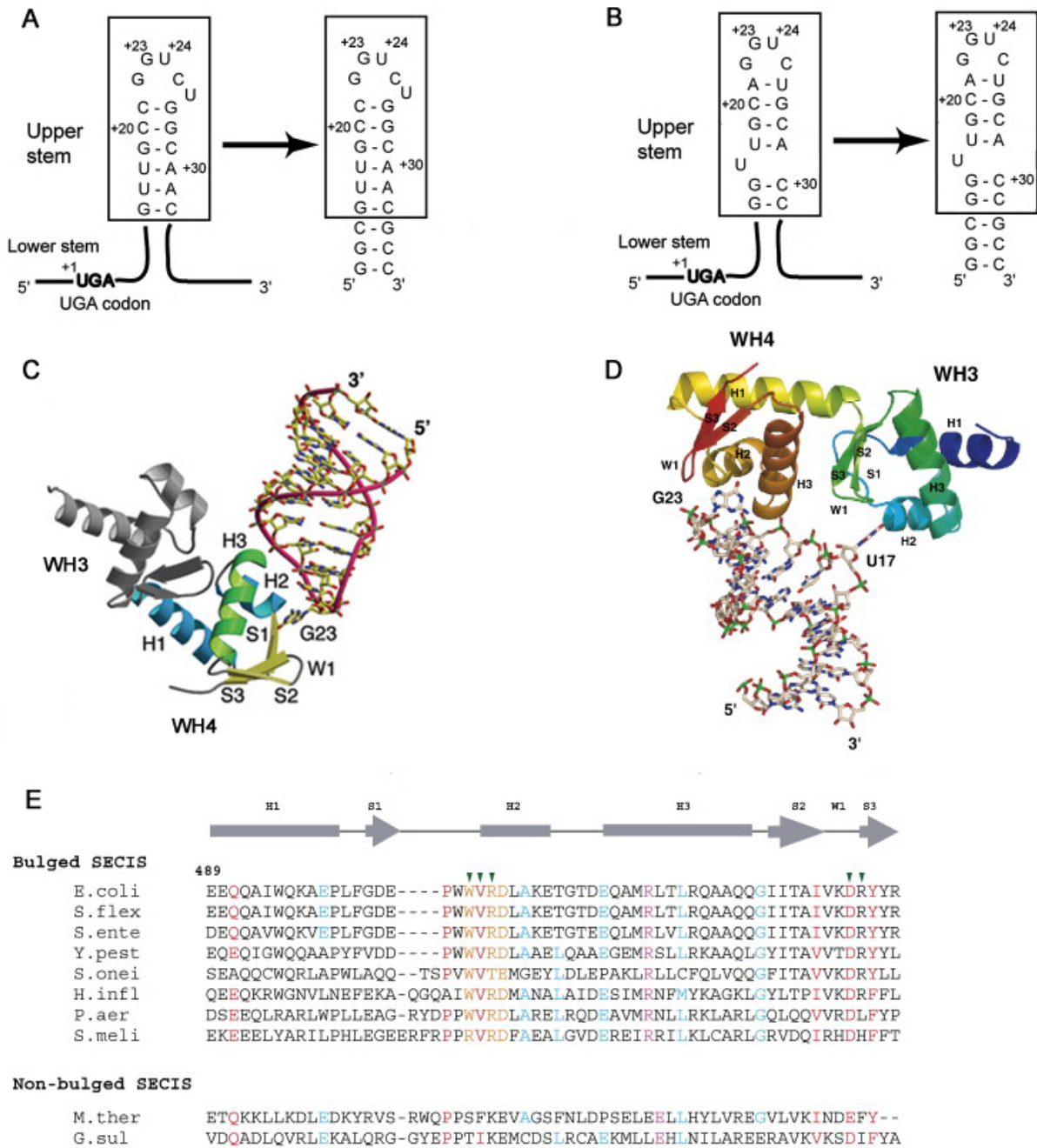
U17 which is extruded from the double helix. The complex has an overall V-like shape with a 70° angle between the RNA helix and the WH3/4 domain in both crystal structures. This shape may be essential for the interaction of SelB-tRNA^{Sec} with the ribosome. Although the contact of the WH3 module with a conserved bulged uracil does not alter the overall conformation of the complex, the interaction is crucial for high affinity binding of mRNA to *E. coli* SelB (Huttenhofer et al., 1996b; Liu et al., 1998). The surface of interaction between the tip of the RNA hairpin and the C-

Fig. 10. Structure of the WH3/4-SECIS RNA complex. SECIS elements from the *M. thermoacetica* fdhA gene (A) and from the *E. coli* fdhF gene (B). The minimal RNA fragment required for SelB binding is boxed. RNA constructs used for the study are indicated by the arrows. View of the WH3/4-SECIS RNA complex from *M. thermoacetica* (C) (Yoshizawa et al., 2005) and *E. coli* (D) (Soler et al., 2007). The bulged U17 is essential for the binding of SelB from *E. coli*. The RNA is shown in stick representation, the protein is shown as a ribbon model. (E) Structure-based sequence alignment of bacterial SelB WH3 domains. Residues are shown in red if they are identical or chemically similar in other sequences that are not displayed. The motif WVRD which is important for U17 recognition, is shown in orange. RNA-interacting residues are indicated with filled green arrows. Residues with a lower degree of conservation are in blue. Conserved residues from the molecular switch are in magenta. Secondary structural elements observed in the crystal structure of the WH3/4–SECIS RNA complex are shown above the alignment. The numbering for the *E. coli* sequence is indicated. The sequences are: *M. thermoacetica* (M. th), *Geobacter sulfurreducens* (G. sul), *E. coli* (E. coli), *Shigella flexneri* (S. flex), *Salmonella enterica* (S. ente), *Yersinia pestis* (Y. pest), *H. influenzae* (H. inf), *Pseudomonas aeruginosa* (P. aer), *Shewanella oneidensis* (S. onei), *Sinorhizobium meliloti* (S. meli) (Soler et al., 2007).

terminal WH motif, which is small in SelB from *M. thermoacetica* (Yoshizawa et al., 2005), is extended in the *E. coli* SelB-RNA complex because of the coupling between the two C-terminal WH modules (Soler et al., 2007). This observation may explain the higher binding affinity of mRNA for SelB from *E. coli* compared to that from *M. thermoacetica*. In fact, the K_d value for *E. coli* SelB binding to the SECIS hairpin is about 1 nM (Thanbichler et al., 2000), three orders of magnitude lower than of *M. thermoacetica* SelB (Yoshizawa et al., 2005). The interaction of the RNA with the SelB-C-domain, where the structure lacks any contacts with the major or minor grooves of the RNA, represents a new type of interaction between WH motifs and nucleic acids. Instead, the specificity of binding between SelB-C and SECIS is provided by the recognition of the hairpin backbone and nucleotides extruded from the helix.

Communication between the tRNA- and mRNA-binding sites of SelB

Previous reports suggested a possible interdomain communication or conformational changes in SelB. SelB-C binds SECIS about 10 times more tightly than the full-length protein. The addition of Sec-tRNA[Sec] increases the affinity of the full-length SelB for the SECIS element to the same level as for SelB-C (Thanbichler et al., 2000). Similarly to EF-Tu, SelB has a low intrinsic GTPase activity that is

stimulated upon addition of ribosomes even when tRNA is absent (Huttenhofer and Bock, 1998; Parmeggiani and Sander, 1981). The addition of SECIS stimulates GTP hydrolysis by SelB further (Huttenhofer and Bock, 1998), suggesting that mRNA binding to SelB leads to a more active GTPase or a more favorable interaction with the ribosome which, in turn, activates the GTPase. Thus, the binding of Sec-tRNA[Sec] to the N-terminal part and SECIS to the C-terminal part of SelB affect each other. One possibility is that the two parts of the protein interfere with each other's function in the absence of RNA. The other possibility is that RNA binding induces conformational changes in one part that contribute favorably to the activity of the other part in terms of mRNA binding or GTP hydrolysis.

Novel RNA sequences that could bind to SelB were identified by *in vitro* selection (Klug et al., 1997). However, although several of them bound SelB with the similar affinity and - as judged by chemical and enzymatic probing data - in a similar way as the natural SECIS, the artificial RNA fragments did not promote Sec incorporation. It seems that a specific SelB-mRNA interaction is needed to trigger a conformational change necessary to achieve UGA readthrough, or to position SelB in a proper way for subsequent interaction with the ribosome. In agreement with this notion, it was shown that the overproduction of SelB and other components of the Sec insertion machinery fails to induce any detectable Sec incorporation in the absence of the proper RNA hairpin structure (Suppmann et al., 1999). Remarkably, the SECIS element has been shown not only to support Sec incorporation, but also to prevent readthrough by unspecific UGA suppression in the absence of selenium (Liu et al., 1999; Sandman and Noren, 2000). Thus, the function of the mRNA hairpin is more than just increasing the local concentration of SelB in the proximity of the stop codon; rather, some kind of conformational change seems to be induced by the SelB-SECIS interaction (Selmer and Su, 2002).

The comparison of the SelB-C structures in the complex with SECIS (Ose et al., 2007; Soler et al., 2007) and in the absence of RNA (Selmer and Su, 2002) suggests a conformational change of the protein upon binding the SECIS which is possibly due to the small contact area between domains WH2 and WH3 (Kromayer et al., 1999; Selmer and Su, 2002). The two proteins adopt different conformations primarily as a result of rigid-body motions of the WH1/2 and WH3/4 modules within the protein. The hinge movement is accompanied by the disruption of the Arg524 - Glu437 salt bridge in *E. coli* (Glu552-Arg461 in *M. thermoacetica*) (Fig. 11A, B). The
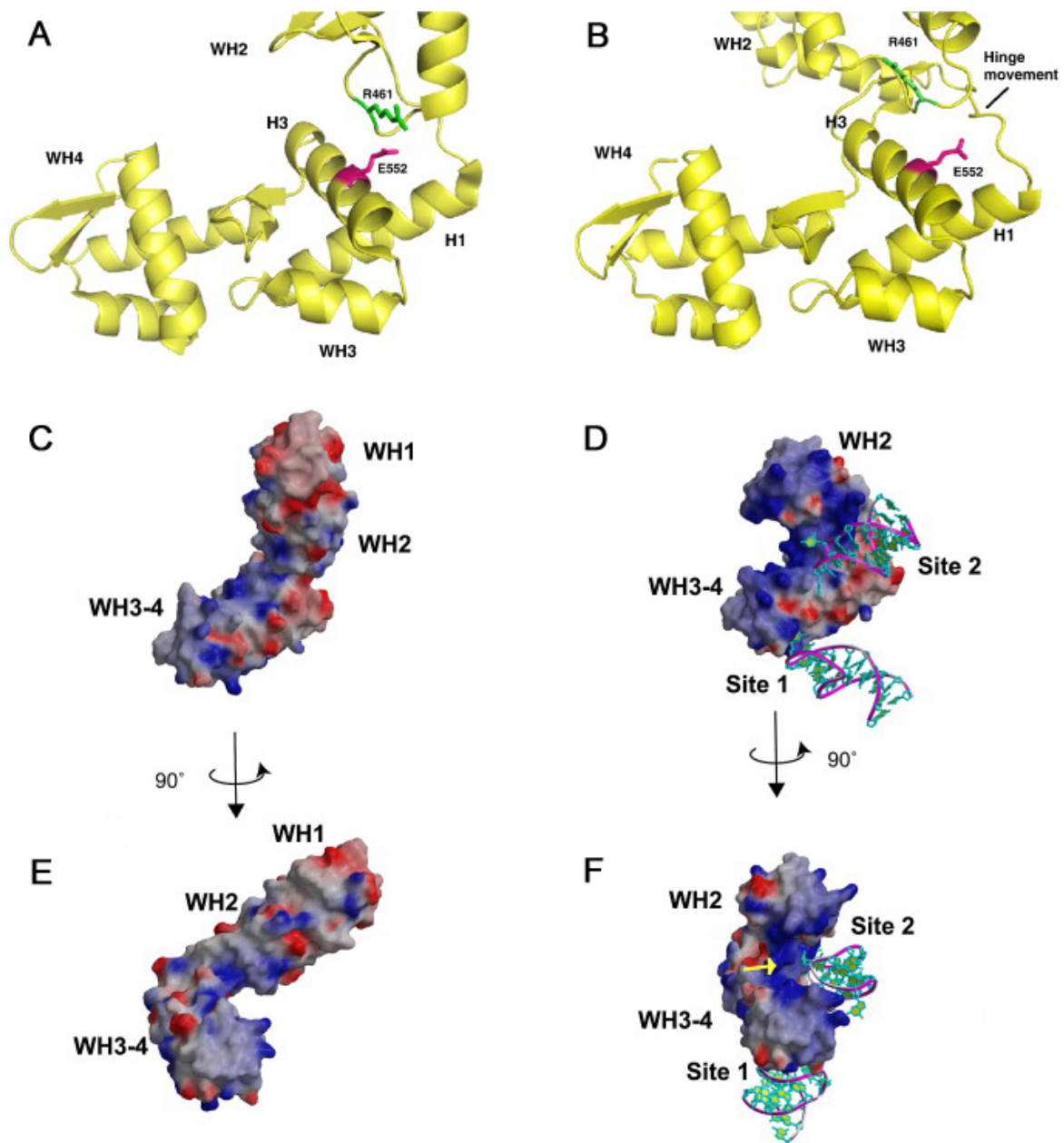
Fig. 11. Structural changes in the domain orientation of SelB-C upon SECIS binding. (A) The pivotal salt bridge in free *M. thermoacetica* SelB-C. E552 in WH3 is in magenta and R461 in WH2 green. (B) In the *M. thermoacetica* SelB-C SECIS-complexed form, the salt bridge is disrupted (Soler et al., 2007). (C–F) Electrostatic potential surface representation of (C and E) free and (D and F) SECIS-complexed SelB-C. (C and D, E and F) The WH3 and WH4 domains are oriented similarly. The yellow arrow (F) indicates the positively charged area consisting of Arg466, Arg485, Arg574, and Arg581 (Ose et al., 2007).

striking feature is that the WH1/2 module is rotated around the hinge region by 60˚ upon disruption of the conserved salt bridge. The importance of the salt bridge can

explain the unexpected results of an *in vivo* genetic study (Kromayer et al., 1999) which suggested that the Glu437Lys mutation in SelB located away from the mRNA binding site rescues the detrimental effect of mutations in the SECIS. As a result of the large conformational rearrangement in the protein, the surface electrostatic potential of the molecule is changed (Ose et al., 2007) (Fig. 11C-F). Basic residues form the continuous π-cation interaction on one side of the WH2/3 interdomain region. This well-ordered positively charged area is suitable for binding an RNA molecule other than the SECIS element. The negatively charged RNA molecule may allow SelB to expose its positively charged area, further resulting in an increase of the contact area between the WH2 and WH3 domains. In contrast, the positively charged area can provide charge repulsion in free SelB-C; hence the elongated shape of SelB-C in the absence of the SECIS. The area which becomes exposed upon the conformational rearrangement of SelB-C does not form contacts with RNA bases, but rather with the phosphate backbone. This recognition mode ensures sequence-independent RNA interactions, which could be beneficial for the transient recognition of stem regions of any RNA molecule. There are two types of RNA molecules involved in Sec incorporation process: tRNA^{Sec} and rRNA. Either or both of these RNA might consecutively interact with the WH2/3 domain of SelB.

mRNA structures directing selenocysteine incorporaton

The specific incorporation of Sec into proteins in bacteria is directed by an in-frame UGA codon that is immediately followed by a SECIS element (Berg et al., 1991; Zinoni et al., 1990). In fact, a new selenoprotein could be designed by introducing the UGA codon followed by SECIS into the *fdhA* gene from *Methanobacterium fonnicicum*, which codes for Cys-containing FDH$_H$ (Heider and Bock, 1992; Zinoni et al., 1987). The elements required for SECIS function include both the sequence of the loop and the stem region as well as the correct folding of the RNA hairpin structure (Heider et al., 1992). As Sec incorporation does not involve frameshifting (Heider et al., 1992), the SECIS element ensures that the UGA codon is recognized as a sense codon rather than serving as termination signal.

Studies of the solution structure of the hairpins in mRNAs coding for *E. coli* FDH$_H$ (*fdhF*) and FDH$_N$ (*fdnG*) revealed the presence of two separate structural domains that possibly exert different functions: the UGA region and the loop structure

of the mRNA hairpin (Huttenhofer et al., 1996b). The UGA codon, previously predicted to be single-stranded, appeared to be a part of an extended helix within the mRNA hairpin in which U and G of the UGA codon are base paired, whereas the A is located in a bulge (Huttenhofer et al., 1996b). Evidence for an *in vivo* function of the extended stem structure comes from the in-frame deletion analysis of mRNA (Zinoni et al., 1990), where deletions up to position -7 had no effect on UGA readthrough, whereas further deletion of sequences up to position -1 (preceding the UGA codon) reduced UGA readthrough to about 25%. Similar results were obtained for sequences 3' of the hairpin which were previously thought to be single-stranded. The possible function of the extended stem could be to facilitate mRNA hairpin folding by enhancing the stability of the hairpin. Interestingly, the UGAC sequence present in both *fdhF* and *fdnG* mRNA hairpins was shown to be the least efficient in termination (Poole et al., 1995). Therefore, the entrapment of the UGA codon in the secondary structure, together with the least efficient termination signal – UGAC – might allow the Sec incorporation system to compete effectively with termination at these UGA codons.

Sec incorporation into the *E. coli fdhF* gene product does not strictly require the presence of UGA and occurs also when the UGA codon is mutated to a Cys codon (UGC or UGU), which requires wobble base pairing with the anticodon of Sec-tRNA[Sec]. When the second position was changed, resulting in a serine codon (UCA), Sec incorporation was abolished but could be rescued by a compensatory mutation in the anticodon of tRNA[Sec] (Baron et al., 1990). Notably, Sec-tRNA[Sec] with an altered anticodon did not read the Cys or serine codons other than the one preceding the SECIS. Sec insertion can be directed also by other stop codons, UAA or UAG, when the complementary changes are introduced into the anticodon of tRNA[Sec] (Heider et al., 1992), suggesting that the SECIS element prevents all three termination codons from being efficient translational stop signals. Furthermore, the presence of SECIS led to a 6-fold increase in tryptophan insertion by the opal suppressor Su7-tRNA in response to UGA (Suppmann et al., 1999). These data underline the necessity of additional mRNA elements outside of the UGA codon that enable tRNA[Sec] to compete with RF2.

The apical loop of the SECIS is the second element that is crucial for Sec insertion (Huttenhofer et al., 1996b). The region has a well-defined structure with bases G23 and U24 exposed to the solvent on the deep groove side of the helix,

following a sharp turn after G22 (A22 in *fdnG* mRNA). The bulged residue U17 points in the same direction as do loop residues G23 and U24 and, at the same time, opens up the deep groove at the top of the hairpin helix. These residues, i.e. G23 and U24 in the loop and U17 in the bulge, are highly reactive in the free mRNA and become strongly protected by SelB. This may indicate that SelB preferentially recognizes distinct bases of the RNA hairpin that are exposed to SelB within the three-dimensional structure of the stem loop.

Extensive site-directed mutagenesis identified the bases in the loop and the adjacent stem that are crucial for Sec incorporation (Heider et al., 1992). Only a few of them are involved in SelB binding directly, whereas the others are presumably needed to maintain the tertiary structure of the loop. Both overall stem structure and length of the stem are essential to keep the loop region at the proper distance from the UGA codon. The deletion of three base pairs at the bottom of the stem results in a complete loss of readthrough activity. Surprisingly, readthrough was observed with a gene fusion containing a three base pair longer stem-loop structure, albeit the efficiency of readthrough was reduced to 50% in comparison with that promoted by the wild-type stem-loop (Heider et al., 1992). Moving the UGA codon six bases in the 5' direction resulted in an 80% decrease in efficiency and the UGA readthrough became independent of selenium (Chen et al., 1993). Thus, while a minimum distance between the UGA codon and the loop region seems to be absolutely required, the constraint on the maximum length is less stringent. If similar structures are in fact present in all bacterial mRNAs that contain a Sec codon, it seems likely that they also function by binding to an *E. coli* SelB homolog. Therefore, within the same organism, all mRNA hairpins that direct Sec incorporation should exhibit similar if not identical secondary and tertiary structures, despite differences in their sequence, as do *fdhF* and *fdnG* mRNA from *E. coli* (Huttenhofer et al., 1996b).

The mRNA hairpin which is believed to direct Sec incorporation into FDH$_H$ in *Enterobacter aerogenes* shows close resemblance to the *fdhF* and *fdnG* secondary structures from *E. coli*, especially within the upper part of the helix (Heider et al., 1991). The RNA hairpin 3' to a UGA codon in *Desulfomicrobium baculatum* in the mRNA coding for a [NiFeSe] hydrogenase-selenoprotein (Menon et al., 1987) also bears some resemblance in the upper part of the SECIS in *E. coli* and *E. aerogenes* (Menon et al., 1987). The conserved G and U bases are present within the loop region; however, a bulged C is found in the stem instead of a bulged U. The length of

the hairpin seems to be conserved in all hairpin structures known to date (Hüttenhofer and Böck, 1998). Although most of the bacterial organisms govern the Sec incorporation with the help of SECIS elements that are conserved by structure, there are some exceptions, such as *Clostridium sticklandii* (Garcia and Stadtman, 1992) or *E. acidaminophilum* (Gursinsky et al., 2000), in which no such structures can be formed within the reading frames of the mRNAs coding for selenoproteins.

Model of SelB action on the ribosome

The mechanism of SelB action on the ribosome is not known in detail. Based on kinetic and affinity measurements (Thanbichler et al., 2000), (Paper 3), it is likely that in the cell practically all SelB is present as a SelB·GTP·Sec-tRNA^{Sec} complex with the SECIS element. SelB is delivered to the ribosome by the movement of mRNA through the ribosome up to the point when the lower part of the SECIS is disrupted (Thanbichler and Bock, 2001). In the crystal structure of the 70S ribosome in complex with mRNA (Yusupova et al., 2001), approximately 12 nucleotides of the mRNA, from the decoding site to the entrance of the mRNA tunnel, are buried inside the ribosome. This is the exact length of the spacer between UGA codon and the 5' end of the minimal RNA fragment necessary to bind SelB (Liu et al., 1998). Thus, upon translation, the UGA codon is positioned in the decoding site, while the intact upper part of SECIS is bound to domain IV of SelB and may appear just at the mRNA entrance of the ribosome (Hüttenhofer and Böck, 1998).

The cryo-EM structure of the SelB·Sec-tRNA^{Sec}·ribosome shows that SelB brings Sec-tRNA^{Sec} to the ribosome in a manner similar to EF-Tu and canonical tRNAs (Paper 4) (Fig. 12A, B). SelB bridges the factor binding site on the 50S subunit and the mRNA entry tunnel on the 30S subunit. The main contacts of the EF-Tu-like domains I-III of SelB on the ribosome are the sarcin-ricin loop on the 50S subunit and helix 5 on the 30S subunit, and the interactions of Sec-tRNA^{Sec} with the ribosome closely resemble the contacts of canonical tRNAs in the EF-Tu complex (Stark et al., 2002; Valle et al., 2003). The sarcin-ricin loop is the only ribosomal element that contacts SelB at the nucleotide-binding pocket (Paper 4). The contact may play a role in GTP hydrolysis by SelB by stabilizing the switch regions of the G domain in the catalytically active conformation (Rodnina et al., 2005). The anticodon of Sec-tRNA^{Sec} can pair with the UGA codon in the A site, and the codon-anticodon

interaction is expected to activate GTP hydrolysis in SelB. The connection between the elbow region of Sec-tRNA^{Sec} and the L11-binding region of 23S rRNA observed in the cryo-EM structure may be important for transmitting the GTPase-activating signal from the codon-anticodon complex, positioning the tRNA relative to other elements of the ribosome, and guiding the tRNA towards the A site during accommodation (Paper 4).
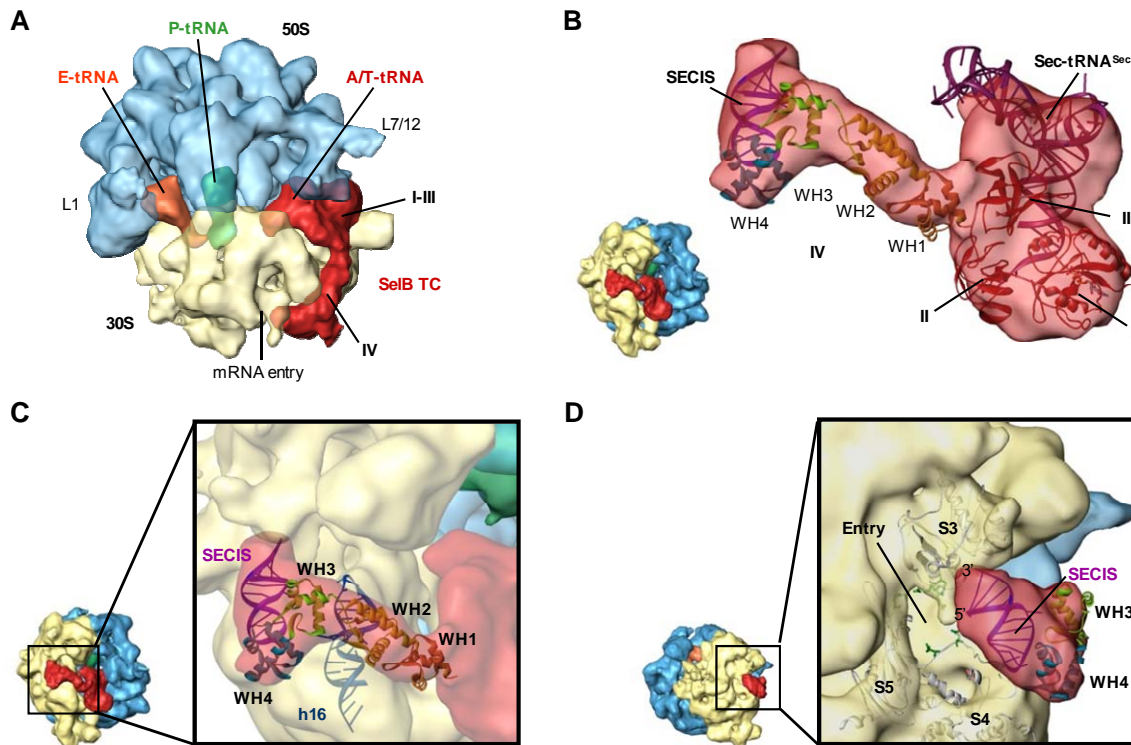

Fig. 12. Cryo-EM structure of the SelB·Sec-tRNA^{Sec}·ribosome complex. The ribosomal 50S subunit is depicted in semitransparent light-blue, the 30S ribosomal subunit in beige. Ligand densities entail SelB·Sec-tRNA^{Sec} (SelB TC, red), P-site tRNA (green) and E-site tRNA (orange). The difference density for the SECIS element is pink. (A) Overall structure. The domains of SelB (I to IV), the mRNA entry channel (mRNA entry), the L1 stalk (L1) and the L7/12 stalk (L7/12) are labeled. (B) Model of the SelB ternary complex with semitransparent EM density in red. WH1 to WH4 indicate the winged helix motifs of domain IV. (C) Interaction of SelB domain IV with helix 16 (h16) and the SECIS. (D) View onto the mRNA entry channel (Entry). Superposition of the SECIS as observed in a SECIS·WH3/4 crystal structure (Yoshizawa et al., 2005) places the SECIS next to the mRNA entry channel (Paper 4).

The role of the SECIS element in GTPase stimulation, be it a mere carrier of SelB to the ribosome or a regulatory factor for SelB function on the ribosome, is not clear. Taking together the size and shape of SelB-C (Selmer and Su, 2002), the

46

location of the mRNA entrance tunnel (Yusupova et al., 2001), and the position and orientation of the EF-Tu·Phe-tRNA[Phe] complex on the ribosome (Stark et al., 1997; Stark et al., 2002; Valle et al., 2002), domain IV of SelB has to span a distance of about 90 Å between the C terminus of domain III of the factor and the SECIS binding site, compared to about 75 Å measured at the diagonal of the L-shaped SelB-C structure (Selmer and Su, 2002). A notable feature of the SelB-C·SECIS complex isthe angle of 70º between the RNA helix and SelB-C (Ose et al., 2007; Soler et al., 2007; Yoshizawa et al., 2005), which seems essential for SelB·tRNA[Sec] interaction on the ribosome. This angle, together with the L-shape of SelB-C, allows the SelB-C·SECIS complex to wrap around the 30S subunit, covering the required distance (Fig. 12C, D). The recent crystal structure of SelB-C in complex with the SECIS element suggested that domain IV may undergo large interdomain conformational changes due to the highly flexible hinge region between WH2 and WH3 motifs and confer a positively charged area in SelB-C suitable for binding an RNA molecule other than the SECIS RNA (Ose et al., 2007) (Fig. 12D, F). Indeed, docking the homology model in the cryo-EM density places WH2 and WH3 motifs in close contact to helix 16 of 16S rRNA (Paper 4) (Fig. 12C). The functional significance of this interaction is not known. It is possible that binding of WH2/3 to 16S rRNA stabilizes the conformation of domain IV and thereby helps to position SelB at the factor binding site. On the other hand, interactions of WH2/3 with helix 16 may affect the relative mobility of the head and body of the 30S subunit, as helix 16 belongs to the elements involved in the open-to-close transition during decoding of sense codons (Ogle et al., 2002). A global conformational change of the 30S subunit is crucial for tRNA selection in the A site and for the GTPase activation of EF-Tu (Gromadski et al., 2006; Gromadski and Rodnina, 2004a, b; Ogle et al., 2001; Ogle et al., 2002). By analogy, the interaction of domain IV of SelB with helix 16 of 16S rRNA may be involved in signaling the recognition of the UGA codon by Sec-tRNA[Sec] and modulating the timing of GTP hydrolysis by SelB (Paper 4).

After GTP hydrolysis, SelB switches to the GDP form, Sec-tRNA[Sec] is rapidly released from the factor (Paper 3) and accommodates into the A site, and Sec is incorporated into the nascent peptide. SelB·GDP must dissociate from the ribosome and the SECIS element to allow for the translation of the downstream mRNA sequence (Thanbichler and Bock, 2001). However, given the high affinity of SelB·GDP to SECIS (Thanbichler et al., 2000), the mechanism of dissociation is not

easy to understand. The molecular details of SelB function on the ribosome are largely deduced by analogy with EF-Tu, which, however is not bound to any specific mRNA elements. Furthermore, given that SelB and EF-Tu have dramatically different nucleotide binding properties (Thanbichler et al., 2000) and there are important differences in the structures of the G domains of SelB and EF-Tu (Leibundgut et al., 2005), there may be differences in the way the two factors interact with the ribosome after GTP hydrolysis. Clarification of these issues will require further biochemical and kinetic work.

Evolution of selenocysteine insertion

The genetic code, formerly thought to be frozen, is now known to be in a state of evolution, and there are several examples of reassigning the meaning of codons. Thus, the AUA codon, which stands for isoleucine in most cells, encodes methionine in human mitochondria (Barrell et al., 1979). The stop codon UAA codes for glutamine in the green alga *Acetabularia*. Candida yeast use CUG (leucine) for serine. Other deviations from the universal code, all in nonplant mitochondria, are CUN (leucine) to code for threonine (in yeast), AAA (lysine) for asparagine (in platyhelminths and echinoderms), and UAA (stop) for tyrosine (in planaria) (Osawa et al., 1992).

UGA is a unique and the most fascinating codon within the genetic code because it can assume five meanings, more than any other code word in evolution. UGA can function as a termination codon (Nirenberg et al., 1966), a Sec codon (Bock et al., 1991), a Cys codon in *Euplotes octocarinatus* (Meyer et al., 1991) and *Euplotes crassus* (Turanov et al., 2009), a tryptophan codon in mitochondria and *Mycoplasma* (Osawa et al., 1992), and an inefficiently read tryptophan codon in *Bacillus subtilis* (Lovett et al., 1991) and *E. coli* (Weiner and Weber, 1973). As to mammals, the UGA codon in rabbit β-globin mRNA has been shown to serve as many as eight functions, including a stop signal, a suppressor codon that supports partial readthrough for Arg-, Cys-, Trp-, and Ser-tRNA, and a translation reading gap codon with the breach consisting of one, two, or three codons (Chittum et al., 1998). The finding that the other two stop codons, UAA or UAG, do not appear to serve as suppressor codons or promote translation reading gaps, suggests that these functions are associated solely with UGA. The variety of UGA functions implies that

this codon has been loosely programmed in evolution and therefore is the most likely code word to have evolved for the infrequently used amino acid selenocysteine (Hatfield and Gladyshev, 2002).

It should be noted that there are two contrasting proposals as to when living organisms acquired the ability to synthesize selenoproteins. One suggests that UGA was a component of the primordial genetic code and existed in the anaerobic world as a codon for Sec (Leinfelder et al., 1988). An argument in favour of this hypothesis is that UGA has been conserved as a codon for Sec in all three lines of descent, suggesting that it existed before bacteria, archaea, and eukarya separated. In archaic organisms that presumably lived in the ocean, Sec could have been chemically stable due to the absence of oxygen and may have been used in many enzymes. On the other hand, selenium is far less abundant in seawater than sulfur (Weast, 1964); therefore, the use of Sec may have been somewhat restricted by the rarity of selenium. The subsequent increase of oxygen in the atmosphere counter-selected against the use of Sec, because of its sensitivity to oxidation. However, certain anaerobic and well-protected organisms retained selenoproteins and the Sec insertion system. The presumed couterselection against Sec left UGA codons unused, resulting in the adaptation to utilize UGA as a termination signal. The original coding role could have only been maintained by masking it against recognition by release factors and by developing a special translation factor that guaranteed insertion at a specific site only and not at other UGA termination codons. Only when UGA became a stop codon would it have been necessary for SelB to appear, together with the mRNA hairpin structure recognized by it (Bock et al., 1991).

An alternative hypothesis suggests that Sec evolved at later stages of evolution, after the other 20 amino acids with their initially specified codons developed (Gladyshev and Kryukov, 2001). This proposal is consistent with the observation that many eukaryotic selenoproteins serving as antioxidant and redox proteins are employed by aerobic organisms to function in antioxidant systems, which was not required in the anaerobic world. The additional support for this viewpoint is that some enzymes containing Sec are found to function also if Sec is replaced by Cys, albeit with diminished efficiency (Zinoni et al., 1986). For example, the FDH of *E. coli* and *Methanobacterium formicicum* (Shuber et al., 1986) have very similar active sites, yet one (*E. coli*) functions with Sec and the other (*M. formicicum*) with Cys. The *E. coli* enzyme has four to five times higher specific activity than the *M.*

formicicum enzyme. This could indicate that Sec is a recent evolutionary improvement to catalysis and that the more primitive form of the enzymes used Cys. Such modifications have the appearance of sophisticated evolutionary innovation rather than the survival of primitive systems (Osawa et al., 1992). Despite of the above arguments, the late appearance of Sec is difficult to conceive, since the existence in all three lineages could only be explained by lateral gene transfer (Bock et al., 1991). This could have conceivably occurred in the case of genes homologous to *selA, selC and selD.* However, the horizontal transfer of *selB* would have to involve the co-transfer or co-evolution of the cognate mRNA hairpin structure. This is difficult to imagine since the Sec-containing enzymes catalyze very different reactions. Irrespective of when the incorporation of Sec into protein originated, this amino acid serves as an example of a unique modification that emerged for its specific use within the universal genetic code.

References

Abel, K., Yoder, M.D., Hilgenfeld, R., and Jurnak, F. (1996). An alpha to beta conformational switch in EF-Tu. Structure 4, 1153-1159.

Abrahamson, J.K., Laue, T.M., Miller, D.L., and Johnson, A.E. (1985). Direct determination of the association constant between elongation factor Tu·GTP and aminoacyl-tRNA using fluorescence. Biochemistry 24, 692-700.

AEvarsson, A., Brazhnikov, E., Garber, M., Zheltonosova, J., Chirgadze, Y., al-Karadaghi, S., Svensson, L.A., and Liljas, A. (1994). Three-dimensional structure of the ribosomal translocase: elongation factor G from Thermus thermophilus. EMBO J 13, 3669-3677.

Agirrezabala, X., Lei, J., Brunelle, J.L., Ortiz-Meoz, R.F., Green, R., and Frank, J. (2008). Visualization of the hybrid state of tRNA binding promoted by spontaneous ratcheting of the ribosome. Mol Cell 32, 190-197.

Agris, P.F. (2004). Decoding the genome: a modified view. Nucl Acids Res 32, 223-238.

Alfano, C., Sanfelice, D., Babon, J., Kelly, G., Jacks, A., Curry, S., and Conte, M.R. (2004). Structural analysis of cooperative RNA binding by the La motif and central RRM domain of human La protein. Nat Struct Mol Biol 11, 323-329.

Allen, G.S., Zavialov, A., Gursky, R., Ehrenberg, M., and Frank, J. (2005). The cryo-EM structure of a translation initiation complex from Escherichia coli. Cell 121, 703-712.

Allmang, C., and Krol, A. (2006). Selenoprotein synthesis: UGA does not end the story. Biochimie 88, 1561-1571.

Allmang, C., Wurth, L., and Krol, A. (2009). The selenium to selenoprotein pathway in eukaryotes: more molecular partners than anticipated. Biochim Biophys Acta.

Andreesen, J.R., Wagner, M., Sonntag, D., Kohlstock, M., Harms, C., Gursinsky, T., Jager, J., Parther, T., Kabisch, U., Grantzdorffer, A., et al. (1999). Various functions of selenols and thiols in anaerobic gram-positive, amino acids-utilizing bacteria. Biofactors 10, 263-270.

Asahara, H., and Uhlenbeck, O.C. (2002). The tRNA specificity of Thermus thermophilus EF-Tu. Proc Natl Acad Sci USA 99, 3499-3504.

Axley, M.J., Bock, A., and Stadtman, T.C. (1991). Catalytic properties of an Escherichia coli formate dehydrogenase mutant in which sulfur replaces selenium. Proc Natl Acad Sci USA 88, 8450-8454.

Baron, C., and Bock, A. (1991). The length of the aminoacyl-acceptor stem of the selenocysteine-specific tRNA(Sec) of Escherichia coli is the determinant for binding to elongation factors SELB or Tu. J Biol Chem 266, 20375-20379.

Baron, C., Heider, J., and Bock, A. (1990). Mutagenesis of selC, the gene for the selenocysteine-inserting tRNA-species in E. coli: effects on in vivo function. Nucl Acids Res 18, 6761-6766.

Baron, C., Westhof, E., Bock, A., and Giege, R. (1993). Solution structure of selenocysteine-inserting tRNA(Sec) from Escherichia coli. Comparison with canonical tRNA(Ser). J Mol Biol 231, 274-292.

Barrell, B.G., Bankier, A.T., and Drouin, J. (1979). A different genetic code in human mitochondria. Nature 282, 189-194.

Berchtold, H., Reshetnikova, L., Reiser, C.O., Schirmer, N.K., Sprinzl, M., and Hilgenfeld, R. (1993). Crystal structure of active elongation factor Tu reveals major domain rearrangements. Nature 365, 126-132.

Berg, B.L., Baron, C., and Stewart, V. (1991). Nitrate-inducible formate dehydrogenase in Escherichia coli K-12. II. Evidence that a mRNA stem-loop structure is essential for decoding opal (UGA) as selenocysteine. J Biol Chem 266, 22386-22391.

Biou, V., Yaremchuk, A., Tukalo, M., and Cusack, S. (1994). The 2.9 Å crystal structure of T. thermophilus seryl-tRNA synthetase complexed with tRNA(Ser). Science 263, 1404-1410.

Böck, A. (2001). Selenium metabolism in bacteria. In Selenium: its molecular biology and role in human health, D.L. Hatfield, ed. (Kluwer Academic Publishers, Norwell, Mass), pp. 7-22.

Bock, A., Forchhammer, K., Heider, J., and Baron, C. (1991). Selenoprotein synthesis: an expansion of the genetic code. Trends Biochem Sci 16, 463-467.
Bosl, M.R., Takaku, K., Oshima, M., Nishimura, S., and Taketo, M.M. (1997). Early embryonic lethality caused by targeted disruption of the mouse selenocysteine tRNA gene (Trsp). Proc Natl Acad Sci USA 94, 5531-5534.

Bouadloun, F., Srichaiyo, T., Isaksson, L.A., and Bjork, G.R. (1986). Influence of modification next to the anticodon in tRNA on codon context sensitivity of translational suppression and accuracy. J Bacteriol 166, 1022-1027.

Brigelius-Flohe, R. (1999). Tissue-specific functions of individual glutathione peroxidases. Free Radic Biol Med 27, 951-965.

Bult, C.J., White, O., Olsen, G.J., Zhou, L., Fleischmann, R.D., Sutton, G.G., Blake, J.A., FitzGerald, L.M., Clayton, R.A., Gocayne, J.D., et al. (1996). Complete genome sequence of the methanogenic archaeon, Methanococcus jannaschii. Science 273, 1058-1073.

Carlson, B.A., Martin-Romero, F.J., Kumaraswamy, E., Moustafa, M.E., Zhi, H., Hatfield, D.L., and Lee, B.J. (2001). Mammalian selenocysteine tRNA. In Selenium: its molecular biology and role in human health D.L. Hatfield, ed. (Kluwer Academic Publishers, Norwell, Mass.), pp. 23-32.

Cate, J.H., Yusupov, M.M., Yusupova, G.Z., Earnest, T.N., and Noller, H.F. (1999). X-ray crystal structures of 70S ribosome functional complexes. Science 285, 2095-2104.

Chambers, I., Frampton, J., Goldfarb, P., Affara, N., McBain, W., and Harrison, P.R. (1986). The structure of the mouse glutathione peroxidase gene: the selenocysteine in the active site is encoded by the 'termination' codon, TGA. EMBO J 5, 1221-1227. Chen, G.F., Fang, L., and Inouye, M. (1993). Effect of the relative position of the UGA codon to the unique secondary structure in the fdhF mRNA on its decoding by selenocysteinyl tRNA in Escherichia coli. J Biol Chem 268, 23128-23131.

Ching, W.M., Tsai, L., and Wittwer, A.J. (1985). Selenium-containing transfer RNAs. Curr Top Cell Regul 27, 497-507.

Chittum, H.S., Lane, W.S., Carlson, B.A., Roller, P.P., Lung, F.D., Lee, B.J., and Hatfield, D.L. (1998). Rabbit beta-globin is extended beyond its UGA stop codon by multiple suppressions and translational reading gaps. Biochemistry 37, 10866-10870. Clark, K.L., Halay, E.D., Lai, E., and Burley, S.K. (1993). Co-crystal structure of the HNF-3/fork head DNA-recognition motif resembles histone H5. Nature 364, 412-420. Cochella, L., and Green, R. (2005). An active role for tRNA in decoding beyond codon:anticodon pairing. Science 308, 1178-1180.

Cone, J., Rio, R.M.d., Davis, J., and Stadtman, T. (1976). Chemical characterization of the selenoprotein component of clostridial glycine reductase: Identification of selenocysteine as the organoselenium moiety. Proc Natl Acad Sci USA 73, 2659-2663.

Crick, F.H. (1966). Codon--anticodon pairing: the wobble hypothesis. J Mol Biol 19, 548-555.

Czworkowski, J., Wang, J., Steitz, T.A., and Moore, P.B. (1994). The crystal structure of elongation factor G complexed with GDP, at 2.7 Å resolution. EMBO J 13, 3661-3668.

Dale, T., Sanderson, L.E., and Uhlenbeck, O.C. (2004). The affinity of elongation factor Tu for an aminoacyl-tRNA is modulated by the esterified amino acid. Biochemistry 43, 6159-6166.

Daviter, T., Gromadski, K.B., and Rodnina, M.V. (2006). The ribosome's response to codon-anticodon mismatches. Biochimie 88, 1001-1011.

Daviter, T., Wieden, H.J., and Rodnina, M.V. (2003). Essential role of histidine 84 in elongation factor Tu for the chemical step of GTP hydrolysis on the ribosome. J Mol Biol 332, 689-699.

Diaconu, M., Kothe, U., Schlunzen, F., Fischer, N., Harms, J.M., Tonevitsky, A.G., Stark, H., Rodnina, M.V., and Wahl, M.C. (2005). Structural basis for the function of the ribosomal L7/12 stalk in factor binding and GTPase activation. Cell 121, 991-1004.

Diaz, I., and Ehrenberg, M. (1991). ms2i6A deficiency enhances proofreading in translation. J Mol Biol 222, 1161-1171.

Dong, G., Chakshusmathi, G., Wolin, S.L., and Reinisch, K.M. (2004). Structure of the La motif: a winged helix domain mediates RNA binding via a conserved aromatic patch. EMBO J 23, 1000-1007.

Engelhardt, H., Forchhammer, K., Muller, S., Goldie, K.N., and Bock, A. (1992). Structure of selenocysteine synthase from Escherichia coli and location of tRNA in the seryl-tRNA(sec)-enzyme complex. Mol Microbiol 6, 3461-3467.

Fahlman, R.P., Dale, T., and Uhlenbeck, O.C. (2004). Uniform binding of aminoacylated transfer RNAs to the ribosomal A and P sites. Mol Cell 16, 799-805.

Fischer, N., Paleskava, A., Gromadski, K.B., Konevega, A.L., Wahl, M.C., Stark, H., and Rodnina, M.V. (2007). Towards understanding selenocysteine incorporation into bacterial proteins. Biol Chem 388, 1061-1067.

Fleischmann, R.D., Adams, M.D., White, O., Clayton, R.A., Kirkness, E.F., Kerlavage, A.R., Bult, C.J., Tomb, J.F., Dougherty, B.A., Merrick, J.M., et al. (1995). Whole-genome random sequencing and assembly of Haemophilus influenzae Rd. Science 269, 496-512.

Flohe, L., Gunzler, W.A., and Schock, H.H. (1973). Glutathione peroxidase: a selenoenzyme. FEBS Lett 32, 132-134.

Forchhammer, K., and Bock, A. (1991). Selenocysteine synthase from Escherichia coli. Analysis of the reaction sequence. J Biol Chem 266, 6324-6328.

Forchhammer, K., Boesmiller, K., and Bock, A. (1991). The function of selenocysteine synthase and SELB in the synthesis and incorporation of selenocysteine. Biochimie 73, 1481-1486.

Forchhammer, K., Leinfelder, W., and Bock, A. (1989). Identification of a novel translation factor necessary for the incorporation of selenocysteine into protein. Nature 342, 453-456.

Forster, C., Ott, G., Forchhammer, K., and Sprinzl, M. (1990). Interaction of a selenocysteine-incorporating tRNA with elongation factor Tu from E.coli. Nucl Acids Res 18, 487-491.

Fourmy, D., Guittet, E., and Yoshizawa, S. (2002). Structure of prokaryotic SECIS mRNA hairpin and its interaction with elongation factor SelB. J Mol Biol 324, 137-150.

Francklyn, C.S. (2008). DNA polymerases and aminoacyl-tRNA synthetases: shared mechanisms for ensuring the fidelity of gene expression. Biochemistry 47, 11695-11703.

Frank, J., and Agrawal, R.K. (2000). A ratchet-like inter-subunit reorganization of the ribosome during translocation. Nature 406, 318-322.

Gajiwala, K.S., and Burley, S.K. (2000). Winged helix proteins. Curr Opin Struct Biol 10, 110-116.

Gao, H., Zhou, Z., Rawat, U., Huang, C., Bouakaz, L., Wang, C., Cheng, Z., Liu, Y., Zavialov, A., Gursky, R., et al. (2007). RF3 induces ribosomal conformational changes responsible for dissociation of class I release factors. Cell 129, 929-941.

Garcia, G.E., and Stadtman, T.C. (1992). Clostridium sticklandii glycine reductase selenoprotein A gene: cloning, sequencing, and expression in Escherichia coli. J Bacteriol 174, 7080-7089.

Garcin, E., Vernede, X., Hatchikian, E.C., Volbeda, A., Frey, M., and Fontecilla-Camps, J.C. (1999). The crystal structure of a reduced [NiFeSe] hydrogenase provides an image of the activated catalytic center. Structure 7, 557-566.

Gefter, M.L., and Russell, R.L. (1969). Role modifications in tyrosine transfer RNA: a modified base affecting ribosome binding. J Mol Biol 39, 145-157.

Giege, R., Sissler, M., and Florentz, C. (1998). Universal rules and idiosyncratic features in tRNA identity. Nucl Acids Res 26, 5017-5035.

Gillam, I., Blew, D., Warrington, R.C., von Tigerstrom, M., and Tener, G.M. (1968). A general procedure for the isolation of specific transfer ribonucleic acids. Biochemistry 7, 3459-3468.

Gladyshev, V.N. (2001). Identity, evolution and function of selenoproteins and selenoprotein genes. In Selenium: its molecular biology and role in human health, D.L. Hatfield, ed. (Kluwer Academic Publishers, Norwell, Mass), pp. 99-114.

Gladyshev, V.N., Khangulov, S.V., Axley, M.J., and Stadtman, T.C. (1994). Coordination of selenium to molybdenum in formate dehydrogenase H from Escherichia coli. Proc Natl Acad Sci USA 91, 7708-7711.

Gladyshev, V.N., and Kryukov, G.V. (2001). Evolution of selenocysteine-containing proteins: significance of identification and functional characterization of selenoproteins. Biofactors 14, 87-92.

Gromadski, K.B., Daviter, T., and Rodnina, M.V. (2006). A uniform response to mismatches in codon-anticodon complexes ensures ribosomal fidelity. Mol Cell 21, 369-377.

Gromadski, K.B., and Rodnina, M.V. (2004a). Kinetic determinants of high-fidelity tRNA discrimination on the ribosome. Mol Cell 13, 191-200.

Gromadski, K.B., and Rodnina, M.V. (2004b). Streptomycin interferes with conformational coupling between codon recognition and GTPase activation on the ribosome. Nat Struct Mol Biol 11, 316-322.

Gromadski, K.B., Wieden, H.J., and Rodnina, M.V. (2002). Kinetic mechanism of elongation factor Ts-catalyzed nucleotide exchange in elongation factor Tu. Biochemistry 41, 162-169.

Gualerzi, C.O., Brandi, L., Caserta, E., La Teana, A., Spurio, R., Tomsic, J., and Pon, C.L. (2000). Translation initiation in bacteria. In The Ribosome: Structure, Function, Antibiotics, and Cellular Interactions, R.A. Garrett, Douthwaite, S.R., Liljas, A., Matheson, A.-T., Moore, P.B. and Noller, H.F., ed. (Washington, D.C., USA:ASM Press), pp. 477-494.

Guimaraes, M.J., Peterson, D., Vicari, A., Cocks, B.G., Copeland, N.G., Gilbert, D.J., Jenkins, N.A., Ferrick, D.A., Kastelein, R.A., Bazan, J.F., et al. (1996). Identification of a novel selD homolog from eukaryotes, bacteria, and archaea: is there an autoregulatory mechanism in selenocysteine metabolism? Proc Natl Acad Sci USA 93, 15086-15091.

Gursinsky, T., Jager, J., Andreesen, J.R., and Sohling, B. (2000). A selDABC cluster for selenocysteine incorporation in Eubacterium acidaminophilum. Arch Microbiol 174, 200-212.

Hansson, S., Singh, R., Gudkov, A.T., Liljas, A., and Logan, D.T. (2005). Crystal structure of a mutant elongation factor G trapped with a GTP analogue. FEBS Lett 579, 4492-4497.

Hatfield, D.L., and Gladyshev, V.N. (2002). How selenium has altered our understanding of the genetic code. Mol Cell Biol 22, 3565-3576.

Heider, J., Baron, C., and Bock, A. (1992). Coding from a distance: dissection of the mRNA determinants required for the incorporation of selenocysteine into protein. EMBO J 11, 3759-3766.

Heider, J., and Bock, A. (1992). Targeted insertion of selenocysteine into the alpha subunit of formate dehydrogenase from Methanobacterium formicicum. J Bacteriol 174, 659-663.

Heider, J., Forchhammer, K., Sawers, G., and Bock, A. (1991). Interspecies compatibility of selenoprotein biosynthesis in Enterobacteriaceae. Arch Microbiol 155, 221-228.

Hilgenfeld, R., Bock, A., and Wilting, R. (1996). Structural model for the selenocysteine-specific elongation factor SelB. Biochimie 78, 971-978.

Huttenhofer, A., and Bock, A. (1998). Selenocysteine inserting RNA elements modulate GTP hydrolysis of elongation factor SelB. Biochemistry 37, 885-890.

Hüttenhofer, A., and Böck, A. (1998). Selenoprotein Synthesis. In RNA Structure and Function, R.W. Simons, and M. Grunberg-Manago, eds. (Cold Spring Harbor Laboratory Press), pp. 603-639.

Huttenhofer, A., Heider, J., and Bock, A. (1996a). Interaction of the Escherichia coli fdhF mRNA hairpin promoting selenocysteine incorporation with the ribosome. Nucl Acids Res 24, 3903-3910.

Huttenhofer, A., Westhof, E., and Bock, A. (1996b). Solution structure of mRNA hairpins promoting selenocysteine incorporation in Escherichia coli and their base-specific interaction with special elongation factor SELB. RNA 2, 354-366.

Ibba, M., and Soll, D. (2000). Aminoacyl-tRNA synthesis. Annu Rev Biochem 69, 617-650.

Jukes, T.H. (1990). Genetic code 1990. Outlook. Experientia 46, 1149-1157.

Julian, P., Konevega, A.L., Scheres, S.H., Lazaro, M., Gil, D., Wintermeyer, W., Rodnina, M.V., and Valle, M. (2008). Structure of ratcheted ribosomes with tRNAs in hybrid states. Proc Natl Acad Sci USA 105, 16924-16927.

Kawashima, T., Berthet-Colominas, C., Wulff, M., Cusack, S., and Leberman, R. (1996). The structure of the Escherichia coli EF-Tu.EF-Ts complex at 2.5 Å resolution. Nature 379, 511-518.

Kim, I.Y., Veres, Z., and Stadtman, T.C. (1992). Escherichia coli mutant SELD enzymes. The cysteine 17 residue is essential for selenophosphate formation from ATP and selenide. J Biol Chem 267, 19650-19654.

Kjeldgaard, M., Nissen, P., Thirup, S., and Nyborg, J. (1993). The crystal structure of elongation factor EF-Tu from Thermus aquaticus in the GTP conformation. Structure 1, 35-50.

Klaholz, B.P., Myasnikov, A.G., and Van Heel, M. (2004). Visualization of release factor 3 on the ribosome during termination of protein synthesis. Nature 427, 862-865.

Klug, S.J., Huttenhofer, A., Kromayer, M., and Famulok, M. (1997). In vitro and in vivo characterization of novel mRNA motifs that bind special elongation factor SelB. Proc Natl Acad Sci USA 94, 6676-6681.

Komine, Y., Adachi, T., Inokuchi, H., and Ozeki, H. (1990). Genomic organization and physical mapping of the transfer RNA genes in Escherichia coli K12. J Mol Biol 212, 579-598.

Konevega, A.L., Soboleva, N.G., Makhno, V.I., Semenkov, Y.P., Wintermeyer, W., Rodnina, M.V., and Katunin, V.I. (2004). Purine bases at position 37 of tRNA stabilize codon-anticodon interaction in the ribosomal A site by stacking and Mg2+-dependent interactions. RNA 10, 90-101.

Korostelev, A., Asahara, H., Lancaster, L., Laurberg, M., Hirschi, A., Zhu, J., Trakhanov, S., Scott, W.G., and Noller, H.F. (2008). Crystal structure of a translation termination complex formed with release factor RF2. Proc Natl Acad Sci USA 105, 19684-19689.

Kothe, U., Paleskava, A., Konevega, A.L., and Rodnina, M.V. (2006). Single-step purification of specific tRNAs by hydrophobic tagging. Anal Biochem 356, 148-150.

Kothe, U., and Rodnina, M.V. (2006). Delayed release of inorganic phosphate from elongation factor Tu following GTP hydrolysis on the ribosome. Biochemistry 45, 12767-12774.

Kothe, U., and Rodnina, M.V. (2007). Codon reading by tRNAAla with modified uridine in the wobble position. Mol Cell 25, 167-174.

Kromayer, M., Neuhierl, B., Friebel, A., and Bock, A. (1999). Genetic probing of the interaction between the translation factor SelB and its mRNA binding element in Escherichia coli. Mol Gen Genet 262, 800-806.

Kromayer, M., Wilting, R., Tormay, P., and Bock, A. (1996). Domain structure of the prokaryotic selenocysteine-specific elongation factor SelB. J Mol Biol 262, 413-420.

Kryukov, G.V., Kryukov, V.M., and Gladyshev, V.N. (1999). New mammalian selenocysteine-containing proteins identified with an algorithm that searches for selenocysteine insertion sequence elements. J Biol Chem 274, 33888-33897.

Lacourciere, G.M., Mihara, H., Kurihara, T., Esaki, N., and Stadtman, T.C. (2000). Escherichia coli NifS-like proteins provide selenium in the pathway for the biosynthesis of selenophosphate. J Biol Chem 275, 23769-23773.

LaRiviere, F.J., Wolfson, A.D., and Uhlenbeck, O.C. (2001). Uniform binding of aminoacyl-tRNAs to elongation factor Tu by thermodynamic compensation. Science 294, 165-168.

Laurberg, M., Asahara, H., Korostelev, A., Zhu, J., Trakhanov, S., and Noller, H.F. (2008). Structural basis for translation termination on the 70S ribosome. Nature 454, 852-857.

Ledoux, S., and Uhlenbeck, O.C. (2008). Different aa-tRNAs are selected uniformly on the ribosome. Mol Cell 31, 114-123.

Ledoux, S., Uhlenbeck, O.C. (2008). Misacylated tRNAs can Decode Both Cognate and Mismatched Codons on the Ribosome. In RNA (Berlin, Germany), pp. 79.

Leibundgut, M., Frick, C., Thanbichler, M., Bock, A., and Ban, N. (2005). Selenocysteine tRNA-specific elongation factor SelB is a structural chimaera of elongation and initiation factors. EMBO J 24, 11-22.

Leinfelder, W., Zehelein, E., Mandrand-Berthelot, M.A., and Bock, A. (1988). Gene for a novel tRNA species that accepts L-serine and cotranslationally inserts selenocysteine. Nature 331, 723-725.

58

Li, W.Q., and Yarus, M. (1992). Bar to normal UGA translation by the selenocysteine tRNA. J Mol Biol 223, 9-15.

Liu, Z., Reches, M., and Engelberg-Kulka, H. (1999). A sequence in the Escherichia coli fdhF "selenocysteine insertion Sequence" (SECIS) operates in the absence of selenium. J Mol Biol 294, 1073-1086.

Liu, Z., Reches, M., Groisman, I., and Engelberg-Kulka, H. (1998). The nature of the minimal 'selenocysteine insertion sequence' (SECIS) in Escherichia coli. Nucl Acids Res 26, 896-902.

Louie, A., and Jurnak, F. (1985). Kinetic studies of Escherichia coli elongation factor Tu-guanosine 5'-triphosphate-aminoacyl-tRNA complexes. Biochemistry 24, 6433-6439.

Louie, A., Ribeiro, N.S., Reid, B.R., and Jurnak, F. (1984). Relative affinities of all Escherichia coli aminoacyl-tRNAs for elongation factor Tu-GTP. J Biol Chem 259, 5010-5016.

Lovett, P.S., Ambulos, N.P., Jr., Mulbry, W., Noguchi, N., and Rogers, E.J. (1991). UGA can be decoded as tryptophan at low efficiency in Bacillus subtilis. J Bacteriol 173, 1810-1812.

Matsui, M., Oshima, M., Oshima, H., Takaku, K., Maruyama, T., Yodoi, J., and Taketo, M.M. (1996). Early embryonic lethality caused by targeted disruption of the mouse thioredoxin gene. Dev Biol 178, 179-185.

Menon, N.K., Peck, H.D., Jr., Gall, J.L., and Przybyla, A.E. (1987). Cloning and sequencing of the genes encoding the large and small subunits of the periplasmic (NiFeSe) hydrogenase of Desulfovibrio baculatus. J Bacteriol 169, 5401-5407.

Meyer, F., Schmidt, H.J., Plumper, E., Hasilik, A., Mersmann, G., Meyer, H.E., Engstrom, A., and Heckmann, K. (1991). UGA is translated as cysteine in pheromone 3 of Euplotes octocarinatus. Proc Natl Acad Sci USA 88, 3758-3761.

Mihara, H., Kato, S., Lacourciere, G.M., Stadtman, T.C., Kennedy, R.A., Kurihara, T., Tokumoto, U., Takahashi, Y., and Esaki, N. (2002). The iscS gene is essential for the biosynthesis of 2-selenouridine in tRNA and the selenocysteine-containing formate dehydrogenase H. Proc Natl Acad Sci USA 99, 6679-6683.

Milon, P., Tischenko, E., Tomsic, J., Caserta, E., Folkers, G., La Teana, A., Rodnina, M.V., Pon, C.L., Boelens, R., and Gualerzi, C.O. (2006). The nucleotide-binding site of bacterial translation initiation factor 2 (IF2) as a metabolic sensor. Proc Natl Acad Sci USA 103, 13962-13967.

Mitra, S.K., Lustig, F., Akesson, B., Axberg, T., Elias, P., and Lagerkvist, U. (1979). Relative efficiency of anticodons in reading the valine codons during protein synthesis in vitro. J Biol Chem 254, 6397-6401.

Myasnikov, A.G., Marzi, S., Simonetti, A., Giuliodori, A.M., Gualerzi, C.O., Yusupova, G., Yusupov, M., and Klaholz, B.P. (2005). Conformational transition of initiation

factor 2 from the GTP- to GDP-bound state visualized on the ribosome. Nat Struct Mol Biol 12, 1145-1149.

Nasvall, S.J., Chen, P., and Bjork, G.R. (2004). The modified wobble nucleoside uridine-5-oxyacetic acid in tRNAPro(cmo5UGG) promotes reading of all four proline codons in vivo. RNA 10, 1662-1673.

Nirenberg, M., Caskey, T., Marshall, R., Brimacombe, R., Kellogg, D., Doctor, B., Hatfield, D., Levin, J., Rottman, F., Pestka, S., et al. (1966). The RNA code and protein synthesis. Cold Spring Harb Symp Quant Biol 31, 11-24.

Nissen, P., Thirup, S., Kjeldgaard, M., and Nyborg, J. (1999). The crystal structure of Cys-tRNACys-EF-Tu-GDPNP reveals general and specific features in the ternary complex and in tRNA. Structure 7, 143-156.

Noble, C.G., and Song, H. (2008). Structural studies of elongation and release factors. Cell Mol Life Sci 65, 1335-1346.

Normanly, J., Ollick, T., and Abelson, J. (1992). Eight base changes are sufficient to convert a leucine-inserting tRNA into a serine-inserting tRNA. Proc Natl Acad Sci USA 89, 5680-5684.

Ogle, J.M., Brodersen, D.E., Clemons, W.M., Jr., Tarry, M.J., Carter, A.P., and Ramakrishnan, V. (2001). Recognition of cognate transfer RNA by the 30S ribosomal subunit. Science 292, 897-902.

Ogle, J.M., Murphy, F.V., Tarry, M.J., and Ramakrishnan, V. (2002). Selection of tRNA by the ribosome requires a transition from an open to a closed form. Cell 111, 721-732.

Ohama, T., Yang, D.C., and Hatfield, D.L. (1994). Selenocysteine tRNA and serine tRNA are aminoacylated by the same synthetase, but may manifest different identities with respect to the long extra arm. Arch Biochem Biophys 315, 293-301.

Olejniczak, M., Dale, T., Fahlman, R.P., and Uhlenbeck, O.C. (2005). Idiosyncratic tuning of tRNAs to achieve uniform ribosome binding. Nat Struct Mol Biol 12, 788-793.

Osawa, S., Jukes, T.H., Watanabe, K., and Muto, A. (1992). Recent evidence for evolution of the genetic code. Microbiol Rev 56, 229-264.

Ose, T., Soler, N., Rasubala, L., Kuroki, K., Kohda, D., Fourmy, D., Yoshizawa, S., and Maenaka, K. (2007). Structural basis for dynamic interdomain movement and RNA recognition of the selenocysteine-specific elongation factor SelB. Structure 15, 577-586.

Ott, G., Faulhammer, H.G., and Sprinzl, M. (1989). Interaction of elongation factor Tu from Escherichia coli with aminoacyl-tRNA carrying a fluorescent reporter group on the 3' terminus. Eur J Biochem 184, 345-352.

Pape, T., Wintermeyer, W., and Rodnina, M.V. (1998). Complete kinetic mechanism of elongation factor Tu-dependent binding of aminoacyl-tRNA to the A site of the E. coli ribosome. EMBO J 17, 7490-7497.

Parmeggiani, A., and Sander, G. (1981). Properties and regulation of the GTPase activities of elongation factors Tu and G, and of initiation factor 2. Mol Cell Biochem 35, 129-158.

Piepenburg, O., Pape, T., Pleiss, J.A., Wintermeyer, W., Uhlenbeck, O.C., and Rodnina, M.V. (2000). Intact aminoacyl-tRNA is required to trigger GTP hydrolysis by elongation factor Tu on the ribosome. Biochemistry 39, 1734-1738.

Pingoud, A., Riesner, D., Boehme, D., and Maass, G. (1973). Kinetic studies on the interaction of seryl-tRNA synthetase with tRNA(Ser) and ser-tRNA(ser) from yeast. FEBS Lett 30, 1-5.

Pinsent, J. (1954). The need for selenite and molybdate in the formation of formic dehydrogenase by members of the coli-aerogenes group of bacteria. Biochem J 57, 10-16.

Polekhina, G., Thirup, S., Kjeldgaard, M., Nissen, P., Lippmann, C., and Nyborg, J. (1996). Helix unwinding in the effector region of elongation factor EF-Tu-GDP. Structure 4, 1141-1151.

Pon, C.L., Paci, M., Pawlik, R.T., and Gualerzi, C.O. (1985). Structure-function relationship in Escherichia coli initiation factors. Biochemical and biophysical characterization of the interaction between IF-2 and guanosine nucleotides. J Biol Chem 260, 8918-8924.

Poole, E.S., Brown, C.M., and Tate, W.P. (1995). The identity of the base following the stop codon determines the efficiency of in vivo translational termination in Escherichia coli. EMBO J 14, 151-158.

Putz, J., Wientges, J., Sissler, M., Giege, R., Florentz, C., and Schwienhorst, A. (1997). Rapid selection of aminoacyl-tRNAs based on biotinylation of alpha-NH2 group of charged amino acids. Nucl Acids Res 25, 1862-1863.

Ribeiro, S., Nock, S., and Sprinzl, M. (1995). Purification of aminoacyl-tRNA by affinity chromatography on immobilized Thermus thermophilus EF-Tu.GTP. Anal Biochem 228, 330-335.

Rodnina, M.V., Fricke, R., and Wintermeyer, W. (1994). Transient conformational states of aminoacyl-tRNA during ribosome binding catalyzed by elongation factor Tu. Biochemistry 33, 12267-12275.

Rodnina, M.V., Gromadski, K.B., Kothe, U., and Wieden, H.J. (2005). Recognition and selection of tRNA in translation. FEBS Lett 579, 938-942.

Rodnina, M.V., Pape, T., Fricke, R., Kuhn, L., and Wintermeyer, W. (1996). Initial binding of the elongation factor Tu.GTP.aminoacyl-tRNA complex preceding codon recognition on the ribosome. J Biol Chem 271, 646-652.

Rodnina, M.V., Pape, T., Fricke, R., and Wintermeyer, W. (1995). Elongation factor Tu, a GTPase triggered by codon recognition on the ribosome: mechanism and GTP consumption. Biochem Cell Biol 73, 1221-1227.

Rodnina, M.V., Stark, H., Savelsbergh, A., Wieden, H.J., Mohr, D., Matassova, N.B., Peske, F., Daviter, T., Gualerzi, C.O., and Wintermeyer, W. (2000). GTPases mechanisms and functions of translation factors on the ribosome. Biol Chem 381, 377-387.

Roll-Mecak, A., Alone, P., Cao, C., Dever, T.E., and Burley, S.K. (2004). X-ray structure of translation initiation factor eIF2gamma: implications for tRNA and eIF2alpha binding. J Biol Chem 279, 10634-10642.

Roll-Mecak, A., Cao, C., Dever, T.E., and Burley, S.K. (2000). X-Ray structures of the universal translation initiation factor IF2/eIF5B: conformational changes on GDP and GTP binding. Cell 103, 781-792.

Rotruck, J.T., Pope, A.L., Ganther, H.E., Swanson, A.B., Hafeman, D.G., and Hoekstra, W.G. (1973). Selenium: biochemical role as a component of glutathione peroxidase. Science 179, 588-590.

Rudinger, J., Blechschmidt, B., Ribeiro, S., and Sprinzl, M. (1994). Minimalist aminoacylated RNAs as efficient substrates for elongation factor Tu. Biochemistry 33, 5682-5688.

Rudinger, J., Hillenbrandt, R., Sprinzl, M., and Giege, R. (1996). Antideterminants present in minihelix(Sec) hinder its recognition by prokaryotic elongation factor Tu. EMBO J 15, 650-657.

Saks, M.E., Sampson, J.R., and Abelson, J.N. (1994). The transfer RNA identity problem: a search for rules. Science 263, 191-197.

Sampson, J.R., and Saks, M.E. (1993). Contributions of discrete tRNA(Ser) domains to aminoacylation by E.coli seryl-tRNA synthetase: a kinetic analysis using model RNA substrates. Nucl Acids Res 21, 4467-4475.

Sandman, K.E., and Noren, C.J. (2000). The efficiency of Escherichia coli selenocysteine insertion is influenced by the immediate downstream nucleotide. Nucl Acids Res 28, 755-761.

Savchenko, A., Krogan, N., Cort, J.R., Evdokimova, E., Lew, J.M., Yee, A.A., Sanchez-Pulido, L., Andrade, M.A., Bochkarev, A., Watson, J.D., et al. (2005). The Shwachman-Bodian-Diamond syndrome protein family is involved in RNA metabolism. J Biol Chem 280, 19213-19220.

Savelsbergh, A., Katunin, V.I., Mohr, D., Peske, F., Rodnina, M.V., and Wintermeyer, W. (2003). An elongation factor G-induced ribosome rearrangement precedes tRNA-mRNA translocation. Mol Cell 11, 1517-1523.

Savelsbergh, A., Mohr, D., Kothe, U., Wintermeyer, W., and Rodnina, M.V. (2005). Control of phosphate release from elongation factor G by ribosomal protein L7/12. EMBO J 24, 4316-4323.

Schmitt, E., Blanquet, S., and Mechulam, Y. (2002). The large subunit of initiation factor aIF2 is a close structural homologue of elongation factors. EMBO J 21, 1821-1832.

Schon, A., Bock, A., Ott, G., Sprinzl, M., and Soll, D. (1989). The selenocysteine-inserting opal suppressor serine tRNA from E. coli is highly unusual in structure and modification. Nucl Acids Res 17, 7159-7165.

Schuette, J.C., Murphy, F.V.t., Kelley, A.C., Weir, J.R., Giesebrecht, J., Connell, S.R., Loerke, J., Mielke, T., Zhang, W., Penczek, P.A., et al. (2009). GTPase activation of elongation factor EF-Tu by the ribosome during decoding. EMBO J 28, 755-765.

Schwarz, K., and Foltz, C. (1957). Selenium as an integral part of factor 3 against dietary necrotic liver degeneration. J Am Chem Soc 79, 3292-3293.

Selmer, M., Dunham, C.M., Murphy, F.V.t., Weixlbaumer, A., Petry, S., Kelley, A.C., Weir, J.R., and Ramakrishnan, V. (2006). Structure of the 70S ribosome complexed with mRNA and tRNA. Science 313, 1935-1942.

Selmer, M., and Su, X.D. (2002). Crystal structure of an mRNA-binding fragment of Moorella thermoacetica elongation factor SelB. EMBO J 21, 4145-4153.

Shuber, A.P., Orr, E.C., Recny, M.A., Schendel, P.F., May, H.D., Schauer, N.L., and Ferry, J.G. (1986). Cloning, expression, and nucleotide sequence of the formate dehydrogenase genes from Methanobacterium formicicum. J Biol Chem 261, 12942-12947.

Simonetti, A., Marzi, S., Myasnikov, A.G., Fabbretti, A., Yusupov, M., Gualerzi, C.O., and Klaholz, B.P. (2008). Structure of the 30S translation initiation complex. Nature 455, 416-420.

Soler, N., Fourmy, D., and Yoshizawa, S. (2007). Structural insight into a molecular switch in tandem winged-helix motifs from elongation factor SelB. J Mol Biol 370, 728-741.

Spiegel, P.C., Ermolenko, D.N., and Noller, H.F. (2007). Elongation factor G stabilizes the hybrid-state conformation of the 70S ribosome. RNA 13, 1473-1482. Stadtman, T.C. (1996). Selenocysteine. Annu Rev Biochem 65, 83-100.

Stark, H., Rodnina, M.V., Rinke-Appel, J., Brimacombe, R., Wintermeyer, W., and van Heel, M. (1997). Visualization of elongation factor Tu on the Escherichia coli ribosome. Nature 389, 403-406.

Stark, H., Rodnina, M.V., Wieden, H.J., van Heel, M., and Wintermeyer, W. (2000). Large-scale movement of elongation factor G and extensive conformational change of the ribosome during translocation. Cell 100, 301-309.

Stark, H., Rodnina, M.V., Wieden, H.J., Zemlin, F., Wintermeyer, W., and van Heel, M. (2002). Ribosome interactions of aminoacyl-tRNA and elongation factor Tu in the codon-recognition complex. Nat Struct Biol 9, 849-854.

Steinberg, S., Misch, A., and Sprinzl, M. (1993). Compilation of tRNA sequences and sequences of tRNA genes. Nucl Acids Res 21, 3011-3015.

Sun, Q.A., Kirnarsky, L., Sherman, S., and Gladyshev, V.N. (2001). Selenoprotein oxidoreductase with specificity for thioredoxin and glutathione systems. Proc Natl Acad Sci USA 98, 3673-3678.

Sun, Q.A., Wu, Y., Zappacosta, F., Jeang, K.T., Lee, B.J., Hatfield, D.L., and Gladyshev, V.N. (1999). Redox regulation of cell signaling by selenocysteine in mammalian thioredoxin reductases. J Biol Chem 274, 24522-24530.

Suppmann, S., Persson, B.C., and Bock, A. (1999). Dynamics and efficiency in vivo of UGA-directed selenocysteine insertion at the ribosome. EMBO J 18, 2284-2293.

Thanbichler, M., and Bock, A. (2001). Functional analysis of prokaryotic SELB proteins. Biofactors 14, 53-59.

Thanbichler, M., Bock, A., and Goody, R.S. (2000). Kinetics of the interaction of translation factor SelB from Escherichia coli with guanosine nucleotides and selenocysteine insertion sequence RNA. J Biol Chem 275, 20458-20466.

Tomsic, J., Vitali, L.A., Daviter, T., Savelsbergh, A., Spurio, R., Striebeck, P., Wintermeyer, W., Rodnina, M.V., and Gualerzi, C.O. (2000). Late events of translation initiation in bacteria: a kinetic analysis. EMBO J 19, 2127-2136.

Tormay, P., Wilting, R., Heider, J., and Bock, A. (1994). Genes coding for the selenocysteine-inserting tRNA species from Desulfomicrobium baculatum and Clostridium thermoaceticum: structural and evolutionary implications. J Bacteriol 176, 1268-1274.

Tormay, P., Wilting, R., Lottspeich, F., Mehta, P.K., Christen, P., and Bock, A. (1998). Bacterial selenocysteine synthase--structural and functional properties. Eur J Biochem 254, 655-661.

Turanov, A.A., Lobanov, A.V., Fomenko, D.E., Morrison, H.G., Sogin, M.L., Klobutcher, L.A., Hatfield, D.L., and Gladyshev, V.N. (2009). Genetic code supports targeted insertion of two amino acids by one codon. Science 323, 259-261.

Vacher, J., Grosjean, H., Houssier, C., and Buckingham, R.H. (1984). The effect of point mutations affecting Escherichia coli tryptophan tRNA on anticodon-anticodon interactions and on UGA suppression. J Mol Biol 177, 329-342.

Valle, M., Sengupta, J., Swami, N.K., Grassucci, R.A., Burkhardt, N., Nierhaus, K.H., Agrawal, R.K., and Frank, J. (2002). Cryo-EM reveals an active role for aminoacyl-tRNA in the accommodation process. EMBO J 21, 3557-3567.

64

Valle, M., Zavialov, A., Li, W., Stagg, S.M., Sengupta, J., Nielsen, R.C., Nissen, P., Harvey, S.C., Ehrenberg, M., and Frank, J. (2003). Incorporation of aminoacyl-tRNA into the ribosome as seen by cryo-electron microscopy. Nat Struct Biol 10, 899-906.

Villa, E., Sengupta, J., Trabuco, L.G., LeBarron, J., Baxter, W.T., Shaikh, T.R., Grassucci, R.A., Nissen, P., Ehrenberg, M., Schulten, K., et al. (2009). Ribosome-induced changes in elongation factor Tu conformation control GTP hydrolysis. Proc Natl Acad Sci USA 106, 1063-1068.

Wagner, M., Sonntag, D., Grimm, R., Pich, A., Eckerskorn, C., Sohling, B., and Andreesen, J.R. (1999). Substrate-specific selenoprotein B of glycine reductase from Eubacterium acidaminophilum. Biochemical and molecular analysis. Eur J Biochem 260, 38-49.

Wagner, R., and Andreesen, J.R. (1979). Selenium requirement for active xanthine dehydrogenase from Clostridium acidiurici and Clostridium cylindrosporum. Arch Microbiol 121, 255-260.

Wang, Y., Jiang, Y., Meyering-Voss, M., Sprinzl, M., and Sigler, P.B. (1997). Crystal structure of the EF-Tu.EF-Ts complex from Thermus thermophilus. Nat Struct Biol 4, 650-656.

Weast, R.C. (1964). Handbook of chemistry and physics, 45th edn (Cleveland, Chemical Rubber Co.).

Wei, Z., Zhang, P., Zhou, Z., Cheng, Z., Wan, M., and Gong, W. (2004). Crystal structure of human eIF3k, the first structure of eIF3 subunits. J Biol Chem 279, 34983-34990.

Weiner, A.M., and Weber, K. (1973). A single UGA codon functions as a natural termination signal in the coliphage q beta coat protein cistron. J Mol Biol 80, 837-855. Weixlbaumer, A., Jin, H., Neubauer, C., Voorhees, R.M., Petry, S., Kelley, A.C., and Ramakrishnan, V. (2008). Insights into translational termination from the structure of RF2 bound to the ribosome. Science 322, 953-956.

Wilden, B., Savelsbergh, A., Rodnina, M.V., and Wintermeyer, W. (2006). Role and timing of GTP binding and hydrolysis during EF-G-dependent tRNA translocation on the ribosome. Proc Natl Acad Sci USA 103, 13670-13675.

Wilson, R.K., and Roe, B.A. (1989). Presence of the hypermodified nucleotide N6-(delta 2-isopentenyl)-2-methylthioadenosine prevents codon misreading by Escherichia coli phenylalanyl-transfer RNA. Proc Natl Acad Sci USA 86, 409-413.

Wintermeyer, W., Peske, F., Beringer, M., Gromadski, K.B., Savelsbergh, A., and Rodnina, M.V. (2004). Mechanisms of elongation on the ribosome: dynamics of a macromolecular machine. Biochem Soc Trans 32, 733-737.

Wittwer, A.J., and Stadtman, T.C. (1986). Biosynthesis of 5-methylaminomethyl-2-selenouridine, a naturally occurring nucleoside in Escherichia coli tRNA. Arch Biochem Biophys 248, 540-550.

Xu, X.M., Carlson, B.A., Mix, H., Zhang, Y., Saira, K., Glass, R.S., Berry, M.J., Gladyshev, V.N., and Hatfield, D.L. (2007). Biosynthesis of selenocysteine on its tRNA in eukaryotes. PLoS Biol 5, e4.

Yoshizawa, S., Rasubala, L., Ose, T., Kohda, D., Fourmy, D., and Maenaka, K. (2005). Structural basis for mRNA recognition by elongation factor SelB. Nat Struct Mol Biol 12, 198-203.

Youngman, E.M., He, S.L., Nikstad, L.J., and Green, R. (2007). Stop codon recognition by release factors induces structural rearrangement of the ribosomal decoding center that is productive for peptide release. Mol Cell 28, 533-543.

Yusupova, G.Z., Yusupov, M.M., Cate, J.H., and Noller, H.F. (2001). The path of messenger RNA through the ribosome. Cell 106, 233-241.

Zaher, H.S., and Green, R. (2009). Fidelity at the molecular level: lessons from protein synthesis. Cell 136, 746-762.

Zavialov, A.V., Buckingham, R.H., and Ehrenberg, M. (2001). A posttermination ribosomal complex is the guanine nucleotide exchange factor for peptide release factor RF3. Cell 107, 115-124.

Zinoni, F., Birkmann, A., Leinfelder, W., and Bock, A. (1987). Cotranslational insertion of selenocysteine into formate dehydrogenase from Escherichia coli directed by a UGA codon. Proc Natl Acad Sci USA 84, 3156-3160.

Zinoni, F., Birkmann, A., Stadtman, T.C., and Bock, A. (1986). Nucleotide sequence and expression of the selenocysteine-containing polypeptide of formate dehydrogenase (formate-hydrogen-lyase-linked) from Escherichia coli. Proc Natl Acad Sci USA 83, 4650-4654.

Zinoni, F., Heider, J., and Bock, A. (1990). Features of the formate dehydrogenase mRNA necessary for decoding of the UGA codon as selenocysteine. Proc Natl Acad Sci USA 87, 4660-4664.

Paper 1

ELSEVIER

Notes & Tips

Single-step purification of specific tRNAs by hydrophobic tagging

Ute Kothe, Alena Paleskava, Andrey L. Konevega, Marina V. Rodnina *

Institute of Physical Biochemistry, University of Witten/Herdecke, D-58448 Witten, Germany

Received 14 March 2006
Available online 11 May 2006

Studies on translation frequently require large amounts of purified individual tRNAs. However, few purified tRNAs are commercially available. Individual tRNAs can be easily produced by in vitro transcription, but the lack of modifications of the tRNA transcripts may influence or impair their function [1,2]. The purification of specific tRNAs from total tRNA is a laborious process that requires several chromatographic steps [3]. Therefore, developing a simple and rapid method for purification of specific tRNA is of great importance. Here we describe a method for purification of individual tRNAs based on selective tagging of the amino group of specifically charged aminoacyl-tRNAs (aa-tRNAs)[1] with 9-fluorenylmethylsuccinimidylcarbonat (FmocOSu) (Fig. 1), followed by a single chromatographic purification step, using reversed-phase HPLC or hydrophobic interaction chromatography. The method is suitable for all tRNAs and allows up to 20-fold enrichment of a specific tRNA in less than 1 day effective working time. The materials used are readily available at low cost.

We tested the procedure for two different tRNAs from *Escherichia coli:* tRNA^{Ala} and tRNA^{Sec} (the latter being tRNA specific for selenocysteine). As starting material, we used total tRNA, which is commercially available or can be prepared by standard procedures [4]. For the purification of tRNA^{Ala}, we used total tRNA from MRE 600 cells that contained approximately 3% tRNA^{Ala} according to charging with [^{14}C]alanine in an analytical aminoacylation assay. tRNA^{Sec} is a rare tRNA that is hardly detected in total tRNA (<1%). To increase the amount of tRNA^{Sec} in the initial tRNA preparation, we overproduced tRNA^{Sec}

in BL21(DE3) cells [5] and isolated total tRNA from these cells. tRNA^{Sec} and tRNA^{Ser} in total tRNA can be aminoacylated with serine by seryl-tRNA synthetase [5], yielding Ser-tRNA^{Sec} and Ser-tRNA^{Ser} [6]. (Further conversion of Ser-tRNA^{Sec} to Sec-tRNA^{Sec} requires a number of additional factors and is not addressed here.) Analytical aminoacylation of total tRNA enriched in tRNA^{Sec} with [^{14}C]serine indicated the presence of approximately 30% tRNA$^{Sec/Ser}$ in total tRNA. For preparative aminoacylation, 50–100 μM total tRNA, 3% (v/v) S100 fraction as a source of aa-tRNA synthetases [7], 3 mM ATP, 50–80 μM ^{14}C-labeled amino acid (alanine [MP Biomedicals] or serine [Moravic Biochemicals]), and 0.005 U/μl inorganic pyrophosphatase (Sigma) were incubated for 60 min at 37 °C in aminoacylation buffer (50 mM Hepes [pH 7.5], 30 mM KCl, 10 mM MgCl$_2$, and 2 mM dithiothreitol [DTT]). For the following purification steps, it is crucial to obtain specific charging by only one given amino acid. To avoid charging of other tRNAs, the preparation of aminoacyl-tRNA synthetase must be absolutely free of endogenous amino acids, and this can be achieved by a dialysis step. Alternatively, purified aminoacyl-tRNA synthetases can be used. The aminoacylation efficiency was controlled in an aliquot of the reaction mixture by trichloroacetic acid (TCA) precipitation, filtration through a nitrocellulose filter (Sartorius), and scintillation counting in Quickszint 361 cocktail (Zinsser Analytic). Potassium acetate (pH 4.5) was added to the reaction mixture to a final concentration of 0.3 M, followed by extraction with an equal volume of water-saturated phenol to remove proteins. The aa-tRNA was precipitated from the aqueous phase with 2.5 volumes of cold ethanol, and the pellet of aa-tRNA was dissolved in 0.1 M sodium acetate (pH 4.5) [8].

In principle, individual tRNAs (or aa-tRNAs) can be separated by chromatography on a reversed-phase HPLC column (LiChrospher WP, instruction manual, Merck). However, when large amounts of tRNA are used, the

---

* Corresponding author. Fax: +49 2302 926 117.
  E-mail address: rodnina@uni-wh.de (M.V. Rodnina).
  [1] *Abbreviations used:* aa-tRNA, aminoacyl-tRNA; FmocOSu, 9-fluorenylmethylsuccinimidylcarbonat; DTT, dithiothreitol; TCA, trichloroacetic acid; DMSO, dimethyl sulfoxide; Fmoc-aa-tRNA, fluoren-9-ylmethoxycarbonyl-aa-tRNA; EF-Tu, elongation factor Tu.
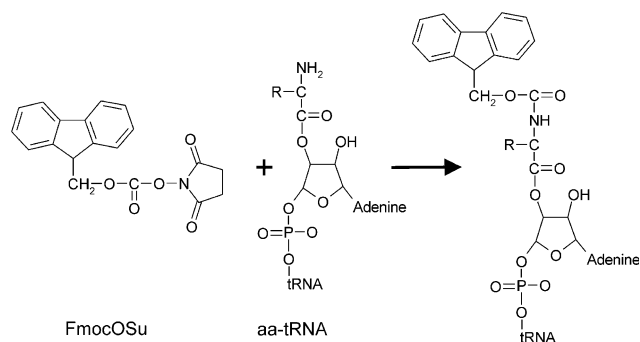
Fig. 1. Formation of fluoren-9-ylmethoxycarbonyl-aa-tRNA (Fmoc-aa-tRNA). FmocOSu reacts with the free amino group of aa-tRNA. The hydrophobicity of the resulting Fmoc-aa-tRNA is increased significantly compared with deacylated tRNA or unmodified aa-tRNA.

separation of the individual tRNA peaks is quite poor. To change the retention time of a specific aa-tRNA on the column and thereby improve its separation from other (deacylated) tRNAs, we modified the amino group of aa-tRNA with FmocOSu (Sigma–Aldrich), which adds a large aromatic group to the tRNA, thereby increasing its hydrophobicity and retention time on the column (Fig. 1). Succinimide esters selectively modify the amino group of amino acid and do not react with other amino groups in the tRNA molecule [9]. FmocOSu was dissolved in dimethyl sulfoxide (DMSO), 1 volume of tRNA was mixed with 4 volumes of FmocOSu to final concentrations of 20 µM aa-tRNA and 35 mM FmocOSu, and the reaction was carried out for 60 min at 0 °C, resulting in the formation of fluoren-9-ylmethoxycarbonyl-aa-tRNA (Fmoc-aa-tRNA). Potassium acetate (pH 4.5) was added to 0.3 M final concentration, and Fmoc-aa-tRNA was precipitated with ethanol and dissolved in 0.3 M potassium acetate (pH 4.5). To remove unreacted FmocOSu, the sample was phenol-extracted and Fmoc-aa-tRNA was purified by two ethanol precipitations. For the subsequent chromatography, Fmoc-aa-tRNA was dissolved in buffer A (20 mM ammonium acetate [pH 5.0], 10 mM magnesium acetate, and 400 mM NaCl).

Separation of Fmoc-aa-tRNA from total tRNA was achieved by chromatography on reversed-phase HPLC using a LiChrospher WP-300 RP-18 (5 µm) column (250 × 10 mm) (Merck) (Figs. 2A and B). The HPLC system allows the efficient separation of Fmoc-aa-tRNA from deacylated tRNAs and residual unmodified aa-tRNA within 2 h. The tRNA mixture (up to 1700 A_{260} units) was applied to the column equilibrated with buffer A, followed by further washing of the column with buffer A at a flow rate of 3 ml/min. The tRNAs were eluted by a linear gradient from buffer A to 100% buffer B (20 mM ammonium acetate [pH 5.0], 10 mM magnesium acetate, 400 mM NaCl, and 30% [v/v] ethanol). The elution profile was monitored by measuring absorption (A_{260}) and scintillation counting of aliquots of eluted fractions to detect Fmoc-[^{14}C]aa-tRNA. The first small A_{260} peak eluting at 0–15% buffer B contained traces of ATP from the aminoacylation
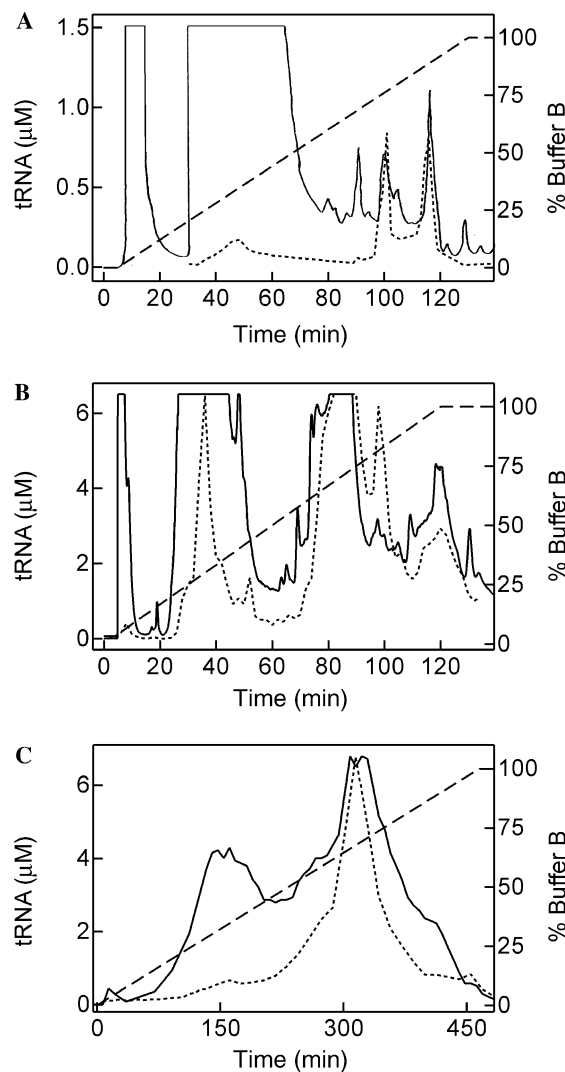

Fig. 2. Separation of Fmoc-aa-tRNA from total tRNA. Elution profiles were monitored by absorption at 260 nm (—) and ^{14}C radioactivity (--). The increase in buffer B percentage (––) is indicated. (A) Separation of Fmoc-Ala-tRNA^{Ala} from total tRNA by reversed-phase HPLC on a LiChrospher WP300 RP-18 (5 µm) column (250 × 10 mm) (Merck). [^{14}C]Alanine (50 dpm/pmol) was detected by scintillation counting of 50 µl of each fraction (4.5 ml) in Lumasafe Plus cocktail (Lumac∗LSC). (B) Separation of Fmoc-Ser-tRNA$^{Sec/Ser}$ from total tRNA (containing overexpressed tRNA^{Sec}) by reversed-phase HPLC. To measure [^{14}C]serine (5 dpm/pmol), 50 µl of each fraction (6 ml) was counted. (C) Separation of Fmoc-Ser-tRNA$^{Sec/Ser}$ from total tRNA on Phenyl Sepharose (75 ml). Here 100 µl of each fraction (10 ml) was counted to detect [^{14}C]serine (6 dpm/pmol).

reaction. The second large peak at 20–50% buffer B contained total tRNA. The radioactivity profile indicated in this peak the presence of aa-tRNA that was not modified with FmocOSu. Finally, Fmoc-aa-tRNA eluted at 60–100% buffer B. For either tRNA^{Ala} or tRNA$^{Sec/Ser}$ preparations, two peaks that were well separated from bulk tRNA were found. For Fmoc-Ser-tRNA$^{Sec/Ser}$, we could show (using analytical assays for the conversion of serine to selenocysteine) that the first of the two peaks contained tRNA-^{Sec} (60–90% buffer B), whereas tRNA^{Ser} isoacceptors eluted

in the second peak (90–100% buffer B) [10]. The two peaks of Fmoc-Ala-tRNA^Ala presumably contain the two isoacceptors of tRNA^Ala [11]; the isoacceptor identity was not analyzed here. The modification efficiency of aa-tRNA with FmocOSu was approximately 70–80%, as estimated from the ratio of ^{14}C radioactivity in the fractions containing aa-tRNA and Fmoc-aa-tRNA. The fractions containing Fmoc-aa-tRNA were pooled and precipitated with ethanol. As an alternative to reversed-phase HPLC, Phenyl Sepharose 6 Fast Flow (high sub) (GE Healthcare) can be used to separate the modified aa-tRNA from bulk tRNA (Fig. 2C) using a 1.4- to 0-M gradient of ammonium sulfate in 50 mM sodium acetate (pH 6.5) and 10 mM MgCl$_2$.

To recover deacylated tRNA, Fmoc-aa-tRNA was deacylated by incubation with 1 M Tris–HCl (pH 9.0) at room temperature for 4 h. This procedure resulted in more than 90% deacylation, as verified by analytical reversed-phase HPLC under conditions similar to the preparative HPLC described above. Thus, efficient deacylation can be achieved without using expensive enzymes [12]. Deacylated tRNA was recovered by the addition of potassium acetate (pH 4.5) to 0.3 M and ethanol precipitation. The purified tRNA^Ala could be charged by alanine to 60%, corresponding to approximately a 20-fold enrichment in a single chromatographic step. The isolated tRNA^Sec, which was purified after overexpression in E. coli, also had a 60% acceptor activity.

The current method of tRNA purification has several advantages compared with previously published procedures [9,12–14]. It is generally applicable for all tRNAs without any adaptations in the described protocol because it relies solely on the selective aminoacylation by highly specific aa-tRNA synthetases and the subsequent modification of the amino group. In contrast to a previously published method [9], the ester used in the current work (FmocOSu) is readily available at low cost and is stable. By our method, the tRNA can be rapidly enriched up to 20-fold after only a single purification step. Both chromatographic materials (LiChrospher WP-300 RP-18 and Phenyl Sepharose) are more readily available than the BD cellulose that was used previously for tRNA purification by a similar approach [15]. Compared with other methods, such as affinity chromatography with immobilized elongation factor Tu (EF-Tu) [13] and streptavidin binding of N-biotinylated aa-tRNAs [14], the current method uses chromatographic materials that are significantly less expensive and allows purification in one chromatographic step of tRNAs in very large preparative amounts—up to 1700 A_{260} units on the LiChrospher WP-300 RP-18 column or 4000 A_{260} units/200 ml Phenyl Sepharose. Thus, we have described a fast, inexpensive, and efficient method for the isolation of specific tRNAs of good purity. For more demanding tasks, such as the purification of individual tRNA isoacceptors, the described procedure represents an ideal first step that can be followed by further purification steps using HPLC or hydrophobic chromatography [3].

References

[1] A.L. Konevega, N.G. Soboleva, V.I. Makhno, Y.P. Semenkov, W. Wintermeyer, M.V. Rodnina, V.I. Katunin, Purine bases at position 37 of tRNA stabilize codon–anticodon interaction in the ribosomal A site by stacking and Mg^{2+}-dependent interactions, RNA 10 (2004) 90–101.
[2] P.F. Agris, Decoding the genome: a modified view, Nucleic Acids Res. 32 (2004) 223–238.
[3] N. Horie, Z. Yamaizumi, Y. Kuchino, K. Takai, E. Goldman, T. Miyazawa, S. Nishimura, S. Yokoyama, Modified nucleosides in the first positions of the anticodons of tRNA$_4^{Leu}$ and tRNA$_5^{Leu}$ from Escherichia coli, Biochemistry 38 (1999) 207–217.
[4] G. Ehrenstein, Isolation of sRNA from intact Escherichia coli cells, Methods Enzymol. 12 (1967) 588–596.
[5] M. Thanbichler, A. Bock, Selenoprotein biosynthesis: purification and assay of components involved in selenocysteine biosynthesis and insertion in Escherichia coli, Methods Enzymol. 347 (2002) 3–16.
[6] C. Baron, A. Bock, The length of the aminoacyl-acceptor stem of the selenocysteine-specific tRNA^Sec of Escherichia coli is the determinant for binding to elongation factors SELB or Tu, J. Biol. Chem. 266 (1991) 20375–20379.
[7] K.S. Kemkhadze, V.B. Odintsov, Y.P. Semenkov, S.V. Kirillov, Quantitative study of the interaction of aminoacyl-tRNA with the A site of Escherichia coli ribosomes: Equilibrium and kinetic parameters of binding in the absence of EF-Tu factor and GTP, FEBS Lett. 125 (1981) 10–14.
[8] M.V. Rodnina, Y.P. Semenkov, W. Wintermeyer, Purification of fMet-tRNA^fMet by fast protein liquid chromatography, Anal. Biochem. 219 (1994) 380–381.
[9] I. Gillam, D. Blew, R.C. Warrington, M. von Tigerstrom, G.M. Tener, A general procedure for the isolation of specific transfer ribonucleic acids, Biochemistry 7 (1968) 3459–3468.
[10] J.T. Kaiser, K. Gromadski, M. Rother, H. Engelhardt, M.V. Rodnina, M.C. Wahl, Structural and functional investigation of a putative archaeal selenocysteine synthase, Biochemistry 44 (2005) 13315–13327.
[11] H. Dong, L. Nilsson, C.G. Kurland, Co-variation of tRNA abundance and codon usage in Escherichia coli at different growth rates, J. Mol. Biol. 260 (1996) 649–663.
[12] E. Cayama, A. Yepez, F. Rotondo, E. Bandeira, A.C. Ferreras, F.J. Triana-Alonso, New chromatographic and biochemical strategies for quick preparative isolation of tRNA, Nucleic Acids Res. 28 (2000) e64.
[13] S. Ribeiro, S. Nock, M. Sprinzl, Purification of aminoacyl-tRNA by affinity chromatography on immobilized Thermus thermophilus EF-Tu · GTP, Anal. Biochem. 228 (1995) 330–335.
[14] J. Putz, J. Wientges, M. Sissler, R. Giege, C. Florentz, A. Schwienhorst, Rapid selection of aminoacyl-tRNAs based on biotinylation of α-NH$_2$ group of charged amino acids, Nucleic Acids Res. 25 (1997) 1862–1863.
[15] I. Gillam, S. Millward, D. Blew, M. von Tigerstrom, E. Wimmer, G.M. Tener, The separation of soluble ribonucleic acids on benzoylated diethylaminoethylcellulose, Biochemistry 6 (1967) 3043–3056.

Paper 2

Towards understanding selenocysteine incorporation into bacterial proteins

Niels Fischer[1], Alena Paleskava[2], Kirill B. Gromadski[2], Andrey L. Konevega[2], Markus C. Wahl[3], Holger Stark[1,*] and Marina V. Rodnina[2,*]

[1] 3D Electron Cryomicroscopy Group, Max-Planck-Institute for Biophysical Chemistry, D-37077 Göttingen, Germany

[2] Institute of Physical Biochemistry, University of Witten/Herdecke, D-58448 Witten, Germany

[3] X-Ray Crystallography Group, Max-Planck-Institute for Biophysical Chemistry, D-37077 Göttingen, Germany

* Corresponding authors
e-mail: rodnina@uni-wh.de; hstark1@gwdg.de

Abstract

In bacteria, UGA stop codons can be recoded to direct the incorporation of selenocysteine into proteins on the ribosome. Recoding requires a selenocysteine incorporation sequence (SECIS) downstream of the UGA codon, a specialized translation factor SelB, and the non-canonical Sec-tRNA^{Sec}, which is formed from Ser-tRNA^{Sec} by selenocysteine synthase, SelA, using selenophosphate as selenium donor. Here we describe a rapid-kinetics approach to study the mechanism of selenocysteine insertion into proteins on the ribosome. Labeling of SelB, Sec-tRNA^{Sec} and other components of the translational machinery allows direct observation of the formation or dissociation of complexes by monitoring changes in the fluorescence of single dyes or fluorescence resonance energy transfer between two fluorophores. Furthermore, the structure of SelA was studied by electron cryomicroscopy (cryo-EM). We report that intact SelA from the thermophilic bacterium *Moorella thermoacetica* (*mth*SelA) can be vitrified for cryo-EM using a controlled-environment vitrification system. Two-dimensional image analysis of vitrified *mth*SelA images shows that SelA can adopt the wide range of orientations required for high-resolution structure determination by cryo-EM. The results indicate that *mth*SelA forms a homodecamer that has a ring-like structure with five bilobed wings, similar to the structure of the *E. coli* complex determined previously.

Keywords: electron cryomicroscopy; fluorescence; protein synthesis; recoding; ribosome; selenocysteine.

Introduction

In addition to the 20 standard amino acids, selenocysteine is the 21st proteinogenic amino acid that is incorporated into protein during ribosomal protein synthesis. Selenocysteine has a structure similar to cysteine, with selenium taking the place of sulfur. In bacteria, the biosynthesis of selenocysteine and its insertion into proteins requires the function of at least four gene products (Böck et al., 1991; Baron and Böck, 1995) (Figure 1). Like the standard amino acids, selenocysteine is transferred to the ribosome by a specific tRNA, tRNA^{Sec}, which is encoded by the *selC* gene. The primary and secondary structures of tRNA^{Sec} differ from those of standard tRNAs in having a longer acceptor stem, a long variable arm, and substitutions at several base positions that are conserved among other elongator tRNAs (Schön et al., 1989; Baron et al., 1990; Baron and Böck, 1991, 1995). tRNA^{Sec} is initially charged with serine by seryl-tRNA synthetase, but the resulting Ser-tRNA^{Sec} is not used for translation because it is not recognized by translation factor EF-Tu, which binds the standard aminoacyl-tRNAs. Rather, the tRNA-bound seryl residue is converted to a selenocysteinyl residue by the pyridoxal phosphate-containing enzyme selenocysteine synthase (the *selA* gene product) using selenomonophosphate as the selenium donor substrate. The latter is synthesized from selenite and ATP by selenophosphate synthetase (the *selD* gene product). Finally, the resulting Sec-tRNA^{Sec} binds to a specific translational elongation factor, SelB, which delivers it to ribosomes translating mRNAs coding for selenoproteins. The codon for selenocysteine is UGA, which usually serves as a stop codon, but, with a specific downstream sequence forming a stem-loop (selenocysteine insertion sequence, SECIS), is recognized as the codon for selenocysteine incorporation.

The mechanism of SelB action on the ribosome is not known in detail. Based on kinetic and affinity measurements (Förster et al., 1990; Thanbichler et al., 2000), it is likely that in the cell practically all SelB is bound in a SelB·GTP·Sec-tRNA^{Sec} complex with the SECIS element. Upon translation, the lower part (10–11 nt) of the SECIS hairpin is expected to melt in order to position the UGA codon in the A site, whereas the intact upper part with SelB may appear just at the mRNA entrance of the ribosomal A site (Hüttenhofer and Böck, 1998b). At the same time, the anticodon of Sec-tRNA^{Sec} may pair with the UGA codon in the A site. By analogy to EF-Tu, codon-anticodon interaction is expected to activate GTP hydrolysis in SelB, although there is no direct evidence for this. Furthermore, the role of the SECIS element in GTPase stimulation, whether as a mere carrier of SelB to the ribosome or a regulatory factor of SelB function on the ribosome, is not clear. SECIS elements bind to SelB domain 4, which consists of four similar winged-helix domains arranged in the shape of an L (Selmer and Su, 2002). The winged-helix domains recognize the hairpin backbone and the nucleotides at the top of the loop of the SECIS element (Yoshizawa et al., 2005; Ose et al., 2007). Taking together the size and shape of domain 4 of SelB (Selmer and Su, 2002), the location of the mRNA entrance tunnel
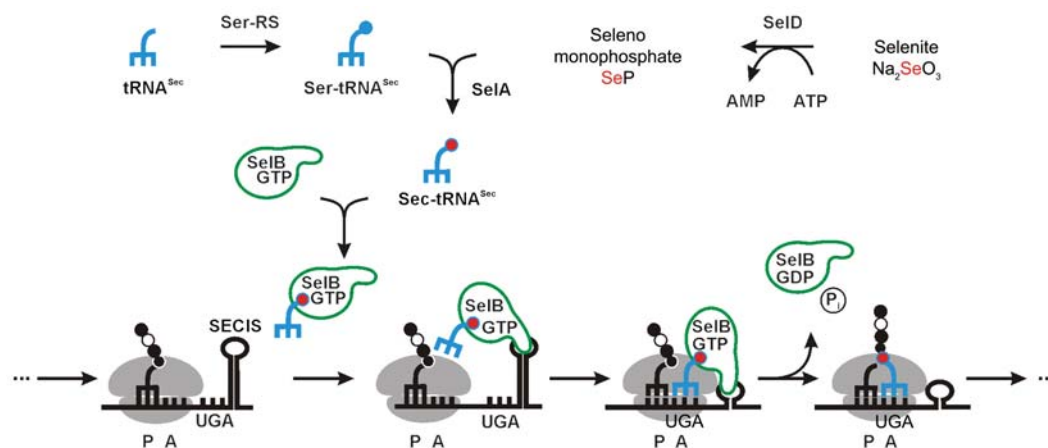
Figure 1 Selenocysteine incorporation into proteins in bacteria. For details, see the text.

(Yusupova et al., 2001), and the position and orientation of the EF-Tu·Phe-tRNA[Phe] complex on the ribosome (Stark et al., 1997, 2002; Valle et al., 2002), domain 4 of SelB has to span a distance of approximately 90 Å between the C-terminus of domain 3 of the factor and the SECIS binding site, compared to approximately 75 Å measured at the diagonal of the L-shaped SelB structure (Selmer and Su, 2002). This may imply that domain 4 opens up to bridge the distance in the ribosome complex with the hairpin (Selmer and Su, 2002). However, other explanations are also possible, e.g., the position of SelB on the ribosome is different from that of EF-Tu, or the interaction of domain 4 with the SECIS element and codon recognition by Sec-tRNA[Sec] take place sequentially, rather than simultaneously. The recently reported crystal structure of SelB domain 4 in complex with the SECIS element suggests that domain 4 may undergo large interdomain conformational changes to confer a positively charged area in domain 4 suitable for binding to an RNA molecule other than the SECIS RNA (Ose et al., 2007).

After GTP hydrolysis, SelB switches to the GDP form, Sec-tRNA[Sec] is released from the factor and is accommodated in the A site, and selenocysteine is incorporated into the nascent peptide. SelB·GDP must dissociate from the ribosome and the SECIS element to allow for translation of the downstream mRNA sequence (Thanbichler and Böck, 2001). However, given the high affinity of SelB·GDP for SECIS (Thanbichler et al., 2000), the mechanism of dissociation is not easy to understand. The molecular details of SelB function on the ribosome are largely deduced from EF-Tu. Given that SelB and EF-Tu have dramatically different nucleotide binding properties (Thanbichler et al., 2000) and the important differences in the structures of the G domains of SelB and EF-Tu (Leibundgut et al., 2004), such analogies may be problematic. To resolve these open questions, a detailed analysis of the events on the ribosome and structural insight into the interactions between the components of the machinery are necessary. Here we describe the experimental approaches used to elucidate the kinetic mechanism of selenocysteine insertion in proteins and to solve the structure of selenocysteine synthase SelA by cryo-EM.

Results and discussion

Fluorescence kinetics studies of selenocysteine incorporation

During protein synthesis in bacterial cells, approximately 10 amino acids are incorporated per ribosome per second. The rate of selenocysteine incorporation appears to be significantly slower, about 0.1 s^{-1} (calculated from Suppmann et al., 1999). Nevertheless, even a reaction as slow as this is completed in less than 10 s, implying that rapid kinetic techniques have to be used to study the kinetics of the reaction. Two main groups of reactions can be studied. First, the rates of the chemical steps, i.e., GTP hydrolysis by SelB and peptide bond formation, can be measured by quench-flow techniques that have been described in detail for EF-Tu (Gromadski and Rodnina, 2004), with only some modifications required for the analysis of selenocysteine-containing peptides (Thanbichler and Böck, 2002). Second, complex formation between various components and conformational changes can be studied by stopped-flow experiments, provided suitable fluorescence reporter groups are attached to the components.

To measure the kinetics of SelB·GTP·Sec-tRNA[Sec] binding to the ribosome, a number of fluorescence-labeled components can be utilized (Figure 2), such as fluorescent derivatives of the P site-bound tRNA, Sec-tRNA[Sec], mRNA, SelB, ribosome, or GTP. Site-specific labeling of the 3′-end of mRNA, tRNA positions in the D loop and at thioU8, as well as random labeling of the ribosomes at surface lysine residues of ribosomal proteins, have been described previously (Wintermeyer and Zachau, 1974; Rodnina et al., 1994a; Savelsbergh et al., 2003; Peske et al., 2005; Milon et al., 2007). Similar to many other tRNAs, tRNA[Sec] contains dihydrouracil at position 20, which can be replaced by the strongly fluorescent proflavin (Wintermeyer and Zachau, 1974). The advantage of this labeling is that the dye usually does not interfere with the functions of the tRNA, but is sensitive to changes in conformation and environment (Rodnina et al., 1994a, 1997; Pape et al., 1999). With conventional elongator aminoacyl-tRNAs, proflavin reports several steps of A-site binding, i.e., initial binding
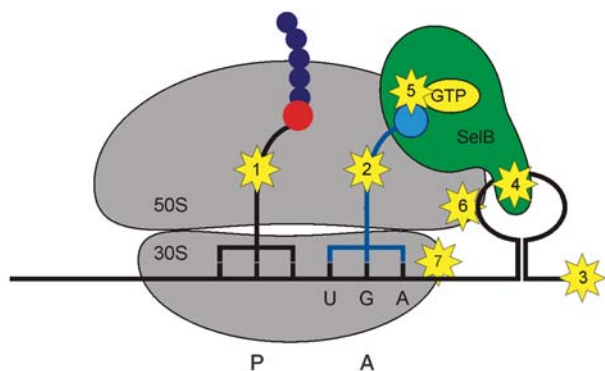
Figure 2 Positions of fluorescent groups attached to components of the selenocysteine insertion machinery.
The dyes are (1) fluorescein, Bodipy, QSY35, or proflavin in P-site tRNA; (2) proflavin attached to position 20 of tRNA^{Sec}; (3) fluorescein at the 3′-end of mRNA; (4) Atto565 coupled to Cys564 in domain 4 of SelB; (5) mant- or Bodipy-GTP/GDP; and (6,7) fluorescein or QSY9 attached randomly at lysine residues of the 50S and 30S subunit, respectively.

of the ternary complex to the ribosome, codon recognition, and accommodation of tRNA in the A site, as assigned on the basis of experiments with different ribosome complexes, non-hydrolyzable GTP analogs, or antibiotics (Rodnina et al., 1994a, 1995). tRNA^{Sec} labeled with proflavin instead of dihydrouracil at position 20 can be aminoacylated and converted to Sec-tRNA^{Sec} with the same efficiency as unmodified tRNA^{Sec} (data not shown).

To label SelB, cysteine residues have to be introduced at the desired positions, which can then be modified using thiol-reactive fluorescent dyes. SelB contains three non-conserved cysteines, and some or all of them have to be removed to achieve site-specific labeling. One of the intrinsic cysteines is located in the G domain of SelB (Cys84), corresponding to the non-conserved Ala108 in *Thermus thermophilus* EF-Tu (Hilgenfeld et al., 1996); Cys84Ala replacement has no effect on the activity of SelB (data not shown). The two other cysteines, Cys564 and Cys568, are located in domain 4 of SelB (*E. coli* numbering). In the crystal structure of *Moorella thermoacetica* SelB (Selmer and Su, 2002), these residues correspond to Thr590 and Gly594, respectively, which are exposed on the surface in the vicinity of the presumed SECIS binding site (Kromayer et al., 1999; Selmer and Su, 2002). Based on the SelB construct with the mutation Cys84Ala, we prepared the double mutant Cys84Ala/Cys568Ser, so that only a single cysteine, Cys564, was available for labeling with a fluorescent dye, Atto565 maleimide. The activity in forming the SelB·GTP·Sec-tRNA^{Sec} complex was measured by nitrocellulose filtration using [^{14}C]Sec-tRNA^{Sec} (Figure 3). The ternary complex was very stable and quantitatively retained on the filter, whereas free [^{14}C]Sec-tRNA^{Sec} passed through the membrane. The affinity of the modified SelB was very similar to that of the wild-type protein, with K_d values of 5±1 and 8±2 nM, respectively. Thus, fluorescence labeling yields SelB preparations that are functionally active and can be used to study SelB binding to the ribosome or conformational changes in the factor upon delivery of selenocysteine into proteins.
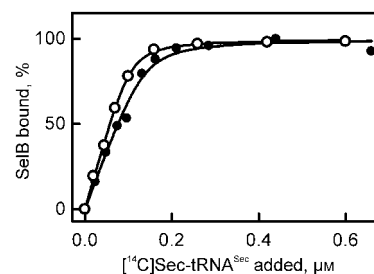

Figure 3 Sec-tRNA^{Sec} binding to SelB (closed circles) and SelB(Cys84Ala, Cys568Ser) labeled with Atto565 dye at Cys564 (open circles) in the presence of GTP.

The role of GTP binding to and hydrolysis by SelB is not known. The conformations of the GTP-bound, GDP-bound, and nucleotide-free forms of archeal SelB are similar (Leibundgut et al., 2004), and Sec-tRNA^{Sec} can bind to SelB irrespective of the presence of a nucleotide (data not shown). To understand the role of GTP hydrolysis by SelB, we studied the incorporation of selenocysteine into peptides on the ribosome in the presence of GTP, GDP, or a non-hydrolyzable GTP analog, GDPNP (Figure 4A). An mRNA with the coding sequence AUGU-GA and a SECIS element at the appropriate distance downstream of the stop codon was used. Although SelB bound Sec-tRNA^{Sec} equally well in the presence of GTP, GDP, or GDPNP, selenocysteine insertion into peptides was strongly impaired or abolished in the presence of GDP or GDPNP, suggesting that GTP binding and hydrolysis were required for SelB function on the ribosome. Nevertheless, even with GTP the incorporation of selenocysteine was quite inefficient (approx. 30%), consistent with *in vivo* data (Suppmann et al., 1999). In comparison, EF-Tu-mediated amino acid incorporation was very efficient (>above 95%), also when a SECIS element was present in the mRNA (data not shown).

To study the interaction of SelB·GTP/GDP with the ribosome, we used a fluorescent derivative of guanine nucleotides, Bodipy-GTP/GDP. The interaction of SelB·Bodipy-GTP/GDP complexes with the ribosomes resulted in a rapid increase in fluorescence that did not depend on the type of nucleotide (Figure 4B). Because
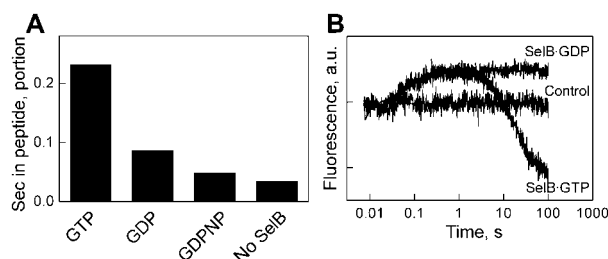

Figure 4 Role of guanine nucleotides.
(A) Effect of guanine nucleotides on selenocysteine incorporation into peptides. SelB·[^{14}C]Sec-tRNA^{Sec} complexes were formed in the presence of the corresponding nucleotide and incubated with ribosome complexes containing mRNA with a SECIS element and a UGA codon at the A site and fMet-tRNA^{fMet} in the P site. fMetSec dipeptides were analyzed by HPLC as previously described (Gromadski and Rodnina, 2004). (B) Time course of SelB·GTP and SelB·GDP binding to ribosome complexes, monitored by fluorescence changes in Bodipy-GTP/GDP. Control, SelB in the absence of ribosomes.

this step is rapid and non-specific, we propose that the fluorescence change reflects the formation of an early complex, comparable to the initial binding complex observed with EF-Tu (Rodnina et al., 1994a), which is dominated by the interactions between SelB and the ribosome. The apparent rate constant of initial complex formation depended linearly on the ribosome concentration (data not shown). The rate constants for SelB·GTP/GDP binding to (k_{on}) and dissociation from (k_{off}) the ribosome were calculated from the slope and the intercept, respectively, of the k_{app} concentration dependence. In the presence of GDP, k_{on}=10 μM^{-1} s^{-1} and k_{off}=10 s^{-1}. With GTP, the stability of the initial complex was increased, with k_{off} decreasing to approximately 1 s^{-1}, and an additional slow step was indicated by a decrease in fluorescence (Figure 4B). At a rate of approximately 0.04 s^{-1}, the fluorescence decrease was still faster than the rate of GTP hydrolysis by SelB on the ribosome, which was 0.003 s^{-1} (Hüttenhofer and Böck, 1998a), and may represent a conformational change in SelB induced by interaction with the ribosome. The rearrangement step is not observed with GDP, suggesting that the conformational change causing the fluorescence decrease does not take place in the absence of GTP. This suggests that the ribosome is capable of discriminating between SelB·GTP and SelB·GDP, despite the similarities in archeal SelB conformations in the GTP and GDP forms (Leibundgut et al., 2004), and efficient binding of both types of complex to the ribosome.

Structural analysis of SelA from *Moorella thermoacetica* by cryo-EM

Structural information about selenocysteine synthase (SelA) has so far been only obtained by two-dimensional (2D) electron-microscopic analysis of negatively stained *E. coli* SelA (*eco*SelA) (Engelhardt et al., 1992). To gain further insight into the molecular architecture, a three-dimensional (3D) reconstruction is needed. However, *eco*SelA binds in preferential orientation to carbon film in negative stain preparations (Engelhardt et al., 1992) and thus does not provide sufficient isotropic views for reliable 3D structure determination at intermediate resolution. Vitrified unstained specimens embedded in amorphous ice usually adopt various orientations and are not subject to the possible artifacts of negatively stained preparations (Frank, 1996). However, first trials showed that bacterial SelA disintegrates upon vitrification under standard preparation conditions. Here we describe a method that allows us to obtain the wide range of particle orientations required for high-resolution structure determination by cryo-EM.

For initial studies by negative stain electron microscopy, SelA from the thermophilic bacterium *Moorella thermoacetica* (*mth*SelA) was stained with the double carbon layer technique using uranyl formate (pH 4.5; Kastner and Luhrmann, 1989) and imaged in the electron microscope at room temperature. Nearly all particle images show *mth*SelA in top-view orientation (Figure 5A). This is in line with previous observations for the highly homologous *eco*SelA (Engelhardt et al., 1992), which was reported to prefer the top-view orientation at low pH, i.e., in the presence of the heavy metal salt uranyl acetate
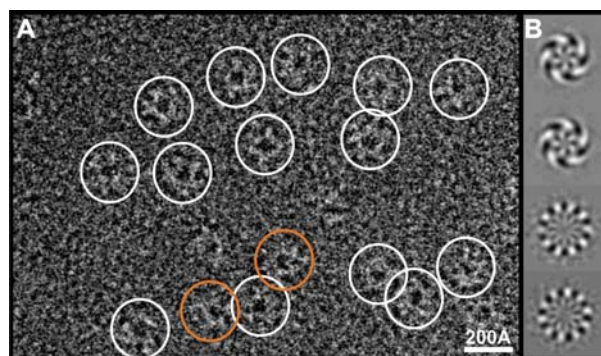

Figure 5 Electron microscopy and symmetry analysis of stained *mth*SelA.
(A) Typical electron micrograph of *mth*SelA stained with uranyl formate showing mainly top-view (white circles) and rarely tilt-view projections (orange circles). (B) Eigenimages one to four (top to bottom) obtained after translational alignment and multivariate statistical analysis of negatively stained *mth*SelA. The first and second eigenimage clearly show a five-fold rotational symmetry. As only a translational alignment was performed, these eigenimages show different in-plane rotations.

(pH 4.8), and the side-on view orientation on staining with uranyl oxalate (pH 6.8).

The 5947 selected particles of stained *mth*SelA were subjected to a reference-free alignment by a classification scheme that led to stable class averages after five iterations. The first eigenimages obtained after translational alignment and subsequent multivariate statistical analysis describe the symmetry aspects of the underlying macromolecular structure (Dube et al., 1993). The present eigenimages clearly show a five-fold rotational symmetry for *mth*SelA (Figure 5B, first and second rows). Class averages for *eco*SelA in earlier studies also suggested a five-fold rotational symmetry (Engelhardt et al., 1992).

For native cryo-EM experiments, *mth*SelA was vitrified with a standard plunger at room temperature. In this case no intact particles were observed in the electron microscope. Chemical fixation of *mth*SelA with paraformaldehyde prior to plunge-freezing yielded intact particles. To our surprise, particles were found nearly exclusively in side-on view orientation (Figure 6A). In contrast, native cryo-EM preparation of non-fixed particles using a controlled environment vitrification system (CEVS; Bellare et al., 1988), at 33°C and 80% humidity resulted in intact particles adopting nearly random orientation (Figure 6B). Since a significant amount of water evaporates during cryo-grid preparation with a standard plunger at room temperature, we expect that *mth*SelA most likely disintegrates upon evaporation due to the rapidly increasing salt concentration and/or cooling of the sample prior to vitrification. In contrast, intact particles can be obtained by (i) reducing evaporation due to high humidity in the CEVS or (ii) stabilization of the complex via cross-linking with paraformaldehyde. For cryopreparations in the CEVS, we are thus able to obtain the desired near-random angular distribution of particles for non-fixed *mth*SelA. Surprisingly, chemical fixation of *mth*SelA forces the particles exclusively into side-on view orientations. This can be explained by changes in the surface charge of the mol-
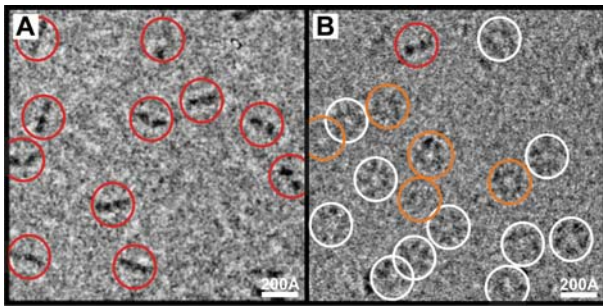
Figure 6 Electron cryomicroscopy of vitrified *mth*SelA.
(A) A typical raw image of *mth*SelA fixed with paraformaldehyde (0.1%) showing particles in side-on-view orientation only. (B) Typical image of non-fixed *mth*SelA, vitrified in a controlled environment vitrification system at 33°C and 80% humidity. Top-view, tilt-view and side-on-view projections are indicated by white, orange and red circles, respectively.

ecules upon paraformaldehyde treatment, which plays an important role in orienting the molecules at the air-water interface on the grid prior to vitrification.

A total of 5602 non-fixed particles were selected from micrographs recorded at liquid nitrogen temperature. Typical class averages for vitrified *mth*SelA with improved signal-to-noise ratio were obtained after alignment by classification, multiple rounds of multi-reference alignment, multivariate statistical analysis and classification (van Heel et al., 1996). Six class averages exhibiting different tilts with respect to the image plane are shown in Figure 7A. Accordingly, *mth*SelA has a ring-like structure with five bilobed wings. *mth*SelA has an overall diameter of 190 Å and a height of 65 Å (Figure 7B). *mth*SelA is thus very similar in shape and size to *eco*SelA (Engelhardt et al., 1992), in line with the sequence conservation and conserved reaction mechanism of bacterial seleno-cysteine synthases (Tormay et al., 1998). Similarly to *eco*SelA, *mth*SelA is likely to form a homodecamer with a molecular mass of 506 kDa constituted of five dimeric subunits (Engelhardt et al., 1992). The wide range of orientations observed here for vitrified, non-fixed *mth*SelA, in conjunction with its five-fold symmetry, should facilitate future 3D structure determination by the angular reconstruction technique (van Heel, 1987).
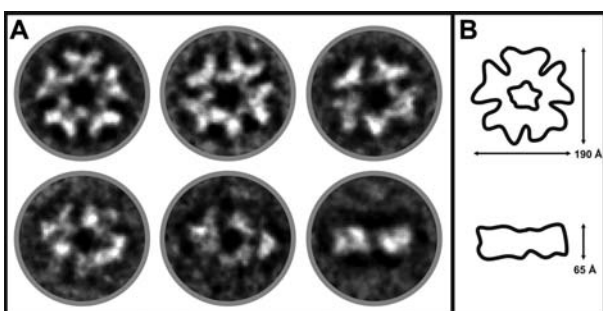

Figure 7 2D analysis of vitrified, non-fixed *mth*SelA.
(A) Class averages revealing a broad range of orientations of vitrified *mth*SelA. *mth*SelA has a ring structure with five bilobed wings and is most likely present as a homodecamer. (B) Dimensions of *mth*SelA in top-view (top) and side-on-view orientation (bottom).

Materials and methods

Purification of SelA from *M. thermoacetica*

*mth*SelA was expressed at 37°C for 18 h from the plasmid pCTA104 (Tormay et al., 1998) in *E. coli* DH5α cells. The cell pellet was resuspended in buffer A [50 mM potassium phosphate, pH 7.5, 3 mM dithiothreitol (DTT), 0.5 mM EDTA, 250 mM ammonium sulfate and 10 mM pyridoxal phosphate], and lysed by sonication. The clarified lysate was heated for 15 min to 70°C and the precipitate was removed by centrifugation. *mth*SelA was collected in the flow-through of a Q-Sepharose-FF column (GE Healthcare, Munich, Germany) equilibrated with buffer A and precipitated by addition of solid ammonium sulfate to 55% saturation. The protein pellet was resuspended in buffer A and purified on a Superdex 200 column (GE Healthcare) equilibrated with buffer A. *mth*SelA fractions were concentrated by ultrafiltration, aliquoted and quick-frozen in liquid nitrogen for storage at -80°C.

Mutagenesis, protein production, fluorescence labeling, and purification of SelB

To construct SelB variants for fluorescence labeling, cysteines at positions 84 and 568 were substituted by alanine and serine, respectively. Mutations were generated in the plasmid pT7SelBH6 coding for SelB extended by six histidines at the C-terminus (Thanbichler and Böck, 2003) by the QuikChange method using Pfu polymerase (Promega, Madison, WI, USA) and confirmed by DNA sequencing. SelB mutants were expressed in *E. coli* BL21(DE3) cells and purified on Ni-NTA agarose under non-denaturing conditions according to the manufacturer's protocol. The protein purity was better than 90% according to SDS-PAGE. For fluorescence labeling, a solution of SelB containing a single cysteine was diluted to 50 μM and the reducing agent (2-mercaptoethanol) was removed by extensive dialysis at 4°C against labeling buffer B (50 mM HEPES, pH 7.0, 500 mM KCl, 5 mM MgCl$_2$, 10% glycerol). Disulfide bond formation was suppressed by treatment for 10 min at 37°C with a 10-fold molar excess of Tris(2-carboxyethyl) phosphine hydrochloride (TCEP; Sigma, St. Louis, MO, USA), a reducing agent that does not compete with thiol modification. Labeling was carried out with a 15-fold molar excess of Atto565 maleimide (Atto-Tec) over the protein at 4°C overnight. Unreacted dye was removed by size-exclusion centrifugation (molecular mass cutoff of 30 kDa; Amicon, Houston, TX, USA).

Biochemical methods

Ribosomes from *E. coli* MRE600, initiation factors, and f[³H]Met-tRNA^{fMet} were prepared as previously described (Rodnina et al., 1994b, 1995, 1999). mRNA (mLP75s) was a derivative of AH75 (Hüttenhofer et al., 1996), modified to have a stronger Shine-Dalgarno sequence and a single AUG codon in all reading frames. The sequence of mLP75s mRNA is 5′-GGG CUA AAU UAA GGA GGU UCA UUA **AUG UGA** CAC GGC CCA UCG G*UU* GCA G*GU* CUG CAC CAA UCG GUC GGU AUU-3′, where the start AUG and the recoding UGA codons are in bold, and the SelB recognition nucleotides in the *fdhF* SECIS element are italicized. mRNA was prepared by T7 RNA polymerase transcription. To attain correct folding, the mRNA was heated in the presence of 100 μM EDTA for 90 s at 80°C and then rapidly cooled on ice. Ribosome initiation complexes were formed in buffer C (50 mM HEPES, pH 7.5, 70 mM NH$_4$Cl, 30 mM KCl, 7 mM MgCl$_2$, 2 mM DTT) by incubating 70S ribosomes (1 μM) with mLP75s mRNA (2 μM), f[³H]Met-tRNA^{fMet} (1.6 μM), initiation factors 1, 2 and 3 (1.5 μM each), and GTP (1 mM) for 70 min at 37°C. Ribosome complexes were purified and concentrated by

centrifugation through a 1.1 M sucrose cushion prepared in buffer C at 259 000 *g* for 2 h on a Sorvall M120GX ultracentrifuge. Binding of f[³H]Met-tRNA^fMet to the P site was quantitated by nitrocellulose filtration.

SelD was a gift from A. Böck. tRNA^Sec was prepared as previously described (Kothe et al., 2006). tRNA^Sec (10 μM) was aminoacylated by seryl-tRNA synthetase (6 μM), [¹⁴C]-serine (30 μM), ATP (4.5 mM), and inorganic pyrophosphatase (0.01 U/μl; Sigma) in buffer C for 60 min at 37°C. Ser-tRNA^Sec was isolated by phenol extraction using potassium acetate-saturated phenol, pH 4.6, and ethanol-precipitated. To convert Ser-tRNA^Sec into Sec-tRNA^Sec, selenite (Na₂SeO₃, 250 μM) was activated to selenomonophosphate by SelD (10 μM) and ATP (4.5 mM), and the Ser-to-Sec conversion was catalyzed by SelA (5 μM) in buffer C for 40 min at 37°C. Sec-tRNA^Sec was phenol-extracted using potassium acetate-saturated phenol, pH 4.6, ethanol-precipitated, and dissolved in 10 mM potassium acetate, pH 4.6, and 5 mM DTT. The extent of conversion was verified by thin-layer chromatography on TLC plates (Thanbichler and Böck, 2002).

The ternary complex SelB·GTP·[¹⁴C]Sec-tRNA^Sec was prepared in buffer C with 5 mM MgCl₂ by mixing [¹⁴C]Sec-tRNA^Sec (concentrations as indicated in Figure 3) with SelB (0.10–0.15 μM) in the presence of GTP (0.2 mM) and incubated for 5 min at 25°C. Ternary complex formation was assayed by nitrocellulose filtration. The data were evaluated by non-linear fitting to a quadratic equation describing ligand binding to one site using Prism 4 (GraphPad Software, San Diego, CA, USA).

Kinetic experiments

Fluorescence changes in Bodipy-GTP/GDP were monitored in a stopped-flow apparatus (SX-18MV spectrometer; Applied Photophysics, Leatherhead, UK) using an excitation wavelength of 470 nm and a 500-nm cutoff filter (KV 500; Schott, Mainz, Germany). SelB (0.2 μM) with Bodipy-GTP/GDP (4 μM) was mixed with ribosome complexes (0.7 μM) in buffer C with 5 mM MgCl₂ and time courses were measured at 25°C.

Electron microscopy and image processing

All experiments were performed at room temperature unless indicated otherwise. For negative staining with 2% (w/v) uranyl formate, the sample was diluted to 18 μg/ml with buffer D (10 mM HEPES, pH 7.5, 100 mM NaCl, 2 mM DTT), sonicated for 10 min and stained with the double carbon layer technique (Kastner and Luhrmann, 1989).

To prepare samples for electron cryomicroscopy, 20 μg/ml *mth*SelA was incubated for 1 h with 0.1% paraformaldehyde for fixation at 4°C and vitrified with the standard plunger at room temperature. Alternatively, 20 μg/ml non-fixed *mth*SelA was vitrified manually using a CEVS (custom-made by the institute's workshop; Bellare et al., 1988). Humidity in the containment system was adjusted to 80% at a temperature of 33°C.

Images of stained and vitrified particles were recorded with a Philips CM200 FEG electron microscope (200 kV, magnification 50 000×) using a Philips holder at room temperature and a Gatan cryoholder at liquid nitrogen temperature, respectively. Images were taken under low-dose conditions at 0.5–1.2 μm defoci for the stained particles and 1.5–5 μm for the vitrified particles on Kodak SO-163 film and were scanned with a rotating drum scanner (Heidelberger Druckmaschinen, Heidelberg, Germany) using a step size of 21 μm. The final pixel size corresponds to 4.233 Å on the specimen scale. A total of 5947 single-particle images of stained *mth*SelA and 5602 of non-fixed vitrified *mth*SelA were processed with the IMAGIC-5 software (van Heel et al., 1996) using corrims-based alignment via polar coordinates (Sander et al., 2003). Each data set was subjected to an alignment by classification procedure (Dube et al., 1993), followed by multivariate statistical analysis and classification. The resulting class averages were used as references in subsequent rounds of refinement until stable class averages were obtained.

References

Baron, C. and Böck, A. (1991). The length of the aminoacyl-acceptor stem of the selenocysteine-specific tRNA(Sec) of *Escherichia coli* is the determinant for binding to elongation factors SELB or Tu. J. Biol. Chem. *266*, 20375–20379.

Baron, C. and Böck, A. (1995). The selenocysteine-inserting tRNA species: structure and function. In: tRNA: Structure, Biosynthesis, and Function, D. Söll and U. RajBhandary, eds. (Washington, DC, USA: American Society for Microbiology), pp. 529–544.

Baron, C., Heider, J., and Böck, A. (1990). Mutagenesis of *selC*, the gene for the selenocysteine-inserting tRNA-species in *E. coli*: effects on *in vivo* function. Nucleic Acids Res. *18*, 6761–6716.

Bellare, J.R., Davis, H.T., Scriven, L.E., and Talmon, Y. (1988). Controlled environment vitrification system: an improved sample preparation technique. J. Electron Microsc. Tech. *10*, 87–111.

Böck, A., Forchhammer, K., Heider, J., and Baron, C. (1991). Selenoprotein synthesis: an expansion of the genetic code. Trends Biochem. Sci. *16*, 463–467.

Dube, P., Tavares, P., Lurz, R., and van Heel, M. (1993). The portal protein of bacteriophage SPP1: a DNA pump with 13-fold symmetry. EMBO J. *12*, 1303–1309.

Engelhardt, H., Forchhammer, K., Müller, S., Goldie, K.N., and Böck, A. (1992). Structure of selenocysteine synthase from *Escherichia coli* and location of tRNA in the seryl-tRNA^sec-enzyme complex. Mol. Microbiol. *6*, 3461–3467.

Förster, C., Ott, G., Forchhammer, K., and Sprinzl, M. (1990). Interaction of a selenocysteine-incorporating tRNA with elongation factor Tu from *E. coli*. Nucleic Acids Res. *18*, 487–491.

Frank, J. (1996). Three-dimensional Electron Microscopy of Macromolecular Assemblies (New York, USA: Academic Press).

Gromadski, K.B. and Rodnina, M.V. (2004). Kinetic determinants of high-fidelity tRNA discrimination on the ribosome. Mol. Cell *13*, 191–200.

Hilgenfeld, R., Böck, A., and Wilting, R. (1996). Structural model for the selenocysteine-specific elongation factor SelB. Biochimie *78*, 971–978.

Hüttenhofer, A. and Böck, A. (1998a). Selenocysteine inserting RNA elements modulate GTP hydrolysis of elongation factor SelB. Biochemistry *37*, 885–890.

Hüttenhofer, A. and Böck, A. (1998b). Selenoprotein synthesis. In: RNA Structure and Function (Cold Spring Harbor, NY, USA: Cold Spring Harbor Laboratory Press), pp. 603–639.

Hüttenhofer, A., Heider, J., and Böck, A. (1996). Interaction of the *Escherichia coli fdhF* mRNA hairpin promoting seleno-cysteine incorporation with the ribosome. Nucleic Acids Res. *24*, 3903–3910.

Kastner, B. and Luhrmann, R. (1989). Electron microscopy of U1 small nuclear ribonucleoprotein particles: shape of the particle and position of the 5′ RNA terminus. EMBO J. *8*, 277–286.

Kothe, U., Paleskava, A., Konevega, A.L., and Rodnina, M.V. (2006). Single-step purification of specific tRNAs by hydro-phobic tagging. Anal. Biochem. *356*, 148–150.

Kromayer, M., Neuhierl, B., Friebel, A., and Böck, A. (1999). Genetic probing of the interaction between the translation factor SelB and its mRNA binding element in *Escherichia coli*. Mol. Gen. Genet. *262*, 800–806.

Leibundgut, M., Frick, C., Thanbichler, M., Böck, A., and Ban, N. (2004). Selenocysteine tRNA-specific elongation factor SelB is a structural chimera of elongation and initiation factors. EMBO J. *24*, 11–22.

Milon, P., Konevega, A.L., Peske, F., Fabbretti, A., Gualerzi, C.O., and Rodnina, M.V. (2007). Transient kinetics, fluorescence, and FRET in studies of initiation of translation in bacteria. Methods Enzymol., in press.

Ose, T., Soler, N., Rasubala, L., Kuroki, K., Kohda, D., Fourmy, D., Yoshizawa, S., and Maenaka, K. (2007). Structural basis for dynamic interdomain movement and RNA recognition of the selenocysteine-specific elongation factor SelB. Structure *15*, 577–586.

Pape, T., Wintermeyer, W., and Rodnina, M.V. (1999). Induced fit in initial selection and proofreading of aminoacyl-tRNA on the ribosome. EMBO J. *18*, 3800–3807.

Peske, F., Rodnina, M.V., and Wintermeyer, W. (2005). Sequence of steps in ribosome recycling as defined by kinetic analysis. Mol. Cell *18*, 403–412.

Rodnina, M.V., Fricke, R., and Wintermeyer, W. (1994a). Transient conformational states of aminoacyl-tRNA during ribosome binding catalyzed by elongation factor Tu. Biochemistry *33*, 12267–12275.

Rodnina, M.V., Semenkov, Y.P., and Wintermeyer, W. (1994b). Purification of fMet-tRNA^fMet^ by fast protein liquid chromato-graphy. Anal. Biochem. *219*, 380–381.

Rodnina, M.V., Fricke, R., Kuhn, L., and Wintermeyer, W. (1995). Codon-dependent conformational change of elongation fac-tor Tu preceding GTP hydrolysis on the ribosome. EMBO J. *14*, 2613–2619.

Rodnina, M.V., Savelsbergh, A., Katunin, V.I., and Wintermeyer, W. (1997). Hydrolysis of GTP by elongation factor G drives tRNA movement on the ribosome. Nature *385*, 37–41.

Rodnina, M.V., Savelsbergh, A., Matassova, N.B., Katunin, V.I., Semenkov, Y.P., and Wintermeyer, W. (1999). Thiostrepton inhibits the turnover but not the GTPase of elongation factor G on the ribosome. Proc. Natl. Acad. Sci. USA *96*, 9586–9590.

Sander, B., Golas, M.M., and Stark, H. (2003). Corrim-based alignment for improved speed in single-particle image pro-cessing. J. Struct. Biol. *143*, 219–228.

Savelsbergh, A., Katunin, V.I., Mohr, D., Peske, F., Rodnina, M.V., and Wintermeyer, W. (2003). An elongation factor G-induced ribosome rearrangement precedes tRNA-mRNA transloca-tion. Mol. Cell *11*, 1517–1523.

Schön, A., Böck, A., Ott, G., Sprinzl, M., and Soll, D. (1989). The selenocysteine-inserting opal suppressor serine tRNA from *E. coli* is highly unusual in structure and modification. Nucleic Acids Res. *17*, 7159–7165.

Selmer, M. and Su, X.D. (2002). Crystal structure of an mRNA-binding fragment of *Moorella thermoacetica* elongation factor SelB. EMBO J. *21*, 4145–4153.

Stark, H., Orlova, E.V., Rinke-Appel, J., Jünke, N., Mueller, F., Rodnina, M.V., Wintermeyer, W., Brimacombe, R., and van Heel, M. (1997). Arrangement of tRNAs in pre- and posttrans-locational ribosomes revealed by electron cryomicroscopy. Cell *88*, 19–28.

Stark, H., Rodnina, M.V., Wieden, H.-J., Zemlin, F., Wintermeyer, W., and van Heel, M. (2002). Ribosome interactions of amino-acyl-tRNA and elongation factor Tu in the codon recognition complex. Nat. Struct. Biol. *9*, 849–854.

Suppmann, S., Persson, B.C., and Böck, A. (1999). Dynamics and efficiency *in vivo* of UGA-directed selenocysteine inser-tion at the ribosome. EMBO J. *18*, 2284–2293.

Thanbichler, M. and Böck, A. (2001). Functional analysis of pro-karyotic SELB proteins. Biofactors *14*, 53–59.

Thanbichler, M. and Böck, A. (2002). Selenoprotein biosynthesis: purification and assay of components involved in selenocys-teine biosynthesis and insertion in *Escherichia coli*. Methods Enzymol. *347*, 3–16.

Thanbichler, M. and Böck, A. (2003). Purification and character-ization of hexahistidine-tagged elongation factor SelB. Pro-tein Expr. Purif. *31*, 265–270.

Thanbichler, M., Böck, A., and Goody, R.S. (2000). Kinetics of the interaction of translation factor SelB from *Escherichia coli* with guanosine nucleotides and selenocysteine insertion sequence RNA. J. Biol. Chem. *275*, 20458–20466.

Tormay, P., Wilting, R., Lottspeich, F., Mehta, P.K., Christen, P., and Bock, A. (1998). Bacterial selenocysteine synthase-structural and functional properties. Eur. J. Biochem. *254*, 655–661.

Valle, M., Sengupta, J., Swami, N.K., Grassucci, R.A., Burkhardt, N., Nierhaus, K.H., Agrawal, R.K., and Frank, J. (2002). Cryo-EM reveals an active role for aminoacyl-tRNA in the accom-modation process. EMBO J. *21*, 3557–3567.

van Heel, M. (1987). Angular reconstitution: a posteriori assign-ment of projection directions for 3D reconstruction. Ultra-microscopy *21*, 111–123.

van Heel, M., Harauz, G., Orlova, E.V., Schmidt, R., and Schatz, M. (1996). A new generation of the IMAGIC image processing system. J. Struct. Biol. *116*, 17–24.

Wintermeyer, W. and Zachau, H.G. (1974). Replacement of odd bases in tRNA by fluorescent dyes. Methods Enzymol. *29*, 667–673.

Yoshizawa, S., Rasubala, L., Ose, T., Kohda, D., Fourmy, D., and Maenaka, K. (2005). Structural basis for mRNA recognition by elongation factor SelB. Nat. Struct. Mol. Biol. *12*, 198–203.

Yusupova, G.Z., Yusupov, M.M., Cate, J.H., and Noller, H.F. (2001). The path of messenger RNA through the ribosome. Cell *106*, 233–241.

Paper 3

Thermodynamic and Kinetic Framework of Selenocysteinyl-tRNA[Sec] Recognition by Elongation Factor SelB

Alena Paleskava[1,2], Andrey L. Konevega[1], Marina V. Rodnina[1,2]*

[1] Department of Physical Biochemistry, Max-Planck-Institute for Biophysical Chemistry, 37077 Göttingen, Germany,

[2] Institute of Physical Biochemistry, University of Witten/Herdecke, 58448 Witten, Germany

*To whom correspondence should be addressed. Tel. 49-2302-926205; Fax. 49-2302-926117; E-mail: rodnina@mpibpc.mpg.de

SelB is a specialized translation elongation factor which delivers selenocysteinyl-tRNA[Sec] (Sec-tRNA[Sec]) to the ribosome. The mechanism of specific selection Sec-tRNA[Sec] by SelB·GTP and the release of the tRNA upon GTP hydrolysis is not known. Here we show that although Sec-tRNA[Sec] can bind tightly to SelB in the presence of GTP, GDP, or in the absence of the nucleotide, the affinity of Sec-tRNA[Sec] binding to SelB·GTP ($K_d = 0.3$ pM) is more than a million-fold higher than that to the GDP-bound or the apo-form of the factor ($K_d = 0.4\text{-}0.5$ μM). The high selectivity for SelB·GTP is restricted to Sec-tRNA[Sec], whereas Ser-tRNA[Sec] and deacylated tRNA[Sec] bind to all forms of SelB with the same affinity. The tight binding of Sec-tRNA to SelB·GTP correlates with the net formation of four ion pairs, three of which seem to involve Sec, and is enthropically driven. The Sec-tRNA[Sec]·SelB·GTP complex also kinetically very stable, with the half-life time in the hours range ($k_{off} = 10^{-3}$ s^{-1}). GTP hydrolysis increases the dissociation rate constant by more than a million ($k_{off} = 230$ s^{-1}), which explains why GTP hydrolysis is required for the delivery of Sec-tRNA[Sec] to the ribosome and why Sec-tRNA[Sec] is released from SelB·GDP despite of the high thermodynamic stability of the complex. The tRNA-binding properties of SelB are reminiscent of those of another specialized factor, eukaryotic translation initiation factor eIF2γ, rather than those of EF-Tu, the common delivery factor for all other aminoacyl-tRNAs, supporting the idea of the common evolutionary ancestry of SelB and eIF2.

_____

SelB is a specialized translation elongation factor responsible for incorporation of selenocysteine (Sec) into proteins. SelB specifically recognizes selenocysteinyl-tRNA, Sec-tRNA[Sec], but not other aminoacyl-tRNAs (aa-tRNAs) (1). In bacteria, tRNA[Sec] is charged with serine by seryl-tRNA synthetase, but the resulting Ser-tRNA[Sec] is not recognized by the translation elongation factor EF-Tu and is not used for translation. Rather, the seryl residue is converted to a selenocysteinyl by the pyridoxal phosphate-containing enzyme selenocysteine synthase (the _selA_ gene product) using selenomonophosphate as the selenium donor substrate (2). The latter is synthesized from selenite and ATP by selenophosphate synthetase (the _selD_ gene product). Finally, Sec-tRNA[Sec] is recognized by SelB, which delivers it to the ribosomes translating mRNAs for selenoproteins. Incorporation of Sec is encoded by a combination of an internal UGA stop codon and a specific mRNA hairpin structure, the SECIS (selenocysteine inserting sequence) located downstream of the UGA codon. In bacteria, SelB binds to the SECIS element directly, without help of auxillary proteins, and targets Sec-tRNA[Sec] to the specific UGA codon (3,4).

SelB shares sequence homology with other translation factors that carry aa-tRNAs to the ribosome, such as EF-Tu which binds all elongator aa-tRNA except for Sec-tRNA[Sec], or eukaryotic eIF2γ which is specific for the initiator Met-tRNA[i], as well as with initiation factors IF2/eIF5B (5,6). SelB consists of four domains arranged in a "chalice"-like fashion (7). SelB domains I (the GTP binding domain), II, and III have the same secondary structure elements as the respective domains of EF-Tu, provide most of the contact surface for Sec-tRNA[Sec], and are conserved among bacteria, archaea, and eukaryotes. The specificity of SelB for tRNA[Sec] is likely determined by the unusual length of the acceptor arm of tRNA[Sec] which is formed by an 8-base pair (bp) acceptor stem and a 5-bp T stem in bacteria (8). Nucleotide-binding properties of SelB (9) differ markedly from those of EF-Tu (10), and rather resemble those of EF-G or IF2 (11,12). The affinities of SelB from _Escherichia coli_ for GTP and GDP are 0.7 μM and 13 μM, respectively (9). The rate of GDP dissociation from SelB is high, 15 s^{-1}. Thus, under _in vivo_ conditions, nucleotide exchange is likely to occur rapidly and spontaneously, explaining the absence of a respective nucleotide exchange factor. In contrast to EF-Tu which undergoes large structural rearrangement when GTP is hydrolyzed to GDP, domains I-III in SelB from _Methanococcus maripaludis_ adopt a similar, GTP-like conformation in the presence of GTP, GDP, or in the absence of the nucleotide (7), in line with the notion that SelB is able to bind Sec-tRNA[Sec] not only in the GTP- but also the apo- and GDP-bound form (1,7). This raises the questions of whether and how the GTP form of SelB is specifically recognized by Sec-tRNA[Sec]. The structure of the SelB complex with Sec-tRNA[Sec] is not available.

1

The structure of domain IV of SelB, which has no analog in EF-Tu or other translational GTPases, is not conserved between pro- and eukaryotes (7,13,14). In bacteria, winged-helix motifs of SelB domain IV recognize the hairpin backbone and nucleotides extruded from the helix of the SECIS (13). *E. coli* SelB binds to SECIS elements very rapidly, with an association rate constant close to the diffusion-controlled limit, and very tightly, with a K_d of the SelB·SECIS complex of about 1 nM (9). The affinity does not depend on the nucleotide (GTP or GDP) bound to the domain I of SelB. Also the affinity of GTP/GDP to SelB does not depend on the presence of a SECIS element, indicating that the respective binding sites do not influence each other (9). In contrast, binding of Sec-tRNA^{Sec} to SelB increased the affinity of the factor to SECIS elements, indicating interplay between the two RNA binding sites (9).

The current model of SelB action on the ribosome is largely based on analogy to EF-Tu. Domains I-III of SelB are expected to bind to the ribosome in a similar fashion as EF-Tu (15-18); in this arrangement, domain IV of SelB spans between the factor binding site and the mRNA entrance tunnel on the 30S subunit (19,20). After GTP hydrolysis, Sec-tRNA^{Sec} should be released from the factor and accommodate in the A site of the ribosome, while SelB·GDP dissociates from the ribosome (21). The release of aa-tRNA from EF-Tu·GDP is rapid and spontaneous, because the affinity of aminoacyl-tRNA for EF-Tu·GDP is very low and thus GTP hydrolysis by EF-Tu can be considered as an all-or-none switch for the release of aminoacyl-tRNA. However, given the sizable affinity of Sec-tRNA^{Sec} to SelB in the GDP-bound form (1,7), the mechanism of dissociation of SelB·GDP·Sec-tRNA^{Sec} complex is less easy to understand. In fact, GTP hydrolysis by SelB is required for selenocysteine incorporation into peptides (22); however, the role of GTP hydrolysis is not known.

In this work, we measured the equilibrium dissociation constants (K_d) as well as association and dissociation rate constants (k_{on} and k_{off}) of interactions between Sec-tRNA^{Sec}, Ser-tRNA^{Sec} and deacylated tRNA^{Sec} with SelB in complexes with GTP, GDP, or in the absence of the nucleotide. We determined the effect of the guanine nucleotide on the affinity of SelB to Sec-tRNA^{Sec} and develop a thermodynamic and kinetic framework for the formation of the ternary complex. We further estimate the contributions of Sec and of the tRNA^{Sec} molecule to the interaction with SelB, provide some insights into the nature of binding contacts, and explain why Sec-tRNA^{Sec} is released to the ribosome after GTP hydrolysis by SelB despite the high affinity of Sec-tRNA^{Sec} to SelB·GDP.

EXPERIMENTAL PROCEDURES

Buffers and reagents-All experiments were performed in buffer A (50 mM HEPES, pH 7.5, 70 mM NH$_4$Cl, 30 mM KCl, 5 mM MgCl$_2$, 2 mM DTT)

2

if not stated otherwise. GDP was purified on MonoQ (5/50 GL, Amersham Biosciences) (11).

Purification of SelA, SelB, SelD, and SerRS-All proteins were expressed in BL21(DE3) cells. The plasmid coding for *E. coli* SelA carried the *selA* gene inserted via NdeI/BamHI sites into pET22b(+); the plasmid was a gift from M. Wahl (Free University of Berlin). Cells were opened in buffer B (10 mM HEPES, pH 7.5, 3 mM DTT, 0.5 mM EDTA, 10 µM pyridoxal 5-phosphate). Solid ammonium sulfate was added to cleared cells extract up to 25% saturation at 0 °C. The precipitated proteins were collected by centrifugation, resolubilized and dialyzed against 2 liters of buffer B. The SelA was purified on a Sephacryl S300 gel filtation column in buffer B. Fractions containing pure protein were pooled, concentrated, and stored at -80 °C.

SelB was expressed from the plasmid pT7SelBH6 coding for SelB extended by six histidines at the C-terminus (23); the construct was a gift from A. Böck (LMU Munich). SelB was expressed and purified on the Ni-NTA agarose under non-denaturing conditions according to the manufacturer's protocol. Protein was dialyzed for 12 hours against 2 liters of buffer C (50 mM HEPES, pH 7.5, 400 mM KCl, 5 mM MgCl$_2$, 2 mM DTT, 20% glycerol) and stored at -80 °C. The protein purity was better than 95% according to SDS-PAGE. Protein concentration was determined spectroscopically at 280 nm (ϵ_{SelB} = 81080 M^{-1}cm^{-1}). The protein activity was approximately 85% in Sec-tRNA^{Sec} binding assay (22). SelB preparation was free of GTP and GDP as determined by HPLC analysis (24).

The plasmid coding for *E. coli* SelD was a kind gift from M. Wahl (Free University of Berlin). The *selD* gene was inserted into pETM-ZZ. SelD extended by the N-terminal histidine-ZZ double tag was expressed and purified on a Ni-NTA agarose under non-denaturing conditions according to the manufacturer's protocol. The protein was dialyzed for 12 hours against 2 liters of buffer A and stored at -80 °C.

SerRS extended by six histidines at the C-terminus was encoded by the pT7SerRS plasmid under the control of T7 promoter. SerRS was expressed and purified on the Ni-NTA agarose under non-denaturing conditions according to the manufacturer's protocol. Protein was dialyzed for 12 hours against 2 liters of buffer D (50 mM HEPES, pH 7.5, 70 mM NH$_4$Cl, 100 mM KCl, 10 mM MgCl$_2$, 2 mM DTT) and stored at -80 °C.

Preparation of tRNA^{Sec}-tRNA^{Sec} was overexpressed in *E. coli* BL21(DE3) strain transformed with the pCB2013 plasmid containing *selC* gene under the control of its own promoter (25); the plasmid was a gift from A. Böck (LMU Munich). Total tRNA was prepared by standard phenol extraction (26) and tRNA^{Sec} was purified as previously described (27). Fluorescence-labeled tRNA^{Sec}(Prf20) was prepared according to the protocol described for tRNA^{Phe} (28,29).

DNA template for preparation of tRNA^{Sec} construct by T7-RNA polymerase transcription was generated by PCR using plasmid pCB2013 and two primers, HT7tSec (5'-ATATTAAGCTTTAATAC-GACTCACTATAGGAAGATCGTCGTCTC-3') and tSec (5'-TGGCGGAAGATCAC-3'). The resulting products were analyzed by agarose gel electrophoresis. tRNA^{Sec} was produced by T7-RNA polymerase transcription and purified under non-denaturing conditions on MonoQ (5/50 GL, Amersham Biosciences) (30)

Ser-tRNA^{Sec} was prepared as previously described (22). To prepare Sec-tRNA^{Sec}, aminoacylation of tRNA^{Sec} and conversion of Ser-tRNA^{Sec} to Sec-tRNA^{Sec} were carried out as described, except that SelB was present in the reaction to improve the yield of Sec-tRNA^{Sec}. The reaction mixture contained tRNA^{Sec} (10 µM), SerRS (6 µM), [^{3}H]- or [^{14}C]-serine (30 µM), ATP (5 mM), inorganic pyrophosphatase (0.01 U/µl), SelA (3 µM), SelD (10 µM), Na$_2$SeO$_3$ (250 µM), SelB (6 µM) and GTP (2 mM) in buffer A with 7 mM MgCl$_2$. After incubation for 60 min at 37ºC, Sec-tRNA^{Sec} was phenol-extracted using potassium acetate-saturated phenol, pH 4.6, ethanol-precipitated, dissolved in 10 mM potassium acetate, pH 4.6, and 4 mM DTT, and purified by gel filtration on Superdex 75 (HiLoad 26/60, Pharmacia). The extent of conversion was verified by thin layer chromatography on TLC plates (25) and in the SelB binding assay.

Equilibrium titrations-Interaction of SelB in apo-, GDP-, GDPNP-, and GTP-bound forms with [^{14}C] or [^{3}H] labeled Sec-tRNA^{Sec} were studied in buffer A at 25ºC if not stated otherwise. Constant amounts of Sec-tRNA^{Sec} were mixed with varying amounts of SelB in the presence or absence of guanine nucleotides and incubated for 15 min. For reactions with low protein amounts (<1 pmol), 50 µg of BSA (Fermentas) was added to the reactions to prevent unspecific adsorption of the protein to the tube walls. The dependence of the K_d value for SelB·GTP·Sec-tRNA^{Sec} on the ionic strength was determined in buffer A containing 150, 250, 350, 450, and 525 mM KCl instead of 70 mM NH$_4$Cl and 30 mM KCl at 37ºC. The temperature dependence of binding was measured in buffer A containing 330, 380, 430, and 480 mM KCl at 20ºC, 25ºC, 30ºC, and 37ºC. The amount of [^{14}C]Sec or [^{3}H]Sec bound to SelB was determined by filtration through nitrocellulose filters (0.45 µm, Sartorius). Filters were dissolved and radioactivity measured in Quickszint 361 scintillation cocktail (Zinsser Analytic). The data were evaluated by non-linear fitting to a quadratic equation describing ligand binding to one site using Prism 5 (GraphPad Software, San Diego, CA, USA). Equilibrium titrations with fluorescence-labeled deacylated or Ser-tRNA^{Sec}(Prf20) were carried out in a PTI fluorimeter (excitation at 470 nm, emission at 510 nm). Increasing concentrations of SelB in the absence or presence of guanine nucleotide (2 mM) was added to a constant amount of tRNA^{Sec}(Prf20) or

Ser-tRNA^{Sec} aminoacylated *in situ* (0.05 µM) and the increase of Prf fluorescence was monitored. The dependence of the K_d value for SelB·GTP·Ser-tRNA^{Sec}(Prf) or SelB·GTP·tRNA^{Sec}(Prf) on the ionic strength was determined in buffer A containing 10, 50, 100, and 150 mM KCl instead of 70 mM NH$_4$Cl and 30 mM KCl at 37ºC. The temperature dependence of binding was measured in buffer A at 20ºC, 25ºC, 30ºC, and 37ºC. The measured fluorescence was corrected for dilution and titrations were evaluated as described in detail in (31). The number of ion pairs between SelB and tRNA^{Sec}, Ser-tRNA^{Sec}, or Sec-tRNA^{Sec} was calculated from the slope of the -log(K_d) *versus* -log[M$^+$] plot according to equation: log(K_d) = (Zψ + k) ·log[M$^+$] − log(K^0), where [M$^+$] is the total concentration of monovalent cations in the reaction (in M); ψ is the fraction of counterions associated with the nucleic acid per phosphate group; Z is a number of cations which interact with the nucleic acid; k is a number of anions released from the protein in the formation of the ternary complex; K^0 is an intrinsic binding constant. The ψ value takes into account the proportion of single-stranded and double-stranded regions of tRNA^{Sec}. ΔH° and ΔS° values were obtained from the slope and Y-axis intercept of the -log(K_d) *versus* 1/T plot, respectively, at each ionic condition. The linear dependence of the ΔH° and ΔS° values on monovalent ions concentration allowed extrapolation to the ionic strength conditions used in other titration experiments, buffer A with 30 mM KCl. The affinity of GTP to SelB·Sec-tRNA^{Sec} complex was measured in the same way using [^{3}H]GTP, SelB (110 nM), Sec-tRNA^{Sec} (3.43 µM) with serial dilutions of GTP for final concentrations spanning 20 nM to 400 nM.

Kinetic measurements-To determine the apparent association rate constants of complex formation, k_{app}, [^{3}H]Sec-tRNA^{Sec} (20 pM) was mixed with SelB (40 pM), GTP or GDPNP (0.1 mM) in buffer A at 25 ºC, 30 ºC, and 37 ºC. The amount of [^{3}H]Sec-tRNA^{Sec} bound to SelB after desired incubation times was determined by nitrocellulose filtration. To measure the dissociation rate constants, k_{off}, [^{3}H]Sec-tRNA^{Sec} (5 nM), SelB (7 nM), and GTP or GDPNP (2 mM) were incubated in buffer A for 15 min at 25 ºC, 30 ºC, or 37 ºC to form the complex and then adding a 10-fold excess of unlabeled Sec-tRNA^{Sec} to induce irreversible dissociation of [^{3}H]Sec-tRNA^{Sec}. The time courses were evaluated by a single-exponential fitting using Prism 5. The association rate constant, k_{on}, was calculated according to the equation $k_{on} = (k_{app} − k_{off})/([\text{SelB·GTP}] + [\text{Sec-tRNA}^{Sec}])$, where [SelB·GTP] and [Sec-tRNA^{Sec}] are equilibrium concentrations of the respective reactants.

Rapid kinetic measurements-Rapid kinetics of Sec-, Ser-, and deacylated tRNA^{Sec} from SelB was measured using a stopped-flow apparatus (SX-18MV; Applied Photophysics, Surrey, U.K.) in buffer A at 25 °C. Fluorescence of tRNA^{Sec}(Prf) was excited at 470 nm and measured after passing a cut-off filter (KV 500; Schott, Mainz, Germany). SelB in the apo-,
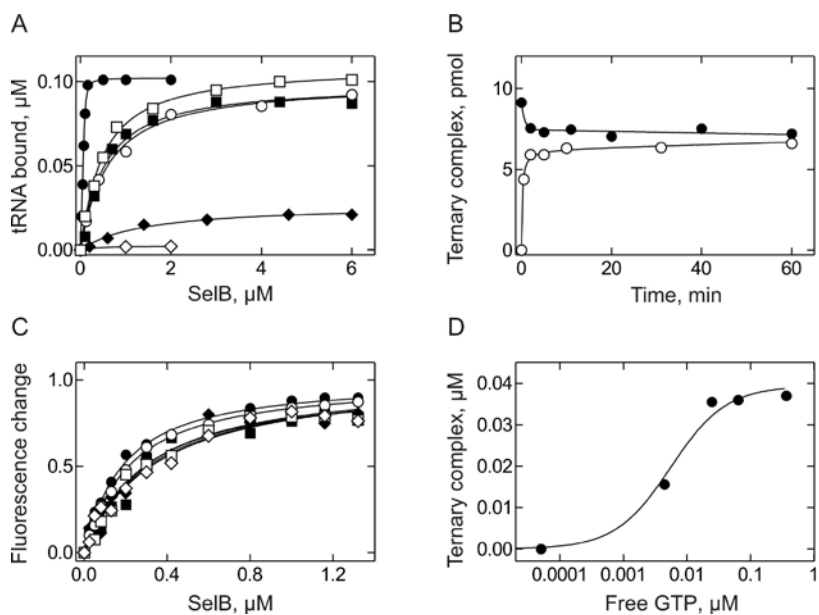
3

FIGURE 1. **Formation of the ternary complex of SelB with guanine nucleotides and different forms of tRNA^{Sec}.** *A*, interaction of native Sec-tRNA^{Sec} with SelB·GTP (●), SelB·GDP (○), SelB in the absence of nucleotide (SelB-apo; □), Sec-tRNA^{Sec} prepared by T7 RNA-polymerase transcription with SelB-apo (■), Phe-tRNA^{Phe} with SelB·GTP (◆), and Sec-tRNA^{Sec} with SelB·GTP attached to filters (◇). *B*, time courses of Sec-tRNA^{Sec} binding to SelB·GTP (○) and dissociation from the SelB·GTP·Sec-tRNA^{Sec} complex upon dilution (●). *C*, binding of Ser-tRNA^{Sec}(Prf20) to SelB·GTP (●), SelB·GDP (■), apo-SelB (◆), and of tRNA^{Sec}(Prf20) to SelB·GTP (◔), SelB·GDP (□), and apo-SelB (◇). Fluorescence change was normalized by defining the maximum signal change as 1.0. The amplitude of fluorescence increase was 29% for SelB·GTP·Ser-tRNA^{Sec}, 28% for SelB·GDP·Ser-tRNA^{Sec}, 22% for SelB-apo·Ser-tRNA^{Sec}, 33% for SelB·GTP·tRNA^{Sec}, 28% for SelB·GDP·tRNA^{Sec}, and 16% for SelB-apo·tRNA^{Sec}. *D*, titration of SelB·Sec-tRNA^{Sec} with [^{3}H]GTP.

TABLE 1. *Summary of the K_d values (nM) for the aa-tRNA complexes with their respective translation factors in the apo-, GDP-, GDPNP-, and GTP-bound form.*

| | Nucleotide bound | | | |
	apo	GDP	GDPNP	GTP
SelB·Sec-tRNA^{Sec} [1]	420±30	540±60	$(5.5±0.8)·10^{-3}$	$(2.1±0.6)·10^{-4}$
SelB·Ser-tRNA^{Sec} [1]	270±60	280±60	n.d.	160±10
SelB·tRNA^{Sec} [1]	290±50	280±50	n.d.	190±10
EF-Tu·Phe-tRNA^{Phe} [2]	n.d.	28,500	180	0.85
eIF2·Met-tRNA$_i^{Met}$ [3]	115	150	n.d.	9
eIF2·tRNA$_i^{Met}$ [3]	n.d.	140	n.d.	130

[1] The K_d values are given for 25 °C except for GDPNP which was measured at 37°C; this work.
[2] The K_d values were measured at 6 °C; data taken from (32) (GDP), (33) (GDPNP), and (34) (GTP).
[3] The K_d values measured at 26 °C; data taken from (35)
n.d., not determined

GTP- or GDP-bound forms (0.4 μM, final concentrations after mixing are given throughout) was preincubated with Sec-, Ser- or deacylated tRNA^{Sec}(Prf) (0.2 μM) and the complexes rapidly mixed with a solution containing unlabeled tRNA^{Sec} (3 μM). Time courses depicted in the figures were obtained by averaging 8–10 individual transients. Data were evaluated by fitting to a single exponential function with a characteristic time constant (k_{app}), amplitude (*A*), and another variable for the final signal (F_∞) according to the equation $F = F_\infty + A·\exp(-k_{app} · t)$ where *F* is the fluorescence at time *t*. Where necessary, two exponential terms were used with two characteristic time constants (k_{app1}, k_{app2}), amplitudes (*A, B*), and another variable for the final signal (F_∞) according to the equation $F = F_\infty + A·\exp(-k_{app1} · t) +$ $B·\exp(-k_{app2} · t)$. The reason for kinetic heterogeneity is not known; the average dissociation rate constant was estimated as described in (36). Calculations were performed using Prism (Graphpad Software). Standard deviations were calculated using the same software.

RESULTS

Affinity of SelB to tRNA and guanine nucleotides-To analyze the complex formation between Sec-tRNA^{Sec} or Ser-tRNA^{Sec} and SelB in the apo-, GTP- or GDP-bound forms, we used filtration assays monitoring retention of radioactive ^{14}C- or ^{3}H-labeled Sec- or Ser-tRNA^{Sec} on the nitrocellulose filters. The tRNA complexes with SelB were bound quantitatively to the filters, whereas free tRNA was

not retained. The specificity of complex formation was tested by (i) applying Sec-tRNA^{Sec} on a filter to which SelB was attached without an incubation and (ii) filtrating SelB mixed with a canonical elongator aa-tRNA (Phe-tRNA^{Phe}) which is not expected to interact with SelB (1) (Fig. 1A); no Sec-tRNA^{Sec} and only minor amounts of Phe-tRNA^{Phe} were retained on the filters. Furthermore, the complex was bound to the filters in a very stable fashion, as tested by extensive rinsing of the filters with up to 100 ml of buffer A (data not shown). The reversibility of Sec-tRNA^{Sec} binding to SelB was demonstrated by the following experiment. The complex was formed either by mixing the components at a particular concentration (Materials and Methods) or by forming the complex at a higher concentration followed by a 100-fold dilution to the final concentration identical to that in the first experiment. At equilibrium conditions the same amount of complex is expected to form regardless of the way the complex was formed, which was indeed the case (Fig. 1B).

Sec-tRNA^{Sec} binds to SelB in the apo-, GTP-, or GDP-bound forms (Fig. 1A), in agreement with earlier observations (1,7), however, the affinity of binding was much higher for SelB·GTP than for the apo- or GDP-bound form. The affinity of native Sec-tRNA^{Sec} is similar for SelB-apo and SelB·GDP with the K_d values of 420 nM and 540 nM, respectively (Table 1). In contrast to SelB·GDP or SelB-apo, a stoichiometric titration was observed with SelB·GTP, indicating a very tight binding ($K_d < 1$ nM), which precluded accurate determination of the respective K_d value at the reaction conditions used. The affinities of the Sec-tRNA^{Sec} prepared from native tRNA or tRNA transcript for SelB-apo were very similar, 420 nM and 470 nM, respectively (Fig. 1A, compare open and closed squares), indicating that the unmodified tRNA^{Sec} behaves identically to native tRNA^{Sec} with respect to binding to SelB; a slightly different final binding level is indicative of a small portion of tRNA transcript (10%) that is inactive in SelB binding.

To determine the affinity of deacylated tRNA^{Sec} to SelB, fluorescence-labeled tRNA^{Sec}(Prf) was prepared containing a reporter group, proflavin, at position 20 in the D loop of the tRNA and the affinity of binding was calculated form equilibrium fluorescence titrations (Fig. 1C); same method was used for Ser-tRNA^{Sec}(Prf), which allowed us to compare the results of the filtration assays with fluorescence titrations. Fluorescence labeling did not impair the activity of the tRNA, because the affinities of SelB·GTP binding to [^{14}C]Ser-tRNA^{Sec}(Prf) measured by the two types of assays were the same and comparable to that for unlabeled [^{14}C]Ser-tRNA^{Sec} (data not shown). Upon binding to SelB, fluorescence of tRNA^{Sec}(Prf) increased; the signal increased hyperbolically with the concentration of SelB, which allowed us to calculate the K_d values of the interaction. The affinities of deacylated and Ser-tRNA^{Sec} to SelB-apo, SelB·GDP, and SelB·GTP were
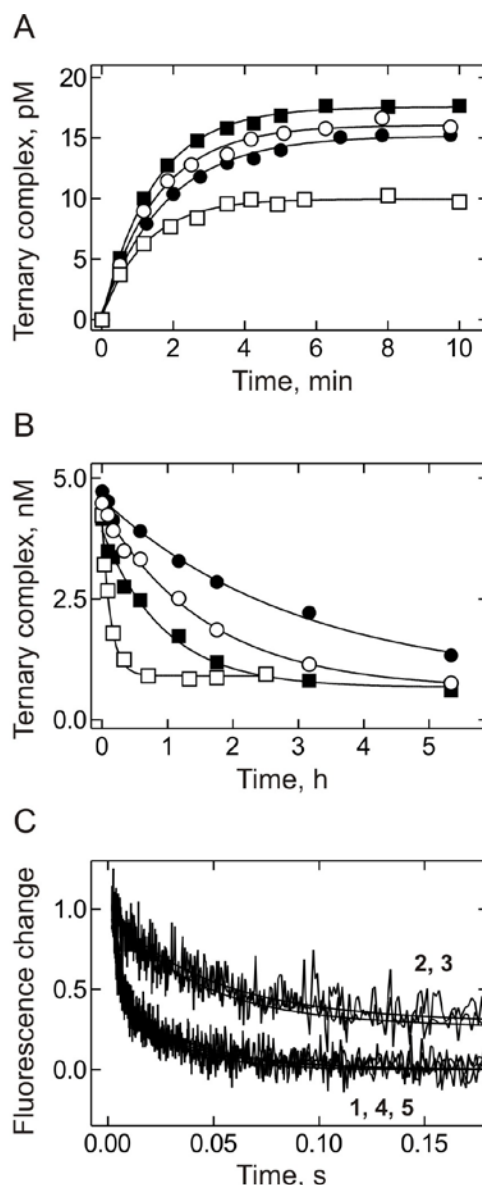

FIGURE 2. **Rate constants of tRNA^{Sec} association with SelB and dissociation of the complex.** *A,* time courses of Sec-tRNA^{Sec} binding to SelB·GTP at 25 °C (◆), 30 °C (○), 37 °C (■), and to SelB·GDPNP at 37 °C (□). *B,* time courses of Sec-tRNA^{Sec} dissociation from SelB·GTP·Sec-tRNA^{Sec} at 25 °C (●), 30 °C (○), 37 °C (■), and from SelB·GDPNP·Sec-tRNA^{Sec} at 37 °C (□). *C,* time courses of dissociation of Sec-tRNA^{Sec}(Prf) from the complex with SelB·GDP (1), Ser-tRNA^{Sec}(Prf) from the complex with SelB·GTP (2), tRNA^{Sec}(Prf) from the SelB·GTP (3), SelB·GDP (4), and SelB-apo (5) at 25 °C. Traces (1), (4), and (5) as well as (2) and (3) are indistinguishable.

not significantly different, about 160-250 nM (Table 1).

SelB-apo binds GTP and Sec-tRNA^{Sec} with the affinities of 0.7 μM (9) and 0.42 μM (this paper), respectively. From the law of mass action, if the affinity of SelB·GTP binding to Sec-tRNA^{Sec} is below 1 nM, then also the binding of GTP to SelB·Sec-tRNA^{Sec} should be similarly tight. To test whether this is the case, we estimated the K_d of [^{3}H]GTP interaction with SelB·Sec-tRNA^{Sec} complex. As expected, the affinity was very high (Fig. 1D); the

TABLE 2. *Rate constants of formation and dissociation of various SelB complexes.*

	k_{on}, M^{-1}s^{-1}	k_{off}, s^{-1}	K_d, pM [a]
SelB·GTP·Sec-tRNA^{Sec} (25°C)	$(4.2 \pm 0.3) \cdot 10^8$	$(0.9 \pm 0.2) \cdot 10^{-4}$	0.21 ± 0.06
SelB·GTP·Sec-tRNA^{Sec} (30°C)	$(4.9 \pm 0.3) \cdot 10^8$	$(1.7 \pm 0.2) \cdot 10^{-4}$	0.35 ± 0.06
SelB·GTP·Sec-tRNA^{Sec} (37°C)	$(5.1 \pm 0.2) \cdot 10^8$	$(2.9 \pm 0.4) \cdot 10^{-4}$	0.6 ± 0.1
SelB·GDPNP·Sec-tRNA^{Sec} (37°C)	$(3.8 \pm 0.2) \cdot 10^8$	$(21 \pm 2) \cdot 10^{-4}$	5.5 ± 0.8
SelB·GDP·Sec-tRNA^{Sec}	$(4.4 \pm 1.2) \cdot 10^{8}$ [b]	240 ± 40	
SelB·GTP·Ser-tRNA^{Sec}	$(0.9 \pm 0.2) \cdot 10^{8}$ [b]	14 ± 2	
SelB·GTP·tRNA^{Sec}	$(1.0 \pm 0.1) \cdot 10^{8}$ [b]	18 ± 1	
SelB·GDP· tRNA^{Sec}	$(8.0 \pm 2.7) \cdot 10^{8}$ [b]	220 ± 30	
SelB-apo·tRNA^{Sec}	$(7.2 \pm 2.4) \cdot 10^{8}$ [b]	210 ± 30	

[a] Calculated from the k_{on} and k_{off} values.
[b] Calculated using the K_d values of Table 1.

upper limit of the K_d value could be estimated at about 5 nM. A more precise value could not be obtained because the concentration of reactants could not be further reduced at the experimental conditions used. By analogy, the affinity of GDP to SelB·Sec-tRNA^{Sec} is expected to be in the 10 μM range; the experimental verification of the K_d value was not feasible because of the high background due to excess [^{3}H]GDP in the titration experiments.

The kinetics of Sec-tRNA^{Sec} binding to SelB- The rate constants of interactions may provide an alternative way to estimate the K_d values and yield additional information beyond the affinities. This prompted us to determine the apparent association rate constants, k_{app}, for the Sec-tRNA^{Sec} binding to SelB·GTP at three different temperatures (Fig. 2A). Excess SelB·GTP was mixed with [^{3}H]Sec-tRNA^{Sec}, aliquots were taken at different incubation times and analyzed by nitrocellulose filtration. The values were $k_{app} = 0.55 \pm 0.04$ min^{-1} at 25 °C, 0.65 ± 0.04 min^{-1} at 30 °C, and 0.69 ± 0.02 min^{-1} at 37 °C. At excess SelB·GTP, the reaction can be considered pseudo-first order; thus, the measured values reflect $k_{app} = k_{on} \cdot ([SelB·GTP]) + k_{off}$. In order to calculate the k_{on} values, k_{off} was measured independently using the chase approach. The SelB·GTP·[^{3}H]Sec-tRNA^{Sec} complex was formed and the chase of [^{3}H]Sec-tRNA^{Sec} initiated by addition of an excess unlabeled Sec-tRNA^{Sec} to prevent rebinding of radioactively labeled tRNA (Fig. 2B). The resulting k_{off} values, together with the k_{on} values calculated from the k_{app} and k_{off}, are summarized in Table 2. The K_d values for the SelB·GTP·Sec-tRNA^{Sec} complex, calculated from $K_d = k_{off}/k_{on}$, are in the low picomolar range, consistent with extremely tight association. For comparison, we also measured the association and dissociation rates and the K_d value for Sec-tRNA^{Sec} interaction with SelB in the complex with GDPNP which is commonly used as a non-hydrolyzable GTP analog in crystallography. While the association rate constants of Sec-tRNA^{Sec} with SelB·GTP or SelB·GDPNP were the same, the dissociation rate constants differed considerably resulting in a 25-fold higher K_d value of the complex with GDPNP. This suggests that the

conformations of SelB with GTP and GDPNP are somewhat different and thus the interactions between SelB and Sec-tRNA^{Sec} modeled on the basis of the SelB·GDPNP crystal structure may not reflect the SelB·GTP complex in every detail. Dissociation of Sec-tRNA^{Sec} from the SelB·GTP (or GDPNP)·Sec-tRNA^{Sec} complex was very slow allowing k_{off} determination by nitrocellulose filtration assay. In contrast, dissociation of almost all other complexes was too rapid to monitor by filtration method. For those complexes, we used fluorescence stopped-flow method to measure the dissociation rate constants (Fig. 2C). Complexes of SelB in the apo-, GDP-, or GTP-bound forms with Sec-, Ser-, and deacylated tRNA^{Sec}(Prf) were mixed with an excess of unlabeled tRNA^{Sec} and the release of the labeled tRNA^{Sec} monitored by decrease in fluorescence. In contrast to the SelB·GTP·Sec-tRNA^{Sec} complex, which dissociated in the hours range, the release of Sec-tRNA^{Sec} from the SelB·GDP complex was extremely rapid, in a milliseconds range. The dissociation rate constant of the complex increased by more than six orders of magnitude upon replacement of GTP for GDP, whereas the association rate constant was unchanged (Table 2). The complexes of Ser-tRNA^{Sec} and tRNA^{Sec} with SelB·GTP also dissociated rapidly, five orders of magnitude faster than the SelB·GTP·Sec-tRNA^{Sec} complex. Dissociation rate of tRNA^{Sec} from SelB was much less sensitive to the nucleotide form of the factor, with tRNA^{Sec} dissociating from SelB·GTP only 10 times slower than from SelB·GDP of SelB–apo.

*Effect of ionic strength on SelB interaction with Sec-tRNA^{Sec}-*To understand the molecular basis for the tight binding of Sec-tRNA^{Sec} to SelB, we examined the ionic strength dependence of the K_d values, which may provide insights into electrostatic interactions between a protein and nucleic acid (37). The experiments were carried out at 37 °C in the presence of increasing KCl concentrations up to 525 mM (Fig. 3A). The decrease in affinity with increasing ionic strength of the buffer (Fig. 3B) suggests that SelB·GTP·Sec-tRNA^{Sec} complex formation involves ionic interactions. In principle, the number of ion
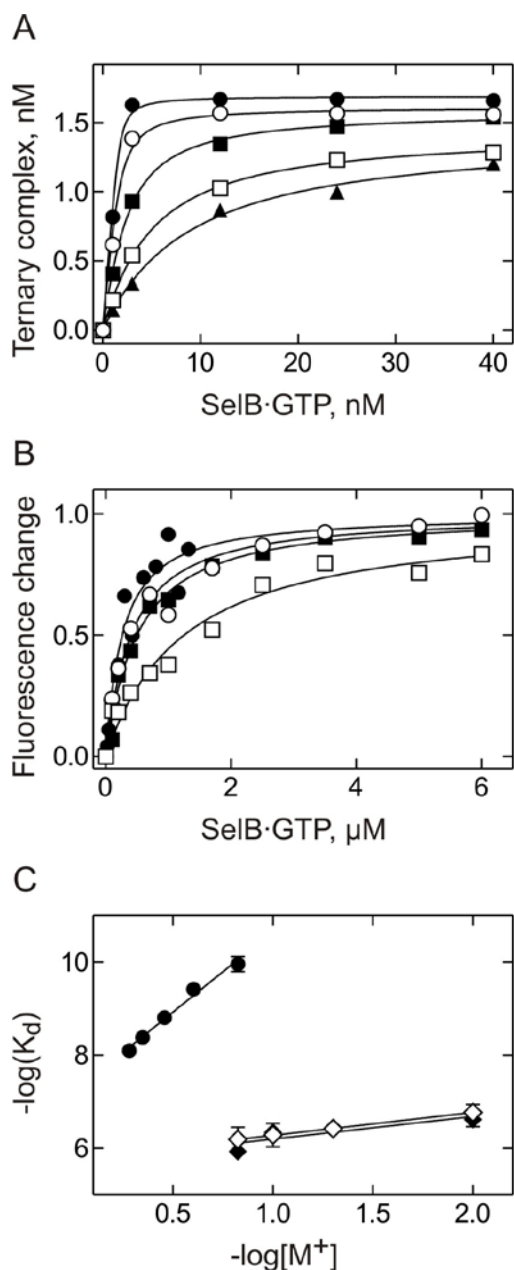
FIGURE 3. **Ionic strength dependence of tRNA^{Sec} binding to SelB·GTP.** *A*, binding of SelB·GTP to Sec-tRNA^{Sec} in buffer A with 150, 250, 350, 450, and 525 mM KCl (from top to bottom). *B*, binding of SelB·GTP to Ser-tRNA^{Sec}(Prf) in buffer A with 10, 50, 100, and 150 mM KCl (from top to bottom). *C*, dependences of the K_d values of SelB·GTP·Sec-tRNA^{Sec} (●), SelB·GTP·Ser-tRNA^{Sec}(Prf) (◆), and SelB·GTP·tRNA^{Sec}(Prf) (◇) on ionic conditions. [M$^+$] is the total concentration of monovalent cations in the reaction (in M).

pairs contributing to the interaction can be estimated from the slope of the plot using the method developed by Record et al (37) and Lohman et al (38). One potential complication for the calculations is the presence of Mg^{2+} ions, which are required both the guanine nucleotide binding and for proper folding of Sec-tRNA^{Sec}. However, as the concentration of Mg^{2+} (4 mM free Mg^{2+}) was low compared to KCl, the uncertainty in estimating the number of ionic

interactions due to the presence of Mg^{2+} ions can be considered negligible.

Another uncertainty in the calculations comes from the unknown portion of single-stranded versus double-stranded regions of tRNA^{Sec} interacting with SelB. A reasonable estimation can be made on the basis of the crystal structures of EF-Tu·GDPNP·Phe-tRNA^{Phe} and EF-Tu·GDPNP·Cys-tRNA^{Cys} complexes (39,40). In both cases three-fourth of the groups that are involved in interaction with EF-Tu are located in double-stranded regions of tRNA. Assuming a similar proportion of the single-stranded and double-stranded regions for tRNA^{Sec}, the number of ionic interactions involved in SelB·GTP·Sec-tRNA^{Sec} formation was 4.2 ± 0.2. In comparison, interaction of SelB with Ser-tRNA^{Sec} or tRNA^{Sec} was much less dependent on salt concentration (Fig. 3B); the estimated number of ion pairs was 0.6.

Another factor involved in the complex formation may be the release of counterions. If the release of anions from SelB were an important factor in the formation of the SelB·GTP·Sec-tRNA^{Sec} complex, a curvature should be observed in log(K_d) *versus* log[M$^+$] plot (38). However, log(K_d) is a linear function of log[M$^+$] over the wide range of salt concentrations suggesting that anion effects are insignificant. To investigate further the role (if any) of the anions released during the formation of the SelB·GTP·Sec-tRNA^{Sec} complex we have measured the K_d dependence on the concentration of potassium acetate (data not shown) and compared it to that on KCl (Fig. 3B). The slopes of the plots log(K_d) *versus* log[M$^+$] were similar suggesting that there are no major differences in the amount of anion released in these buffer conditions. However, the affinity of SelB·GTP to Sec-tRNA^{Sec} was approximately four-fold higher in the presence of acetate than of chloride at the same total ion concentration. The difference in K_d can be explained assuming that Cl$^-$ ions bind to the tRNA binding region of SelB more strongly than CH$_3$COO$^-$ ions do, which is consistent with the lyotropic series (41). Alternatively, acetate might bind to the protein at sites not directly involved in tRNA binding and induce a conformational change in SelB which enhances the affinity of the protein for Sec-tRNA^{Sec}.

Thermodynamic parameters of SelB·GTP·Sec-tRNA^{Sec} complex formation-Usually, thermodynamic parameters of complex formation are calculated from the -log(K_d) plot vs. 1/T (van't Hoff plot) temperature dependence of the K_d values. Because of the high affinity of SelB·GTP·Sec-tRNA^{Sec} binding, the direct measurement of the temperature dependence of the K_d values was not feasible and we used two different approaches to overcome this difficulty. The standard enthalpy and entropy changes were estimated using the K_d values calculated from the rate constants (Fig. 4B). Alternatively, the values for thermodynamic parameters of binding were determined at several high KCl concentrations (Fig. 4A) where the affinity is sufficiently reduced to measure the K_d values reliably.

7

TABLE 3. *Thermodynamic parameters of tRNA binding to SelB and EF-Tu*

	$\Delta H°$ (kcal/mol)	$\Delta G°$ (kcal/mol)	$\Delta S°$ (cal/mol/K)	$T\Delta S°$ (kcal/mol)
SelB·GTP·Sec-tRNA$^{Sec\ (1a)}$	-16.0 ± 0.6	-17.3 ± 0.2	4 ± 2	1.3 ± 0.6
SelB·GTP·Ser-tRNA$^{Sec\ (1b)}$	-4 ± 1	-9.1 ± 0.2	18 ± 4	5 ± 1
SelB·GTP·tRNA$^{Sec\ (1b)}$	-4.0 ± 0.8	-9.2 ± 0.2	18 ± 3	5.3 ± 0.8
EF-Tu·GTP·Phe-tRNA$^{Phe\ (2)}$	-16	-11	-16	-5
EF-Tu·GTP·Tyr-tRNA$^{Tyr\ (3)}$	-8	-12	13	4

[1] $\Delta H°$ and $\Delta S°$ values were determined from the $-\log(K_d)$ *versus* $1/T$ plot (Fig. 4B). [a] K_d values were calculated from the rate constants of Sec-tRNA^{Sec} binding to and dissociation from SelB·GTP, $K_d = k_{off}/k_{on}$. [b] K_d values were measured by equilibrium titrations with fluorescence-labeled tRNA^{Sec}(Prf). $\Delta G°$ values were obtained for 298 K according to the equation $\Delta G° = RT \ln K_d$; this work.
[2] Buffer conditions: 50 mM HEPES, pH 7.6, 50 mM NH$_4$Cl, 10 mM MgCl$_2$, 0.1 mM DTT (34).
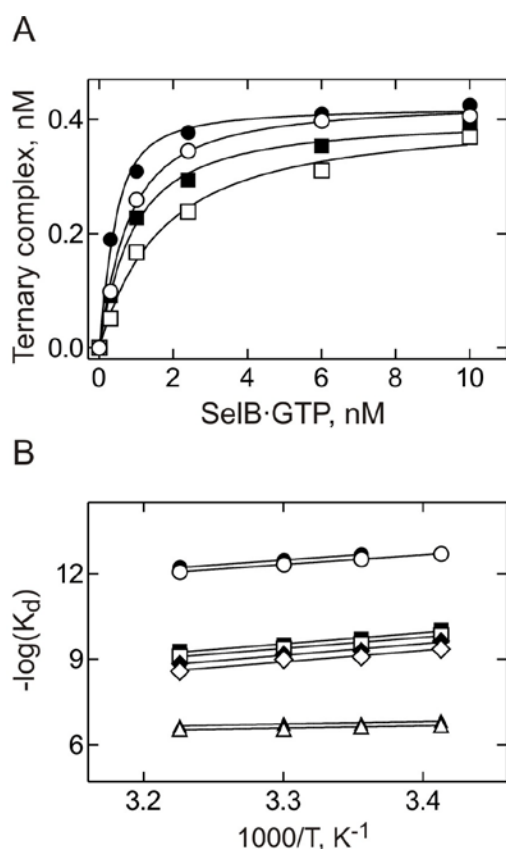[3] Buffer conditions: 50 mM borate, pH 7.0, 50 mM NH$_4$Cl, 10 mM MgCl$_2$ (42).

FIGURE 4. **Temperature dependence of tRNA^{Sec} binding to SelB·GTP.** *A,* binding of SelB·GTP to Sec-tRNA^{Sec} in buffer A with 430 mM KCl at 20°C, 25°C, 30°C, and 37°C (from top to bottom). *B,* temperature dependences of the K_d values of SelB·GTP·tRNA^{Sec}(Prf) (▲), SelB·GTP·Ser-tRNA^{Sec}(Prf) (△), and SelB·GTP·Sec-tRNA^{Sec} calculated from the rate constants of Sec-tRNA^{Sec} binding to and dissociation from SelB·GTP (Figure 2) (●), or extrapolated (○) from the temperature dependences of the K_d values measured in buffer A with 480 mM KCl (◇), 430 mM KCl (◆), 380 mM KCl (□), and 330 mM KCl (■).

The dependence of the $\Delta H°$ and $\Delta S°$ values on monovalent ions concentration was linear, which allowed for the extrapolation to the desired ionic strength conditions; both methods gave identical

results (Table 3). Binding of Sec-tRNA^{Sec} to SelB·GTP is driven by a large favorable change in the interaction enthalpy, while the binding entropy is almost unchanged. With Ser-tRNA^{Sec} and tRNA^{Sec} the decrease in the affinity to SelB·GTP compared Sec-tRNA^{Sec} was entirely due to a less favorable binding enthalpy, while the entropy changes are even slightly more favorable. Comparison of these data to those published for the aa-tRNA interaction with EF-Tu (Table 3) appeared difficult, because the values for thermodynamic parameters reported for Phe-tRNA^{Phe} and Tyr-tRNA^{Tyr} differ significantly from one another; the reasons for this difference are not clear and may be due to different nature of the aa-tRNAs, buffer conditions, or experimental approaches.

DISCUSSION

SelB, EF-Tu and its eukaryotic homolog eEF1A, and eIF2γ are translation factors that deliver different aa-tRNAs to the ribosome. EF-Tu has evolved to bind all correctly aminoacylated elongator aa-tRNAs, except for Sec-tRNA^{Sec}, with approximately the same affinity (43-49). The thermodynamic contributions of the amino acid and the tRNA to the overall binding affinity are independent of and compensate for one another when the tRNA is esterified with cognate amino acid. In contrast, the affinities of EF-Tu for misacylated tRNAs may vary by several thousand-fold due to the lack of thermodynamic compensation between amino acid and the tRNA molecule. While misacylated tRNAs displaying weaker binding properties for EF-Tu are probably not incorporated into the growing peptide, some misacylated tRNAs stably bind to EF-Tu and can be delivered to the ribosome. This explains why some misacylated suppressor tRNAs are active in translation (50,51) or why alanine could be incorporated instead of cysteine (Cys) after reduction of Cys-tRNA^{Cys} to Ala-tRNA^{Cys} (52).

Unlike EF-Tu, SelB has evolved to bind a single aa-tRNA, Sec-tRNA^{Sec}, and the recognition pattern is specific for the SelB-Sec-tRNA^{Sec} pair. The tRNA^{Sec}
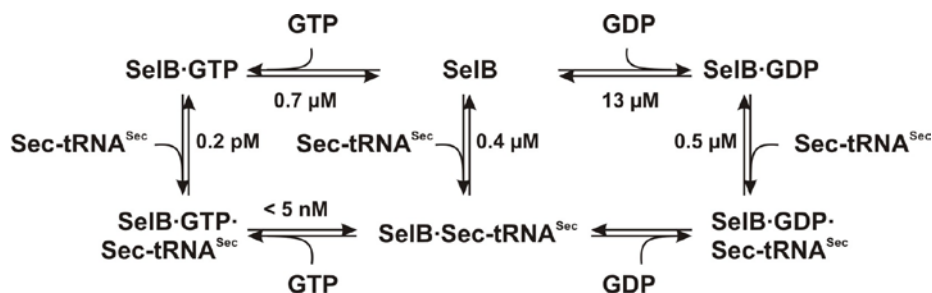
FIGURE 5. **A thermodynamic framework of interactions between Sec-tRNA^{Sec}, SelB, and guanine nucleotides.** The K_d values of the respective interactions are indicated.

molecule is selected by SelB based on specific structural determinants which distinguish tRNA^{Sec} from all other aa-tRNAs (8). The complex is stabilized by both ionic and non-ionic interactions; the latter contribute significantly to the thermodynamic stability of the complex, because the affinity of tRNA^{Sec} to SelB is relatively high even at high salt concentrations. Binding of tRNA^{Sec} or Ser-tRNA^{Sec} to SelB results in the net formation of about one ion pair. This contribution of ionic interactions is comparable to that in the EF-Tu·GTP·Phe-tRNA^{Phe} complex (34); in both cases the interactions do not involve the amino acid of aa-tRNA. Importantly, the Ser residue is not recognized by SelB, as the affinity of the factor for Ser-tRNA^{Sec} and deacylated tRNA^{Sec} is similar and has almost identical binding enthalpy and entropy. The entropy change upon binding is favorable which is somewhat unexpected given that complex formation should lead to losses in degrees of freedom, but may reflect the contribution of non-ionic interactions. Furthermore, the affinity of Ser-tRNA^{Sec} and tRNA^{Sec} to SelB is independent of the guanine nucleotide suggesting that the two tRNAs bind in the same way to SelB irrespectively of the conformational changes in the G domain induced by the nucleotide binding, consistent with the similarity of the overall shape of the three SelB forms in the absence of Sec (7). In contrast, the Sec residue increases the binding affinity to SelB·GTP by six orders of magnitude, allowing for efficient selection of Sec-tRNA^{Sec} against binding of deacylated tRNA^{Sec} or non-converted Ser-tRNA^{Sec}. Such discrimination is crucial, because if the Sec residue is replaced by a Ser in the active site of FDH$_H$, the activity of the enzyme is lost (53). Interestingly, the affinity of misacylated Sec-tRNA^{Val} to EF-Tu is very poor (44), indicating that the discrimination of Sec-tRNA^{Sec} binding to EF-Tu is not simply due to the specific features of tRNA^{Sec} but also due to the lack of specific contacts between the Sec residue and EF-Tu.

Another recognition element in the SelB system is the thermodynamic coupling between binding of Sec-tRNA^{Sec} and GTP to SelB, which is not observed with deacylated tRNA^{Sec} or Ser-tRNA^{Sec} or with the GDP-bound or apo-form of SelB. While all three forms of tRNA^{Sec} have similar affinities to SelB-apo or SelB·GDP, Sec-tRNA^{Sec} appears to make additional interactions with SelB·GTP resulting in a much more stable complex. The specific stabilization of the SelB·GTP·Sec-tRNA^{Sec} complex ensures that Sec-tRNA^{Sec} is channeled into the active GTP-bound form of SelB, rather than to the GDP-bound or apo-forms which are inactive in translation (22). Furthermore, because the production of Sec-tRNA^{Sec} requires considerable use of cellular resources, it should be stringently protected by SelB from hydrolysis or oxidation. Tight binding of Sec-tRNA^{Sec} to SelB·GTP would also minimize the chances of premature release of the factor from the aa-tRNA and the possible passage of Sec-tRNA^{Sec} into the peptidyl transferase center before the ribosome can monitor the correct geometry of the codon-anticodon interactions. In effect, the high affinity of the complex would reduce translational errors by ensuring that maximum discrimination was achieved during the recognition of Sec-tRNA^{Sec} on the ribosome. With respect to thermodynamic coupling, ligand-binding properties of SelB are reminiscent of those of eIF2γ which in the GTP-bound state forms an interaction with the methionine moiety on Met-tRNA$_i$ that is disrupted when GTP is replaced with GDP, while contacts between the factor and the body of the tRNA remain intact (35). Similarly to SelB·GTP·Sec-tRNA^{Sec} complex in elongation, this positive interaction with the methionine residue on tRNA$_i$ may serve to ensure that only charged initiator tRNA enters the initiation pathway. The similar strategies towards the specific recognition and selection of a particular tRNA may indicate a common evolutionary ancestry of SelB and eIF2. In fact, phylogenetic studies suggest that SelB and eIF2 constitute an ancient subfamily of translation GTPases distinct from the EF-Tu/eEF1A subfamily and there might have been a switch in function of the ancestral factor which produced the modern SelB and eIF2γ (6).

Our data suggest that binding of the Sec residue results in the net formation of about three ion pairs. These pairs might involve the Sec group directly or reflect the formation upon Sec binding of salt bridges between other groups, e.g. of additional interactions with the phosphate groups of tRNA^{Sec} or salt bridges within SelB. The important contribution of these ionic interactions is consistent with the large favorable change in binding enthalpy of SelB·GTP binding to Sec-tRNA^{Sec} compared to Ser- of deacylated tRNA^{Sec}. Modeling of the aminoacyl-binding pocket of SelB

9

suggested a potential role for residues Asp180, Arg181, and Arg236, which are unique to SelB (5). Asp180 and Arg236 are conserved among SelB molecules from all kingdoms, whereas Arg181 is present in bacterial proteins and is replaced by a His residue in archaeal and eukaryotic SelB (His192 in *M. maripaludis* (7)). Residues Arg181 and Arg236 may provide two positive charges and either or both of them would have the capacity to interact with the negatively charged selenol group. The importance of these residues for Sec binding was corroborated by mutational analysis which suggested that the presence of at least one positive charge in the aminoacyl-binding pocket of SelB is required for function (7). The identity of other group(s) contributing to ionic interactions is currently unknown.

Another role for the thermodynamic coupling may be to ensure that Sec-tRNA^{Sec} is released rapidly from SelB after GTP hydrolysis on the ribosome. Upon binding of the SelB·GTP·Sec-tRNA^{Sec} to the ribosome in a codon- and SECIS-directed manner, GTP hydrolysis occurs, aa-tRNA is released from SelB·GDP, and enters the ribosomal A site. For most elongator aa-tRNAs, the accommodation step may be rate limiting for peptide bond synthesis (21). If Sec-tRNA^{Sec} were to bind SelB·GDP too tightly, accommodation and peptide bond formation would be too slow. GTP hydrolysis by SelB increases the rate of Sec-tRNA^{Sec} release by six orders of magnitude, from 10^{-3} s^{-1} to 230 s^{-1}; the latter rate is sufficiently high to allow for rapid transfer of Sec-tRNA^{Sec} from the factor to the ribosome. Although the contacts between Sec-tRNA^{Sec} and SelB·GDP after GTP hydrolysis on the ribosome may be different from those in the ternary complex, such as suggested recently by cryo-EM reconstructions of the EF-Tu·GDP·Phe-tRNA^{Phe} complex stalled on the ribosome by kirromycin (15,18), it is likely that the strong effect of GTP hydrolysis on the dissociation rate of Sec-tRNA^{Sec} from SelB would be maintained. In this view, thermodynamic coupling in binding of Sec-tRNA^{Sec} and GTP to SelB ensures both the specificity of Sec- versus Ser-tRNA^{Sec} selection and the efficient protection of Sec-tRNA^{Sec} against premature degradation, combined with the rapid release of Sec-tRNA^{Sec} on the ribosome after GTP hydrolysis.

REFERENCES

1. Forchhammer, K., Leinfelder, W., and Böck, A. (1989) *Nature* **342**, 453-456
2. Commans, S., and Böck, A. (1999) *FEMS Microbiol. Rev.* **23**, 335-351
3. Atkins, J. F., and Gesteland, R. F. (2000) *Nature* **407**, 463, 465
4. Baron, C., and Böck, A. (1995) The selenocystein-inserting tRNA species: structure and function. in *tRNA: structure biosynthesis, and function* (Soll, D., and RajBhandary, U. eds.), American society for microbiology., Washington. pp 529-544
5. Hilgenfeld, R., Böck, A., and Wilting, R. (1996) *Biochimie* **78**, 971-978
6. Keeling, P. J., Fast, N. M., and McFadden, G. I. (1998) *J. Mol. Evol.* **47**, 649-655
7. Leibundgut, M., Frick, C., Thanbichler, M., Böck, A., and Ban, N. (2005) *EMBO J.* **24**, 11-22
8. Baron, C., and Böck, A. (1991) *J. Biol. Chem.* **266**, 20375-20379
9. Thanbichler, M., Böck, A., and Goody, R. S. (2000) *J. Biol. Chem.* **275**, 20458-20466
10. Gromadski, K. B., Wieden, H. J., and Rodnina, M. V. (2002) *Biochemistry* **41**, 162-169
11. Wilden, B., Savelsbergh, A., Rodnina, M. V., and Wintermeyer, W. (2006) *Proc Natl Acad Sci U S A* **103**, 13670-13675
12. Milon, P., Tischenko, E., Tomsic, J., Caserta, E., Folkers, G., La Teana, A., Rodnina, M. V., Pon, C. L., Boelens, R., and Gualerzi, C. O. (2006) *Proc. Natl. Acad. Sci. USA* **103**, 13962-13967
13. Yoshizawa, S., Rasubala, L., Ose, T., Kohda, D., Fourmy, D., and Maenaka, K. (2005) *Nat. Struct. Mol. Biol.*
14. Selmer, M., and Su, X. D. (2002) *EMBO J.* **21**, 4145-4153
15. Schuette, J. C., Murphy, F. V. t., Kelley, A. C., Weir, J. R., Giesebrecht, J., Connell, S. R., Loerke, J., Mielke, T., Zhang, W., Penczek, P. A., Ramakrishnan, V., and Spahn, C. M. (2009) *EMBO J* **28**, 755-765
16. Stark, H., Rodnina, M. V., Wieden, H. J., Zemlin, F., Wintermeyer, W., and van Heel, M. (2002) *Nat. Struct. Biol.* **9**, 849-854
17. Valle, M., Zavialov, A., Li, W., Stagg, S. M., Sengupta, J., Nielsen, R. C., Nissen, P., Harvey, S. C., Ehrenberg, M., and Frank, J. (2003) *Nat. Struct. Biol.* **10**, 899-906
18. Villa, E., Sengupta, J., Trabuco, L. G., LeBarron, J., Baxter, W. T., Shaikh, T. R., Grassucci, R. A., Nissen, P., Ehrenberg, M., Schulten, K., and Frank, J. (2009) *Proc Natl Acad Sci USA* **106**, 1063-1068
19. Hüttenhofer, A., and Böck, A. (1998) Selenoprotein synthesis. in *RNA structure and function*, Cold Spring Harbour Laboratory Press. pp 603-639

20. Ose, T., Soler, N., Rasubala, L., Kuroki, K., Kohda, D., Fourmy, D., Yoshizawa, S., and Maenaka, K. (2007) *Structure* **15**, 577-586

21. Pape, T., Wintermeyer, W., and Rodnina, M. V. (1998) *EMBO J* **17**, 7490-7497

22. Fischer, N., Paleskava, A., Gromadski, K. B., Konevega, A. L., Wahl, M. C., Stark, H., and Rodnina, M. V. (2007) *Biol Chem* **388**, 1061-1067

23. Thanbichler, M., and Böck, A. (2003) *Protein. Expr. Purif.* **31**, 265-270

24. John, J., Sohmen, R., Feuerstein, J., Linke, R., Wittinghofer, A., and Goody, R. S. (1990) *Biochemistry* **29**, 6058-6065

25. Thanbichler, M., and Böck, A. (2002) *Methods. Enzymol.* **347**, 3-16

26. Ehrenstein, G. (1967) *Methods Enzymol* **12**, 588-596

27. Kothe, U., Paleskava, A., Konevega, A. L., and Rodnina, M. V. (2006) *Anal Biochem* **356**, 148-150

28. Wintermeyer, W., and Zachau, H. G. (1974) *Methods Enzymol* **29**, 667-673

29. Rodnina, M. V., Fricke, R., and Wintermeyer, W. (1994) *Biochemistry* **33**, 12267-12275

30. Konevega, A. L., Soboleva, N. G., Makhno, V. I., Semenkov, Y. P., Wintermeyer, W., Rodnina, M. V., and Katunin, V. I. (2004) *RNA* **10**, 90-101

31. Rodnina, M. V., Pape, T., Fricke, R., Kuhn, L., and Wintermeyer, W. (1996) *J Biol Chem* **271**, 646-652

32. Dell, V. A., Miller, D. L., and Johnson, A. E. (1990) *Biochemistry* **29**, 1757-1763

33. Nazarenko, I. A., Harrington, K. M., and Uhlenbeck, O. C. (1994) *EMBO J.* **13**, 2464-2471

34. Abrahamson, J. K., Laue, T. M., Miller, D. L., and Johnson, A. E. (1985) *Biochemistry* **24**, 692-700

35. Kapp, L. D., and Lorsch, J. R. (2004) *J. Mol. Biol.* **335**, 923-936

36. Milon, P., Konevega, A. L., Gualerzi, C. O., and Rodnina, M. V. (2008) *Mol Cell* **30**, 712-720

37. Record, M. T., Jr., Lohman, M. L., and De Haseth, P. (1976) *J Mol Biol* **107**, 145-158

38. Lohman, T. M., deHaseth, P. L., and Record, M. T., Jr. (1980) *Biochemistry* **19**, 3522-3530

39. Nissen, P., Kjeldgaard, M., Thirup, S., Polekhina, G., Reshetnikova, L., Clark, B. F., and Nyborg, J. (1995) *Science* **270**, 1464-1472

40. Nissen, P., Thirup, S., Kjeldgaard, M., and Nyborg, J. (1999) *Structure* **7**, 143-156

41. Record, M. T., Jr., Anderson, C. F., and Lohman, T. M. (1978) *Q Rev Biophys* **11**, 103-178

42. Ott, G., Faulhammer, H. G., and Sprinzl, M. (1989) *Eur J Biochem* **184**, 345-352

43. LaRiviere, F. J., Wolfson, A. D., and Uhlenbeck, O. C. (2001) *Science* **294**, 165-168

44. Asahara, H., and Uhlenbeck, O. C. (2002) *Proc Natl Acad Sci USA* **99**, 3499-3504

45. Dale, T., Sanderson, L. E., and Uhlenbeck, O. C. (2004) *Biochemistry* **43**, 6159-6166

46. Abrahamson, J. K., Laue, T. M., Miller, D. L., and Johnson, A. E. (1985) *Biochemistry* **24**, 692-700

47. Louie, A., and Jurnak, F. (1985) *Biochemistry* **24**, 6433-6439

48. Louie, A., Ribeiro, N. S., Reid, B. R., and Jurnak, F. (1984) *J Biol Chem* **259**, 5010-5016

49. Rudinger, J., Hillenbrandt, R., Sprinzl, M., and Giege, R. (1996) *EMBO J* **15**, 650-657

50. Giege, R., Sissler, M., and Florentz, C. (1998) *Nucl Acids Res* **26**, 5017-5035

51. Saks, M. E., Sampson, J. R., and Abelson, J. N. (1994) *Science* **263**, 191-197

52. Chapeville, F., Lipmann, F., Von Ehrenstein, G., Weisblum, B., Ray, W. J., Jr., and Benzer, S. (1962) *Proc Natl Acad Sci USA* **48**, 1086-1092

53. Axley, M. J., Bock, A., and Stadtman, T. C. (1991) *Proc Natl Acad Sci USA* **88**, 8450-8454

Paper 4

Structure of SelB·GTP·Sec-tRNA^{Sec} bound to the ribosome

Niels Fischer[1], Kirill Gromadski[2], Alena Paleskava[2], Marina V. Rodnina[2,*] and Holger Stark[1,*]

[1] Max-Planck Institute for Biophysical Chemistry, 37077 Göttingen, Germany
[2] Institute of Physical Biochemistry, University of Witten/Herdecke, 58448 Witten, Germany

Corresponding authors:
Dr. Marina Rodnina, University of Witten/Herdecke, 58448 Witten, Germany. Tel. +49 2302 926205. Fax. +49 2302 926117. E-mail: rodnina@uni-wh.de
Dr. Holger Stark, Max-Planck Institute for Biophysical Chemistry, 37077 Göttingen, Germany. Tel.: +49 551 201 1305. Fax: +49 551 201 1197. E-mail: holger.stark@mp bpc.mpg.de

Abstract

The translational recoding of the stop codon UGA as selenocysteine (Sec) requires a specialized elongation factor (EF) SelB that selectively binds Sec-tRNA^{Sec}, and a selenocysteine insertion sequence (SECIS) in the mRNA. Here we report the three-dimensional reconstruction by cryo-electron microscopy of the SelB·Sec-tRNA^{Sec} complex stalled on the ribosome by using a non-hydrolysable analog of GTP, GDPNP. EF-Tu-like domains I-III of SelB bind to the ribosome in a fashion similar to EF-Tu. Domain IV of SelB bridges between the factor binding site and the mRNA entrance tunnel on the 30S subunit. Wing-helix motifs 1 and 2 of domain 4 contact h16 of 16S rRNA, whereas the tip of wing-helix motif 4 contacts the ribosomal protein S3 at the mRNA entry tunnel. The results provide a detailed snapshot view of the ribosome during the recoding of the UGA codon with selenocysteine.

Introduction

Selenocysteine is the 21st "natural" amino acid that is incorporated into protein during ribosomal protein synthesis. It is known to occur in several dozen proteins called selenoproteins (Kryukov and Gladyshev, 2004). Selenoproteins exist in all major forms of life, eukaryotes, eubacteria and archaea, and are vital in animals and humans. In bacteria, the biosynthesis of selenocysteine and its insertion into proteins requires the function of at least four gene products. Like other amino acids used by cells, selenocysteine has a specialized tRNA, which is encoded by the SelC gene in bacteria (Baron and Böck, 1995; Böck et al., 1991). The primary and secondary structure of selenocysteine tRNA, tRNA^{Sec}, differs from those of standard tRNAs in several respects, most notably in having a longer acceptor stem, substitutions at several conserved base positions, and a long variable arm (Baron and Böck, 1991, 1995; Baron et al., 1990; Schön et al., 1989). The selenocysteine tRNA is initially charged with serine by seryl-tRNA ligase, but the resulting Ser-tRNA^{Sec} is not used for translation because it is not recognized by the normal translation factor EF-Tu. Rather, the tRNA-bound seryl residue is converted to a selenocysteyl (Sec) residue by the pyridoxal phosphate-containing enzyme selenocysteine synthase (the selA gene product) using selenomonophosphate as the selenium donor substrate. The latter is synthesized from selenite and ATP by selenophosphate synthetase (the selD gene product). Finally, the resulting Sec-tRNA^{Sec} specifically binds a specific translational elongation factor, SelB, which delivers it in a targeted manner to the ribosomes translating mRNAs for selenoproteins. The mRNA codon for selenocysteine is UGA, which usually serves as a stop codon but, in context with a specific downstream sequence forming a stem-loop (SECIS), is recognized as the site of selenocysteine incorporation into proteins. SelB is a GTP binding protein that belongs to the family of translation factors,

which also includes EF-Tu, EF-G, IF2, RF3, and their eukaryotic homologs. The structure of the full-length SelB from *E. coli* is not known. Sequence comparisons between SelB and EF-Tu suggested that SelB consists of four domains (Hilgenfeld et al., 1996; Kromayer et al., 1996). Domains I-III are conserved among bacteria, archea, and eukaryotes. They are homologous to domains I-III of EF-Tu and provide most of the contact surface for Sec-tRNA^{Sec}. The arrangement of domains I-III in the crystal structure of SelB from an archeon *Methanococcus maripaludis* is very similar to that of *Escherichia coli* or *Thermus aquaticus* EF-Tu·GTP (Leibundgut et al., 2004). The structure of domain IV of SelB, which has no orthologs in EF-Tu or other translational GTPases, is not conserved between pro- and eukaryotes. In bacteria, domain IV of SelB binds the SECIS element of mRNA. Domain IV of SelB from *Moorella thermoacetica* consists of four similar winged-helix (WH) domains arranged into the shape of an L (Selmer and Su, 2002). WH4 domain recognizes the hairpin backbone and nucleotides extruded from the apical loop of the SECIS element (Yoshizawa et al., 2005). The structure of archaeal and eukaryotic domain IV is different (Leibundgut et al., 2004). In eukaryotes, the function of SelB is shared by at least two proteins, EFsec and SBP2 (Copeland et al., 2000). In addition, the ribosomal protein L30, which has no prokaryotic ortholog, was reported to be a component of the recoding machinery in eukaryotes (Chavatte et al., 2005). The current model of SelB action on the ribosome suggests that in the cell practically all SelB is present as a SelB·GTP·Sec-tRNA^{Sec} complex with SECIS (Thanbichler et al., 2000). Upon translation, the lower part (10-11 nucleotides) of the SECIS hairpin is expected to melt in order to position the UGA codon in the A site, whereas the intact upper part is bound to domain IV of SelB and may appear just at the mRNA entrance of the ribosomal A site (Hüttenhofer and Böck, 1998). The efficiency of UGA decoding by SelB·GTP·Sec-tRNA^{Sec} in the presence of SECIS in *E. coli* is low, ranging from about 5% in exponentially growing cells (Suppmann et al., 1999) to 60% during the stationary phase (Mansell et al., 2001). A careful genetic analysis indicated that this low efficiency is caused by termination at UGA codons, rather than by the presence of a (stable) SECIS hairpin or competition of SelB·GTP·Sec-tRNA^{Sec} with the bulk of EF-Tu·GTP·aminoacyl-tRNAs (Mansell et al., 2001; Suppmann et al., 1999). Recoding of the UGA codon by selenocysteine resulted in a translational pause of about 10 ms (Suppmann et al., 1999). A structural explanation for these findings is lacking, as the structure of the ribosome complex is not available.

In the present work, we solved the structure of the recoding complex with *E. coli* SelB and Sec-tRNA^{Sec} stalled in the A site of the ribosome by addition of GDPNP, a non-hydrolyzable GTP analog, using electron cryomicroscopy (cryo-EM).

Results

Overall structure

The overall structure of the ribosome in the complex (Fig. 1) is the same as that obtained by crystallography (Schuwirth et al., 2005) or cryo-EM at lower resolution (Stark et al., 2002; Valle et al., 2003). SelB and the tRNAs (fMet-tRNA^{fMet} in the P site, SelB-bound Sec-tRNA^{Sec} in the A site, and a tRNA in the E site) are clearly visible. The cryo-EM density of the 30S and 50S subunits can be interpreted using the crystal structures of *E. coli* ribosomes (Schuwirth et al., 2005) (Fig. 1), after the following modifications. The relative arrangement of the head and the body of the 30S subunit in the present structure differs from both crystal structures of the *E. coli* 70S ribosome (Schuwirth et al., 2005), but is very similar to that in the kirromycin-stalled complex with EF-Tu and Phe-tRNA^{Phe} (Stark et al., 2002; Valle et al., 2003) or the crystal structure of the 30S subunit from *T. thermophilus* with the anticodon stem-loop parts of tRNA bound (Ogle et al., 2001). To interpret the cryo-EM map, the densities for the head and body were fitted separately using the respective parts of the *E. coli* crystal structure (Schuwirth et al., 2005). The structure of the L11-binding region of 23S rRNA (helices 43/44) is also altered. Automated rigid body fitting of the region
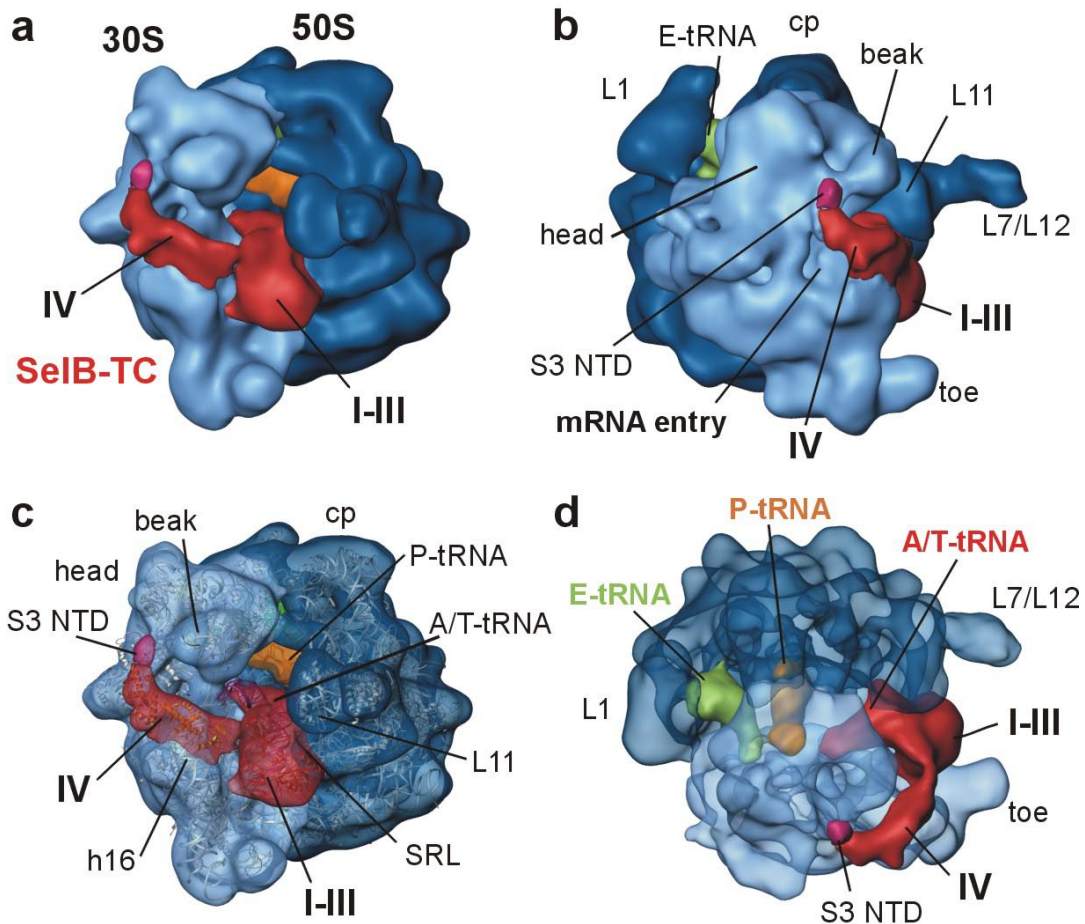
Figure 1 Three-dimensional reconstruction of the 70S *E. coli* ribosome in complex with SelB, Sec-tRNA[Sec] and mRNA containing the SECIS element.

a) View from the A-site side of the ribosome and **b)** from the 30S subunit side. The 50S subunit is shown in dark blue, the 30S subunit in light blue, P-site tRNA in orange, E-site tRNA in green, the difference densities for the Sec-tRNA[Sec]·SelB·GDPNP ternary complex (SelB-TC) in red and for the N-terminal domain of S3 (S3 NTD) in pink. I-IV indicate the domains of SelB; cp, central protuberance; L1, L1 stalk; L7/L12, L7/L12 stalk; mRNA entry, mRNA entry tunnel. **c)** Fitting crystal structures of the 70S ribosome from *E. coli* (PDB entries 2aw4 and 2aw7 (Schuwirth et al., 2005); light grey), homology model of SelB (domains I-III red (Leibundgut et al., 2004); domain IV, orange (Selmer and Su, 2002)), Sec-tRNA[Sec] (coordinates from http://www-ibmc.u-strasbg.fr/upr9002/westhof/ (Baron et al., 1993); violet), the P-site tRNA (PDB entry 1YL4 (Jenner et al., 2005); orange) and E-site tRNA[Sec] (green). SRL, sarcin ricin loop; h16, helix 16 of 16S rRNA. **d)** Position of the SelB ternary complex and tRNAs as seen from top.

resulted in a 7 Å shift of position A1067 towards the central protuberance of the 50S subunit, compared to the crystal structure (Schuwirth et al., 2005). In the cryo-EM map, the region corresponding to the ribosomal protein S3 was altered compared to the crystal structure (Schuwirth et al., 2005). To obtain the best fit, the N-terminal domain of S3 was shifted by 7 Å away from the beak of the 30S subunit. The change in the S3 conformation is most probably induced by SelB binding, because this structure is found only in the presence of SelB, and was not observed in crystal structures

(Ogle et al., 2001; Ogle et al., 2002) or cryo-EM maps with other ligands (Stark et al., 2002; Valle et al., 2003).

P-site and E-site tRNAs

fMet-tRNA[fMet] is positioned between the 30S and 50S subunits in largely the same way as the P-site tRNA in the 70S crystal structure (Jenner et al., 2005; Yusupov et al., 2001). The density was interpreted best by using the structure (Jenner et al., 2005), which is distorted at the anticodon and D stems compared to unbound tRNA (Jovine et al., 2000; Shi and Moore, 2000) (Fig. 1). The anticodon arm points into the 30S P-
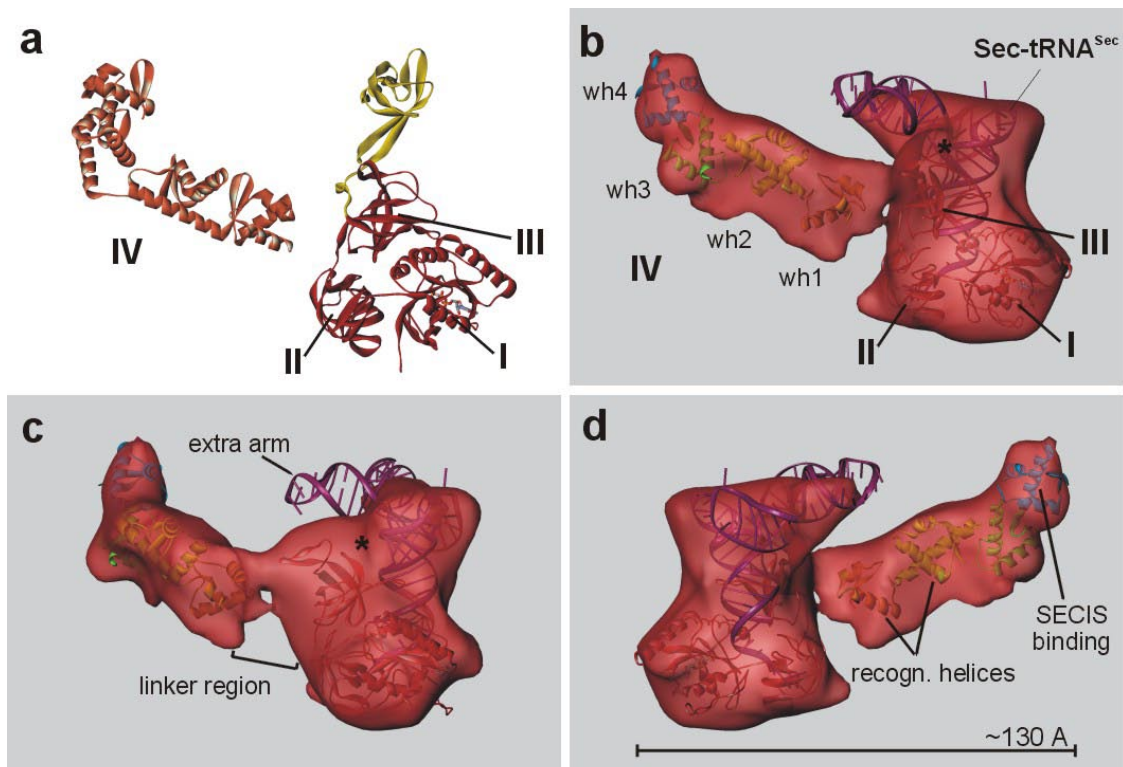
Figure 2 Model of the SelB ternary complex a) Crystal structures used for homology modeling of E. coli SelB. Domains I-III (I-III) were modeled using the structure of free SelB from an Archeon M. maripaludis in the GDPNP-bound form (red, domains I-III; yellow, domain IV) (Leibundgut et al., 2004). The structure of SelB·GDP was used to reconstruct the effector loop, unresolved in the SelB·GDPNP structure (PDB entries 1wb3 and 1wb1 (Leibundgut et al., 2004)). Domain IV of SelB (IV) was modeled using the free structure from the bacterium M. thermoacetica (PDB entry 1lva (Selmer and Su, 2002); orange). b) Molecular model of the Sec-tRNA^{Sec}·SelB·GDPNP complex with semitransparent EM density in red, shown from the factor binding site side, c) from the 50S side, and d) from the L1 stalk side. The flexible extra arm of Sec-tRNA^{Sec} (Baron et al., 1993) may fold back onto SelB domain III and, thus, account for the free density (*). Wh, winged helix motifs of domain IV; recogn. helices, recognition helices of wh1 and wh2; SECIS binding, region of wh4 binding SECIS RNA in the M. thermoacetica crystal structure (PDB entry 1WSU (Yoshizawa et al., 2005)).

site decoding center. The anticodon arm contacts helices 24, 30, and 31. The T loop and the minor groove of the D stem of the P-site tRNA contact the 50S subunit at protein L5 and helix 69 of 23S rRNA, respectively, as in the crystal structure (Jenner et al., 2005; Yusupov et al., 2001). The identity of the tRNA in the E site is not known. Our ribosome preparations, in contrast to *T. thermophilus* ribosomes used for crystallography (Jenner et al., 2005; Yusupov et al., 2001), do not contain deacylated tRNA in the E site (Stark et al., 2000; Stark et al., 2002). The deacylated tRNA found in the E site is most likely tRNA^{Sec} that was added in excess and was not fully charged under the conditions used in the present experiments. The presence of any other tRNAs is unlikely, because tRNA^{Sec} and fMet-tRNA^{fMet} used in the present experiments had >90% purity, and the 70S initiation complex was additionally purified from unbound tRNA by

ultracentrifugation. Direct identification of tRNA^{Sec} in the E site, e.g. due to its extended variable loop was not possible, as the extra arm is not resolved. The tRNA in the E site makes largely the same contacts as seen in the crystal structures (Jenner et al., 2005; Yusupov et al., 2001). The anticodon arm contacts protein S7, the apical loop of helix 23, helices 28/29 on the 30S subunit. Protein L1 and helices 76/77 on the 50S subunit contact the elbow region of tRNA, whereas helix 68 contacts the acceptor arm.

SelB and Sec-tRNA^{Sec}

The density due to SelB-Sec-tRNA^{Sec} attached to the factor binding site of the ribosome (Fig. 1) resembles that of EF-Tu-Phe-tRNA^{Phe} (Stark et al., 2002), except for an additional L-shaped protrusion extended towards the mRNA entry tunnel and the protein S3 on the 30S subunit. To interpret the density of SelB-Sec-tRNA^{Sec} in detail, a
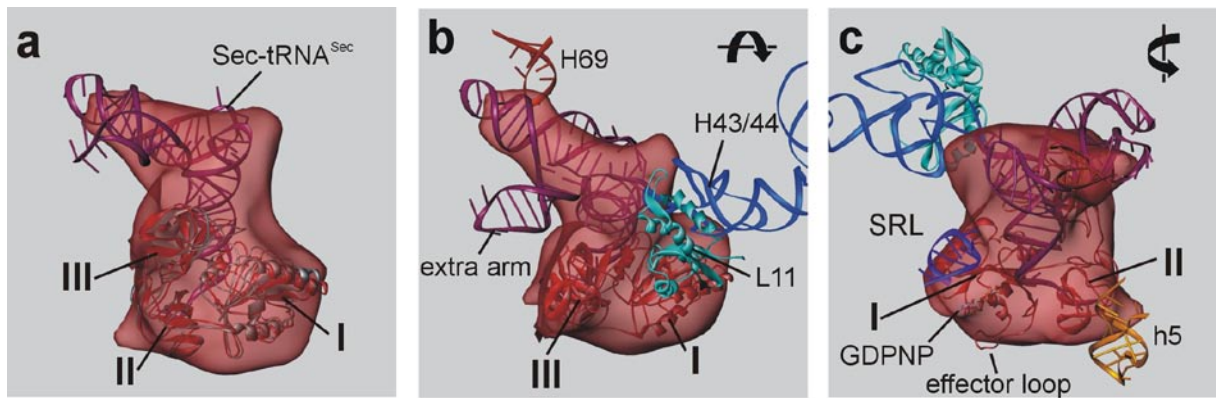
Figure 3 Conformation and contacts of SelB domains I-III and Sec-tRNA^{Sec}.
a) Conformation of SelB domains I-III (I-III, red) and Sec-tRNA^{Sec} (violet) on the ribosome. Domain III was adjusted to a more open arrangement relative to domain I in comparison to the homology model (grey) to fit the cryo-EM density (semitransparent red). **b)** and **c)** Contacts of SelB domains I to III and Sec-tRNA^{Sec} with the ribosome, similar to those of the EF-Tu ternary complex (Stark et al., 2002; Valle et al., 2003). H69 and H43/H44, helices 69 and 43/44 of 23S rRNA; SRL, sarcin ricin loop of 23S rRNA; h5, helix 5 of 16S rRNA.

difference map (indicated red in the Figures) was calculated between the cryo-EM maps of the SelB bound ribosome and the ligand free ribosome (see Methods), which thus represents the SelB·GDPNP·Sec-tRNA^{Sec} ternary complex. The structural model of *E. coli* SelB·GDPNP·Sec-tRNA^{Sec} (Fig. 2) was obtained by docking homology models of domains I-III (Leibundgut et al., 2004), domain IV (Selmer and Su, 2002), and the model of Sec-tRNA^{Sec} (Baron et al., 1993) into the difference map. The EM map shows two connections between domains III and IV of SelB; the connection could not be interpreted in terms of protein structure, because the homology model for the corresponding linker region (10 residues) is not available. Compared to the homology model of SelB domains I-III based on the crystal structure of *M. maripaludis* SelB (Leibundgut et al., 2004), the relative orientation of domains I-III of SelB on the ribosome is changed, with domain III rotated slightly away from domain I. Similar conformational changes were observed upon EF-Tu binding to the ribosome (Stark et al., 2002; Valle et al., 2003).Superposition of domains I-III of SelB and EF-Tu bound to the ribosome (Stark et al., 2002; Valle et al., 2003) suggests that the factors bind to the ribosome in a very similar way. Domain I of SelB is involved in an extensive interaction with the sarcin-ricin stem loop (SRL) of 23S RNA, whereas domain II contacts helix 5 of 16S rRNA (Fig. 3). The SRL interaction seems to constitute the main direct binding interaction between SelB and the ribosome. On SelB, the interaction involves the nucleotide-binding pocket suggesting that the SRL may have a role in GTPase activation of the factor.

Sec-tRNA^{Sec} interacts with helices 69 and 43/44 of 23S rRNA (Fig. 3). The contact of Sec-tRNA^{Sec} to helix 69 is quite similar to that observed with Phe-tRNA^{Phe} in the kirromycin-stalled EF-Tu complex (Stark et al., 2002; Valle et al., 2003). However, the interaction with helix 43, the binding site for the ribosomal protein L11, is somewhat different in the two complexes. In the SelB complex, there is a shift of the L11 arm by 4 Å towards the central protuberance of the 50S subunit in comparison to the map of the initiated complex without ligand, and the position of helices 43/44 is different compared to the kirromycin-stalled EF-Tu complex (see below). The long variable arm of tRNA^{Sec} is not found in the position expected from the solution structure model (Baron et al., 1993).

The variable arm may not be resolved due to its flexibility; however, additional density was observed close to domain 3 of SelB which could not be accounted for by the protein. This suggests that the conformation of Sec-tRNA^{Sec} may be changed compared to the model of the solution structure and the variable loop may be folded back onto the apical part of domain III (Fig. 2).
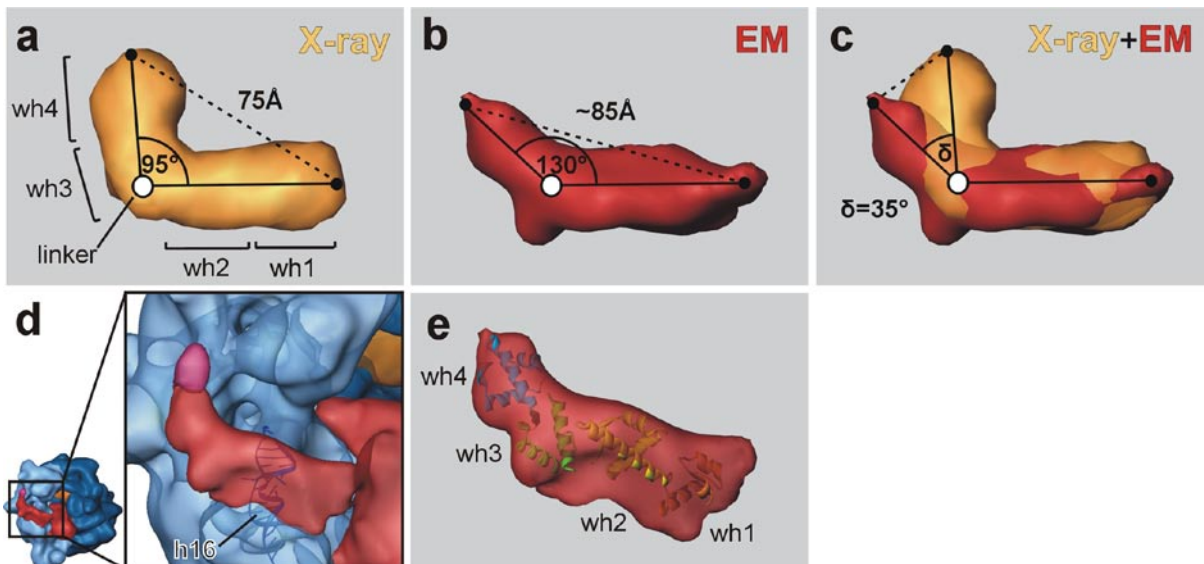
Figure 4 Potential conformational change of SelB domain IV

a) Homology model of free SelB domain IV (semitransparent yellow) obtained from the crystal structure (Selmer and Su, 2002) by filtering to 15 Å resolution. The positions of the wh motifs (wh) and the linker region between wh2 and wh3 are indicated. **b)** Cryo-EM density for SelB domain IV (red) bound to the ribosome. **c)** Overlay of the homology model and cryo-EM density indicating an opening of SelB domain IV upon ribosome binding. **d)** Position of SelB (semitransparent red) on the 30S subunit (semitransparent blue) Wh1 and wh2 of domain IV face helix 16 (h16, blue) of 16S rRNA. **e)** Docking the homology model of *E. coli* SelB domain IV into the cryo-EM density (semitransparent red). WH1 (red) and WH2 (yellow) were docked as a rigid body to face helix 16 with their recognition helices, then WH3 (green) and WH4 (bue) were fit as a rigid body maintaining connectivity with WH2

Conformation and contacts of domain 4 of SelB

Comparison of the difference density of the ribosome-bound domain IV of SelB with the homology model based on the structure of the isolated domain (Selmer and Su, 2002), suggests that the two subdomains of domain IV (comprising WH1/2 and WH3/4, respectively) move apart by 35°. This increases the distance between the N and C termini of the domain from about 75 Å to 85 Å and allows domain IV to reach from the C-terminus of domain III to protein S3 at the mRNA entry tunnel (Fig. 4). The pivot is located in the random-coil linker between WH2 and WH3, and flexibility in this region is further supported by the small contact area between the two WH motifs (Selmer and Su, 2002).

Docking the homology model places WH1 and WH2 motifs in close contact to helix 16 of 16S rRNA (Fig. 4, 5), suggesting

a potential interaction. In fact, isolated helix 16 of 16S rRNA forms a stable complex with SelB, resulting in a band shift in native polyacrylamide gel electrophoresis (data not shown). WH4 contacts the NTD of S3 at the mRNA entry tunnel (Fig. 5). The SECIS binding site of domain IV points to the mRNA entry tunnel. To predict the position of SECIS, the NMR structure of the *E. coli* SECIS hairpin (Fourmy et al., 2002) was modeled assuming the proposed contacts between SECIS and WH4 (Yoshizawa et al., 2005). According to the model, the SECIS element is expected to appear directly in front of the mRNA entry tunnel; however no apparent density was found which could be interpreted in terms of a SECIS element. This suggests that SECIS is either too flexible and is therefore not resolved in the structure, or is unfolded at the present step of UGA recoding.
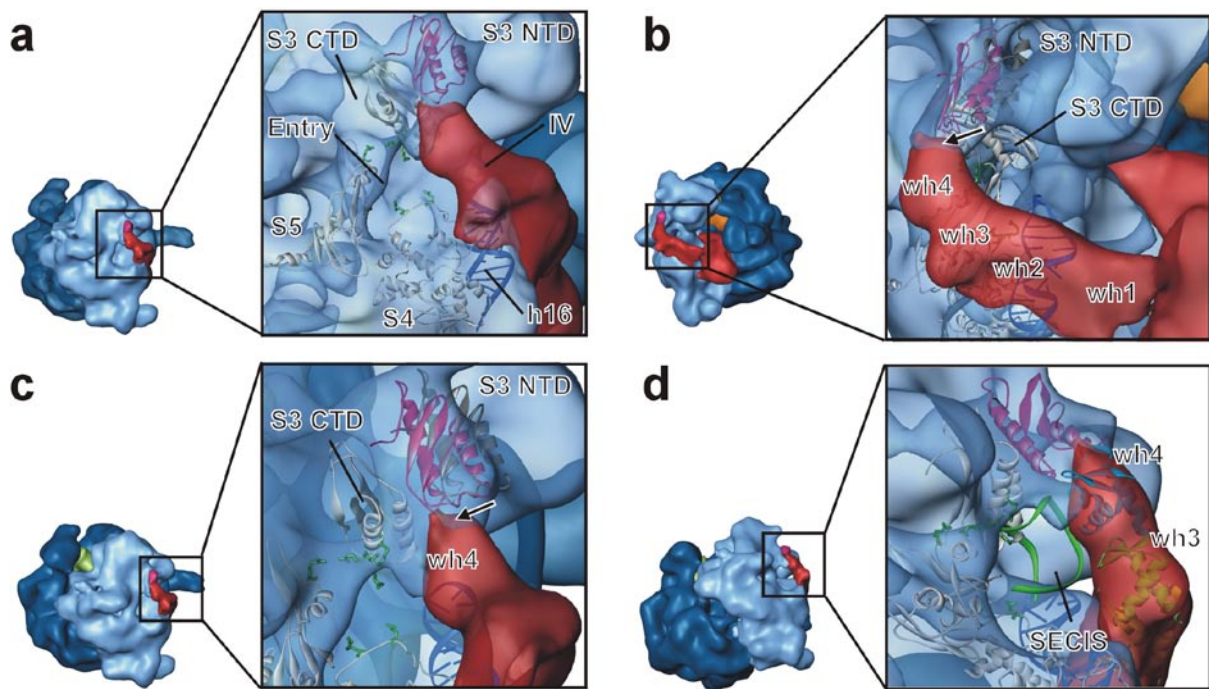
Figure 5 Position of domain IV of SelB on the ribosome
a) Position of SelB domain IV (IV, semitransparent red) on the 30S subunit (semitransparent blue). Domain IV binds the ribosome close to helix 16 (h16, blue) of 16S rRNA and the N- and C-terminal domains of protein S3 (S3 NTD, pink; S3 CTD, white; difference density for S3 NTD, semitransparent pink) at the mRNA entry tunnel (Entry). Two other proteins at the mRNA tunnel are S4 and S5 (white; green stick representations, basic side chains enclosing the mRNA entry tunnel). **b)** View from the factor binding site. The S3 NTD as obtained by fitting the crystal structure of the 30S head (Schuwirth et al., 2005) as rigid body (dark grey) was shifted by about 7 Å (arrow) to fit the EM density (pink, after readjustment). Positions of the wh motifs 1-4 of SelB domain IV are indicated. **c)** and **d)** Different views from the 30S subunit side. Addition of the *E. coli* SECIS assuming the interaction with wh4 as suggested (Yoshizawa et al., 2005) (PDB entry 1mfk (Fourmy et al., 2002); green ribbon) places the SECIS hairpin close to the mRNA tunnel, but outside of the EM density.

Discussion

The cryo-EM structure presented here provides insights into the mechanism of UGA recoding by selenocysteine. It shows that SelB brings Sec-tRNA^{Sec} to the ribosome in a manner similar to EF-Tu and canonical tRNAs. SelB bridges the factor binding site on the 50S subunit and the mRNA entry tunnel on the 30S subunit. The main contacts of the EF-Tu-like domains I-III of SelB on the ribosome are the SRL on the 50S subunit and helix 5 on the 30S subunit, and the interactions of Sec-tRNA^{Sec} with the ribosome resemble very closely the contacts of canonical tRNAs in the EF-Tu complex (Stark et al., 2002; Valle et al., 2003). The conformation of domain IV of SelB is altered compared to the solution structure, with a pivot between WH motifs 1/2 and 3/4. WH motifs 1/2 are close to helix 16 of 16S rRNA, whereas WH4 contacts the protein S3 on the 30S subunit through the NTD of S3, which changes its position upon SelB binding. In addition, the cryo-EM structure reveals the "half-closed" conformation of the L11-binding region of 23S rRNA (Frank et al., 2005) and sheds some light on its role in factor function.

Although the arrangement and contacts of SelB and EF-Tu on the ribosome are very similar, the sequence of events resulting in complex formation may be different. The initial contact of EF-Tu with the ribosome is mediated by the ribosomal protein L7/12, which recruits the factors independently of the codon presented in the A site (Diaconu et al., 2005; Kothe et al., 2004). In contrast, SelB, which binds tightly to the SECIS element (Thanbichler et al., 2000), is delivered to the ribosome by the movement of mRNA through the ribosome up to the point when the lower

Figure 6 Movement of the L11-RNA complex upon ternary complex binding
a) Positions of helices 43/44 (h43/44) of 23S rRNA as observed in cryo-EM maps of different 70S ribosome complexes. Cyan, 'open' position of h43/44 in the initiated and accommodated state (emd entries 1003 and 1056 (Gabashvili et al., 2000; Valle et al., 2003)); dark blue, 'half closed' position of h34/44 in the complexes with Sec-tRNA^{Sec}·SelB·GDPNP (present structure) or Phe-tRNA^{Phe}·EF-Tu·GDPNP (Frank et al., 2005); violet, 'closed' position of h34/44 in the Phe-tRNA^{Phe}·EF-Tu·GDP·kirromycin complex (emd entry 1055 (Valle et al., 2003))

part of the SECIS helix is melted (Thanbichler and Böck, 2001). Early results suggested that positioning the SECIS hairpin closer than about 16 bases to the ribosomal A site resulted in reduced mRNA binding to the 30S subunit (Hüttenhofer et al., 1996).

However, when analogous experiments were carried out with 70S ribosomes in the presence of fMet-tRNA^{fMet} and initiation factors, rather than 30S subunits and deacylated tRNA^{fMet} (Hüttenhofer et al., 1996), we obtained equally efficient initiation independently of the spacer length between the AUG and UGA codons or the SECIC (data not shown), suggesting that the ribosome is capable to unwind the lower part of the SECIS in the absence of SelB or any further accessory proteins.

In the complex prior to codon recognition, SelB binds at the site overlapping with EF-Tu, as decoding of sense codons by EF-Tu is delayed by SelB·Sec-tRNA^{Sec} binding to the ribosome (Suppmann et al., 1999). The major contact of SelB on the 50S subunit is the SRL, and this is the only ribosome element that contacts SelB at the nucleotide-binding pocket. The contact may play a role in GTP hydrolysis by SelB by stabilizing the switch regions of the G domain in the catalytically active conformation (Rodnina et al., 2005).

Another clear contact between the ternary complex and the ribosome is the connection between the elbow region of Sec-tRNA^{Sec} and the L11-binding region of 23S rRNA, termed the GTPase-activating (or associated) center (GAC). As there is no contact between L11 and the nucleotide binding pocket of EF-Tu, a direct involvement of L11 in GTPase activation of SelB (or EF-Tu) is unlikely; hence the term GAC appears to be inappropriate. Rather than activating the GTPase directly, the L11-binding region, and possibly its contact with aa-tRNA, is important for transmitting the GTPase-activating signal from the codon-anticodon complex, positioning the tRNA relative to other elements of the ribosome, and guiding the tRNA towards the A site during accommodation.

In the complex with SelB the L11-binding helices were found in the "half-closed" conformation that differs both from the "open" structure found in the structures in the absence of the factors (Gabashvili et al., 2000; Valle et al., 2003) and from the "closed" conformation observed in the kirromycin-stalled EF-Tu complex (Stark et al., 2002; Valle et al., 2003). A similar "half-closed" conformation of helices 43/44 was found in the EF-Tu·GDPNP complex on the ribosome (Frank et al., 2005). This suggests that the "half-closed" conformation may form transiently upon binding of ternary complexes, either with SelB or EF-Tu, to the ribosome before GTP hydrolysis. This movement may bring the D loop of tRNA in contact with helix 69 of 23S rRNA (Frank et al., 2005). These contacts, together with additional interactions of the factors with the SRL and the formation of the codon-anticodon complex, may be important for the stabilization of the GTPase transition state of the factor. GTP hydrolysis by EF-Tu is not affected by kirromycin (Kothe and Rodnina, 2006); hence, the structure of the kirromycin-stalled EF-Tu complex may represent a further movement of the helices 43/44, together with tRNA, after GTP hydrolysis. The results of MD simulation indicated that A1067 in helix 43 consecutively interacts with tRNA bases 55, 54, 53, 52, and 51 during the accommodation, suggesting that A1067 may monitor the tRNA movement (Sanbonmatsu et al., 2005). In the final stage of the accommodation, the elbow

region of the tRNA does no longer interact with A1067, and helices 43/44 may move to their initial "open" position.

Probably the most interesting set of interactions found in the present structure involve domain IV of SelB. Domain IV of SelB is found on the ribosome in a more open conformation than in the crystal structure (Selmer and Su, 2002). The opening is necessary to accommodate simultaneously the WH4 motif bound at the mRNA entry tunnel and domains I-III of SelB attached to the factor binding site, as proposed previously (Selmer and Su, 2002). WH4 interacts with the protein S3. The position of the NTD of S3 is changed compared to the structure in the absence of the factor, which is probably caused by the binding of the SelB body to the ribosome. The density expected for a SECIS element is absent in the present cryo-EM reconstruction. One explanation for the lack of the respective density is that the SECIS is too flexible and is therefore not resolved in the structure. However, it is also possible that the SECIS is not seen because the upper part of the SECIS is unfolded at the present step of UGA recoding. The unwinding of the upper part of the SECIS is necessary for further translation, because the SECIS helix is too large to pass through the narrow mRNA tunnel. Upon binding of SelB to the ribosome the SECIS helix may be melted by the ribosomal helicase complex consisting of proteins S3, S4, and S5 (Takyar et al., 2005), possibly assisted by domain IV of SelB. In this context, the movement of the NTD of S3 may reflect a rearrangement involved in melting the mRNA secondary structure and thus provide a snapshot of the ribosomal helicase at work.

The functional significance of the interaction between WH1/2 and helix 16 of 16S rRNA is not known. It is possible that binding of WH1/2 to 16S rRNA stabilizes the open conformation of domain IV and thereby helps to position SelB at the factor binding site. On the other hand, interactions of WH1/2 with helix 16 may affect the relative mobility of the head and body of the 30S subunit, as helix 16 belongs to the elements involved in the open-to-close transition during decoding of sense codons (Ogle et al., 2002). Global conformational change of the 30S subunit

is crucial for tRNA selection in the A site and for the GTPase activation in EF-Tu (Gromadski et al., 2006; Gromadski and Rodnina, 2004a, b; Ogle et al., 2001; Ogle et al., 2002). By analogy, interaction of domain 4 of SelB with helix 16 of 16S rRNA may be involved in sensing the recognition of the UGA codon by Sec-tRNA[Sec] and modulating at the distance the timing of GTP hydrolysis by SelB.

The WH motifs of SelB are involved in both protein-protein and RNA-protein interactions, with the protein S3, the SECIS element, and helix 16 of 16S rRNA. WH motifs are widely found in DNA-binding proteins (for review see (Gajiwala and Burley, 2000)), which recognize DNA by inserting the helix 3 and/or wing 1 of the WH motif into the major groove of a DNA double helix. The known structures of WH motifs bound to RNA come from the studies of the SECIS·WH3/4 complex (Yoshizawa et al., 2005); the RNA-protein contacts of another RNA-binding WH-containing protein, the La protein (Alfano et al., 2004; Dong et al., 2004), do not seem to involve the WH motif (Teplova et al., 2006). SelB WH4 recognizes neither the major nor the minor groove of RNA (Yoshizawa et al., 2005). Helix 2 and the N-terminal part of recognition helix 3 of WH4 form specific contacts with the backbone as well as nucleotides extruded from the hairpin loop (Yoshizawa et al., 2005). WH1/2 motifs are close to helix 16 of 16S rRNA and cover the upper double-helical part of helix 16 which contains two G·U base pairs and a large internal bulge. Notably, helix 2 of WH2 contains a conserved basic patch of WH1/2 (Selmer and Su, 2002), which may be involved in the backbone interactions with 16S rRNA. The details of the interaction cannot be deduced at the present level of resolution and await high-resolution structures. However, the type of recognition by WH motifs of the RNA elements or protein S3 on the ribosome and DNA is quite different, emphasizing the versatility of the WH motifs as a module in DNA-protein, RNA-protein, and protein-protein interactions.

Methods
Biochemical methods
Ribosomes from *E. coli* MRE600, initiation factors, and f[³H]Met-tRNA[fMet] were

prepared as described previously (Rodnina et al., 1995; Rodnina et al., 1999; Rodnina et al., 1994). mRNA (mLP75) was a derivative of AH75 (Hüttenhofer et al., 1996), modified to have a stronger Shine-Dalgarno sequence and a single AUG codon in all reading frames. The sequence of mLP75 mRNA is 5'-GGGCUAAAUUAAGGAGGUUCAUUAAU GUUC3CACGGCCCAUCGG*UU*GCAG*GU* CUGCACCAAUCUAUUGGCGCAUUG-3'. mRNA was prepared by T7 RNA polymerase transcription. To remove the traces of salt which strongly favors the formation of biologically inactive dimers, the solutions of mRNA were reactivated in the presence of 100 mM EDTA for 90 s at 80°C and then rapidly cooled on ice. Ribosomal initiation complexes were formed in a buffer A containing 50 mM HEPES, pH 7.5, 70 mM NH_4Cl, 30 mM KCl, 7 mM $MgCl_2$, 1 mM DTT by incubating 70S ribosomes (1 μM) with mLP75 mRNA (3 μM), f[^{3}H]Met-tRNA$_f^{Met}$ (1.5 μM), initiation factors 1, 2 and 3 (1.5 μM each), and GTP (1 mM) for 70 min at 37 °C. Ribosome complex was purified and concentrated by centrifugation through 1.1 M sucrose cushion prepared in buffer A at 200,000 x g for 2 h on a Sorvall M120GX ultracentrifuge. Binding of f[^{3}H]Met-tRNA^{fMet} to the P site was quantitated by nitrocellulose filtration.

SelB was prepared accoding to (Thanbichler and Böck, 2003). SelA, SelD, seryl-tRNA synthetase, and tRNA^{Sec} were kind gifts of A. Böck. tRNA^{Sec} (8.5 µM) was aminoacylated by seryl-tRNA synthetase (1 µM), ^{14}C-serine (30 µM), ATP (3 mM), inorganic pyrophosphatase (0.01 U/µl; Sigma) in buffer B containing 100 mM HEPES, pH 7.0, 10 mM KCl, 10 mM magnesium acetate, 2 mM DTT for 90 min at 37°C. Ser-tRNA^{Sec} was isolated by phenol extraction using potassium acetate-saturated phenol, pH 4.6. To convert Ser-tRNA^{Sec} into Sec-tRNA^{Sec}, selenite (Na_2SeO_3, 150 µM) was activated to selenomonophosphate by SelD (10 µM) and ATP (5 mM), and Ser to Sec conversion was catalyzed by SelA (3 µM) in buffer B for 30 min at 37°C. Sec-tRNA^{Sec} was phenol extracted in the presence of 100 mM potassium acetate-saturated, pH 4.6, and 5 mM DTT, ethanol precipitated, and dissolved in 10 mM potassium acetate,

pH 4.6, and 5 mM DTT. The extent of conversion was verified by thin-layer chromatography on TCA plates (Thanbichler and Böck, 2002).

The ternary complex SelB·GMPPNP·[^{3}H]Sec-tRNA^{Sec} was prepared in buffer A by mixing [^{3}H]Sec-tRNA^{Sec} (6 µM) with SelB (6 µM) containing a C-terminal His-tag, GMPPNP (3 mM), DTT (2 mM) incubated for 10 min at 37°C. Binding of Sec-tRNA^{Sec} to SelB was tested by nitrocellulose filtration. After additional incubation for 5 min at 37°C equal volumes of purified 70S initiation complex (1 µM) and the ternary complex (6 µM) were mixed and the incubation was continued for 2 min at 37°C. The incubation was stopped by shock-freezing of the formed complex in the liquid nitrogen. No dipeptidyl-tRNA, f[^{3}H]MetSec-tRNA^{Sec}, was formed at these conditions, as verified by HPLC analysis.

Electron cryomicroscopy and image processing

Thin carbon foil was floated onto holey carbon grids. Ribosome complexes were applied at a concentration of ~0.05 µM. After blotting excess solution with filter paper, the grid was rapidly plunged into liquid ethane, resulting in a thin film of vitrified ribosome solution covering the carbon foil (Dubochet et al., 1988). Images were taken on a Philips CM200 electron microscope at a magnification of 161,000 with a defocus of 1.0-3.3 µm and an electron dose of about 15-20 e^-/Å^2. Images were acquired at liquid nitrogen temperature on a 2-fold binned 4k x 4k 16 bit CCD camera (TVIPS GmbH) for improved contrast (Sander et al., 2005), resulting in a final pixel size of 1.85 Å/pixel. Ribosomal particles were selected semi-automatically using the program Boxer (Ludtke et al., 1999). The remaining 200000 particles were corrected locally for the CTF (Sander et al., 2003a). Two 3D reconstructions were computed based on two different reference maps for projection matching, an initiated ribosome with fMet-tRNA^{fMet} in the P-site (IC) and a ribosome carrying additionally an EF-Tu ternary complex (TC).

While the reconstruction based on the IC map did not show any density for the SelB·GDPNP·Sec-tRNA^{Sec}·SECIS complex

(SelB complex), the reconstruction based on the TC map showed only scattered density in the factor binding site, indicating low occupancy with the SelB complex. Supervised classification was used to separate particle images according to occupancy with ligand (Valle et al., 2003). For each particle, the maximum cross-correlation coefficient (CCC) with references from the IC map was compared with that of projections from the TC map. The 57798 particles showing a higher CCC when aligned to references from the TC map were then used to reconstruct the SelB complex map. In order to prevent reference bias due to the EF-Tu ternary complex, these particles were first aligned with respect to the IC map. The final reconstruction was calculated from the best matching 25491 particles at a resolution of 19/26 Å (5σ/0.5FSC criterion) and a pixel size of 4.5 Å/pixel. A control map 70S initiation complex with mLP mRNA (SECIS IC) at 17/21 Å resolution (5σ/0.5FSC criterion, Suppl. Fig. S2) was calculated from the best 51681 particles showing a higher CCC for the IC map. A difference map was built by subtracting map SECIS IC from SelB complex map after normalization. The density thresholds for rendering the maps were chosen to represent the dimensions of published atomic structures filtered to the respective resolution. The resulting volumes correspond to about 120 - 130% of the ribosome volume calculated from the atomic structures. All image processing was performed in the context of the IMAGIC-5 software (van Heel et al., 1996) using corrim–based multireference alignment via polar coordinates (Sander et al., 2003b).

Homology modelling and docking of atomic models

A homology model for *E. coli* SelB was built with WHATIF (Vriend, 1990), based on the crystal structure of SelB in complex with GDPNP (PDB entry 1wb3 chain A residues 3-376 (Leibundgut et al., 2004) from the archaeon *M. maripaludis* for the domains I to III and the crystal structure of a fragment of *M. thermoacetica* SelB (PDB entry 1lva residues 380-634 (Selmer and Su, 2002)) for the domain IV. The unresolved region in the SelB·GDPNP model (residues 30-48) was substituted with the corresponding residues of the SelB·GDP model (PDB entry 1wb1 chain C, (Leibundgut et al., 2004)). Target-template alignments were taken from the respective references, with minor changes. Two insertions in *E. Coli* domain III (residues 340/341 and 326/327) could not be modeled and were omitted. The linker between domains III and IV of *E. Coli* (residues 355-364) was not modeled as no matching template could be found. Domain IV was further separated into two parts, the WH motifs 1/2 and 3/4, as separate entities. The model of free tRNA^{Sec} (Baron et al., 1993) was modified by replacing the 3'GCCA end with the 3'UCCA end of Cys-tRNA^{Cys} bound to EF-Tu·GDPNP (PDB entry 1b23 (Nissen et al., 1999)) to account for binding to SelB.

Docking of atomic models as rigid bodies was performed manually using AMIRA 3.1 (TGS software). Atomic models of *E. coli* 30S and 50S subunits (PDB entries 2aw7 and 2aw4, (Schuwirth et al., 2005)) were docked into the SelB complex map, using 30S head and body as separate entities and including a model for proteins L10 and the NTD of the *E. coli* L7/L12 proteins (Diaconu et al., 2005) and the crystal structure of the L1 protein (pdb 1mzp (Nikulin et al., 2003)). Figures were made using Ribbons (Carson, 1997), ViewerLite 4.2 (Accelrys Inc.) and Amira 3.1 (TGS software).

Competing interests statement
The authors declare that they have no competing financial interests.

Correspondence should be addressed to M.V.R. *email: rodnina@uni-wh.de*, or H. S. *email: holger.stark@mpibpc.mpg.de.*

References

Alfano, C., Sanfelice, D., Babon, J., Kelly, G., Jacks, A., Curry, S., and Conte, M.R. (2004). Structural analysis of cooperative RNA binding by the La motif and central RRM domain of human La protein. Nat Struct Mol Biol *11*, 323-329.

Baron, C., and Böck, A. (1991). The length of the aminoacyl-acceptor stem of the selenocysteine-specific tRNA(Sec) of *Escherichia coli* is the determinant for binding to elongation factors SELB or Tu. J Biol Chem *266*, 20375-20379.

Baron, C., and Böck, A. (1995). The selenocystein-inserting tRNA species: structure and function. In tRNA: structure biosynthesis, and function, D. Soll, and U. RajBhandary, eds. (Washington, American society for microbiology.), pp. 529-544.

Baron, C., Heider, J., and Böck, A. (1990). Mutagenesis of selC, the gene for the selenocysteine-inserting tRNA-species in E. coli: effects on in vivo function. Nucl Acids Res *18*, 6761-6716.

Baron, C., Westhof, E., Böck, A., and Giege, R. (1993). Solution structure of selenocysteine-inserting tRNA(Sec) from *Escherichia coli*. Comparison with canonical tRNA(Ser). J Mol Biol *231*, 274-292.

Böck, A., Forchhammer, K., Heider, J., and Baron, C. (1991). Selenoprotein synthesis: an expansion of the genetic code. Trends Biochem Sci *16*, 463-467.

Carson, M. (1997). Ribbons. Macromolecular Crystallography, Pt B *277*, 493-505.

Chavatte, L., Brown, B.A., and Driscoll, D.M. (2005). Ribosomal protein L30 is a component of the UGA-selenocysteine recoding machinery in eukaryotes. Nat Struct Mol Biol *12*, 408-416.

Copeland, P.R., Fletcher, J.E., Carlson, B.A., Hatfield, D.L., and Driscoll, D.M. (2000). A novel RNA binding protein, SBP2, is required for the translation of mammalian selenoprotein mRNAs. EMBO J *19*, 306-314.

Diaconu, M., Kothe, U., Schlunzen, F., Fischer, N., Harms, J.M., Tonevitsky, A.G., Stark, H., Rodnina, M.V., and Wahl, M.C. (2005). Structural basis for the function of the ribosomal L7/12 stalk in factor binding and GTPase activation. Cell *121*, 991-1004.

Dong, G., Chakshusmathi, G., Wolin, S.L., and Reinisch, K.M. (2004). Structure of the La motif: a winged helix domain mediates RNA binding via a conserved aromatic patch. Embo J *23*, 1000-1007.

Dubochet, J., Adrian, M., Chang, J.J., Homo, J.C., Lepault, J., McDowall, A.W., and Schultz, P. (1988). Cryo-electron microscopy of vitrified specimens. Q Rev Biophys *21*, 129-228.

Fourmy, D., Guittet, E., and Yoshizawa, S. (2002). Structure of prokaryotic SECIS mRNA hairpin and its interaction with elongation factor SelB. J Mol Biol *324*, 137-150.

Frank, J., Sengupta, J., Gao, H., Li, W., Valle, M., Zavialov, A., and Ehrenberg, M. (2005). The role of tRNA as a molecular spring in decoding, accommodation, and peptidyl transfer. FEBS Lett *579*, 959-962.

Gabashvili, I.S., Agrawal, R.K., Spahn, C.M.T., Grassucci, R.A., Svergun, D.I., Frank, J., and Penczek, P. (2000). Solution structure of the *E. coli* 70S ribosome at 11.5 Å resolution. Cell *100*, 537-549.

Gajiwala, K.S., and Burley, S.K. (2000). Winged helix proteins. Curr Opin Struct Biol *10*, 110-116.

Gromadski, K.B., Daviter, T., and Rodnina, M.V. (2006). A uniform response to mismatches in codon-anticodon complexes ensures ribosomal fidelity. Mol Cell *21*, 369-377.

Gromadski, K.B., and Rodnina, M.V. (2004a). Kinetic determinants of high-fidelity tRNA discrimination on the ribosome. Mol Cell *13*, 191-200.

Gromadski, K.B., and Rodnina, M.V. (2004b). Streptomycin interferes with conformational coupling between codon recognition and GTPase activation on the ribosome. Nat Struct Mol Biol *11*, 316-322.

Hilgenfeld, R., Böck, A., and Wilting, R. (1996). Structural model for the selenocysteine-specific elongation factor SelB. Biochimie *78*, 971-978.

Hüttenhofer, A., and Böck, A. (1998). Selenoprotein synthesis. In RNA structure and function (Cold Spring Harbour Laboratory Press), pp. 603-639.

Hüttenhofer, A., Heider, J., and Böck, A. (1996). Interaction of the *Escherichia coli fdhF* mRNA hairpin promoting selenocysteine incorporation with the ribosome. Nucl Acids Res *24*, 3903-3910.

Jenner, L., Romby, P., Rees, B., Schulze-Briese, C., Springer, M., Ehresmann, C., Ehresmann, B., Moras, D., Yusupova, G., and Yusupov, M. (2005). Translational operator of mRNA on the ribosome: how repressor proteins exclude ribosome binding. Science *308*, 120-123.

Jovine, L., Djordjevic, S., and Rhodes, D. (2000). The crystal structure of yeast phenylalanine tRNA at 2.0 Å resolution: cleavage by Mg^{2+} in 15-year old crystals. J Mol Biol *301*, 401-414.

Kothe, U., and Rodnina, M.V. (2006). Delayed release of inorganic phosphate from elongation factor Tu following GTP hydrolysis on the ribosome. Biochemistry *submitted for publication*.

Kothe, U., Wieden, H.J., Mohr, D., and Rodnina, M.V. (2004). Interaction of helix D of elongation factor Tu with helices 4 and 5 of protein L7/12 on the ribosome. J Mol Biol *336*, 1011-1021.

Kromayer, M., Wilting, R., Tormay, P., and Böck, A. (1996). Domain structure of the prokaryotic selenocysteine-specific elongation factor SelB. J Mol Biol *262*, 413-420.

Kryukov, G.V., and Gladyshev, V.N. (2004). The prokaryotic selenoproteome. EMBO Rep *5*, 538-543.

Leibundgut, M., Frick, C., Thanbichler, M., Böck, A., and Ban, N. (2004). Selenocysteine tRNA-specific elongation factor SelB is a structural chimaera of elongation and initiation factors. EMBO J *24*, 11-22.

Ludtke, S.J., Baldwin, P.R., and Chiu, W. (1999). EMAN: Semiautomated software for high-resolution single-particle reconstructions. J Struct Biol *128*, 82-97.

Mansell, J.B., Guevremont, D., Poole, E.S., and Tate, W.P. (2001). A dynamic competition between release factor 2 and the tRNA(Sec) decoding UGA at the recoding site of *Escherichia coli* formate dehydrogenase H. EMBO J *20*, 7284-7293.

Nikulin, A., Eliseikina, I., Tishchenko, S., Nevskaya, N., Davydova, N., Platonova, O., Piendl, W., Selmer, M., Liljas, A., Drygin, D*., et al.* (2003). Structure of the L1 protuberance in the ribosome. Nat Struct Biol *10*, 104-108.

Nissen, P., Thirup, S., Kjeldgaard, M., and Nyborg, J. (1999). The crystal structure of Cys-tRNA^{Cys}-EF-Tu-GDPNP reveals general and specific features in the ternary complex and in tRNA. Structure *7*, 143-156.

Ogle, J.M., Brodersen, D.E., Clemons, W.M., Jr., Tarry, M.J., Carter, A.P., and Ramakrishnan, V. (2001). Recognition of cognate transfer RNA by the 30S ribosomal subunit. Science *292*, 897-902.

Ogle, J.M., Murphy, F.V., Tarry, M.J., and Ramakrishnan, V. (2002). Selection of tRNA by the ribosome requires a transition from an open to a closed form. Cell *111*, 721-732.

Rodnina, M.V., Fricke, R., Kuhn, L., and Wintermeyer, W. (1995). Codon-dependent conformational change of elongation factor Tu preceding GTP hydrolysis on the ribosome. EMBO J *14*, 2613-2619.

Rodnina, M.V., Gromadski, K.B., Kothe, U., and Wieden, H.J. (2005). Recognition and selection of tRNA in translation. FEBS Lett *579*, 938-942.

Rodnina, M.V., Savelsbergh, A., Matassova, N.B., Katunin, V.I., Semenkov, Y.P., and Wintermeyer, W. (1999). Thiostrepton inhibits the turnover but not the GTPase of elongation factor G on the ribosome. Proc Natl Acad Sci USA *96*, 9586-9590.

Rodnina, M.V., Semenkov, Y.P., and Wintermeyer, W. (1994). Purification of fMet-tRNA^{fMet} by fast protein liquid chromatography. Anal Biochem *219*, 380-381.

Sanbonmatsu, K.Y., Joseph, S., and Tung, C.S. (2005). Simulating movement of tRNA into the ribosome during decoding. Proc Natl Acad Sci USA *102*, 15854-15859.

Sander, B., Golas, M.M., and Stark, H. (2003a). Automatic CTF correction for single particles based upon multivariate statistical analysis of individual power spectra. J Struct Biol *142*, 392-401.

Sander, B., Golas, M.M., and Stark, H. (2003b). Corrim-based alignment for improved speed in single-particle image processing. J of Struct Biol *143*, 219-228.

Sander, B., Golas, M.M., and Stark, H. (2005). Advantages of CCD detectors for de novo three-dimensional structure determination in single-particle electron microscopy. J Struct Biol *151*, 92-105.

Schön, A., Böck, A., Ott, G., Sprinzl, M., and Soll, D. (1989). The selenocysteine-inserting opal suppressor serine tRNA from *E. coli* is highly unusual in structure and modification. Nucl Acids Res *17*, 7159-7165.

Schuwirth, B.S., Borovinskaya, M.A., Hau, C.W., Zhang, W., Vila-Sanjurjo, A., Holton, J.M., and Cate, J.H. (2005). Structures of the bacterial ribosome at 3.5 Å resolution. Science *310*, 827-834.

Selmer, M., and Su, X.D. (2002). Crystal structure of an mRNA-binding fragment of *Moorella thermoacetica* elongation factor SelB. EMBO J *21*, 4145-4153.

Shi, H., and Moore, P.B. (2000). The crystal structure of yeast phenylalanine tRNA at 1.93 Å resolution: a classic structure revisited. RNA *6*, 1091-1105.

Stark, H., Rodnina, M.V., Wieden, H.J., van Heel, M., and Wintermeyer, W. (2000). Large-scale movement of elongation factor G and extensive conformational change of the ribosome during translocation. Cell *100*, 301-309.

Stark, H., Rodnina, M.V., Wieden, H.J., Zemlin, F., Wintermeyer, W., and van Heel, M. (2002). Ribosome interactions of aminoacyl-tRNA and elongation factor Tu in the codon-recognition complex. Nat Struct Biol *9*, 849-854.

Suppmann, S., Persson, B.C., and Böck, A. (1999). Dynamics and efficiency in vivo of UGA-directed selenocysteine insertion at the ribosome. EMBO J *18*, 2284-2293.

Takyar, S., Hickerson, R.P., and Noller, H.F. (2005). mRNA helicase activity of the ribosome. Cell *120*, 49-58.

Teplova, M., Yuan, Y.R., Phan, A.T., Malinina, L., Ilin, S., Teplov, A., and Patel, D.J. (2006). Structural basis for recognition and sequestration of UUU(OH) 3' temini of nascent RNA polymerase III transcripts by La, a rheumatic disease autoantigen. Mol Cell *21*, 75-85.

Thanbichler, M., and Böck, A. (2001). Functional analysis of prokaryotic SELB proteins. Biofactors *14*, 53-59.

Thanbichler, M., and Böck, A. (2002). Selenoprotein biosynthesis: purification and assay of components involved in selenocysteine biosynthesis and insertion in Escherichia coli. Methods Enzymol *347*, 3-16.

Thanbichler, M., and Böck, A. (2003). Purification and characterization of hexahistidine-tagged elongation factor SelB. Protein Expr Purif *31*, 265-270.

Thanbichler, M., Böck, A., and Goody, R.S. (2000). Kinetics of the interaction of translation factor SelB from *Escherichia coli* with guanosine nucleotides and selenocysteine insertion sequence RNA. J Biol Chem *275*, 20458-20466.

Valle, M., Zavialov, A., Li, W., Stagg, S.M., Sengupta, J., Nielsen, R.C., Nissen, P., Harvey,

S.C., Ehrenberg, M., and Frank, J. (2003). Incorporation of aminoacyl-tRNA into the ribosome as seen by cryo-electron microscopy. Nat Struct Biol *10*, 899-906.

van Heel, M., Harauz, G., Orlova, E.V., Schmidt, R., and Schatz, M. (1996). A new generation of the IMAGIC image processing system. J Struct Biol *116*, 17-24.

Vriend, G. (1990). What If - a molecular modeling and drug design program. J Mol Graphics *8*, 52-&.

Yoshizawa, S., Rasubala, L., Ose, T., Kohda, D., Fourmy, D., and Maenaka, K. (2005). Structural basis for mRNA recognition by elongation factor SelB. Nat Struct Mol Biol.

Yusupov, M.M., Yusupova, G.Z., Baucom, A., Lieberman, K., Earnest, T.N., Cate, J.H., and Noller, H.F. (2001). Crystal structure of the ribosome at 5.5 Å resolution. Science *292*, 883-896.

Curriculum vitae

PERSONAL DATA

Name	Alena Paleskava
Date of Birth	24th October 1981
Place of Birth	Minsk, Belarus

SCIENTIFIC EDUCATION

09/2004 – 05/2009   Ph.D. at the Institute of Physical Biochemistry
University of Witten/Herdecke, Germany

09/1999 – 07/2004   Graduate studies: Radiobiology
International Sakharov Environmental University, Minsk, Belarus
Degree: M. Sc. / Diplom in Radiobiology

SCHOOL EDUCATION

1996 - 1999   Polytechnic gymnasium, Minsk, Belarus
Certificate of Secondary Education

1988 - 1996   Secondary School № 171, Minsk, Belarus

Acknowledgments

I would like to express my sincere gratitude to Marina Rodnina for being a great supervisor during my PhD project. Her continuous support and endless enthusiasm for science always encouraged me.

I am very thankful to Wolfgang Wintermeyer for his wise criticism and productive discussions.

I am grateful to our collaborators: Markus Wahl, Holger Stark, Niels Fischer, and Oleg Ganichkin for the help in visualization of Sec incorporation machinery.

I thank August Böck for generous gifts of components of Sec insertion system and plasmid constructs.

Special thanks go to my lab colleagues for creating a nice atmosphere in Witten and introducing a lot of pleasure in science. In particular, I would like to thank Kirill for being my supervisor at the beginning of the project, Ute for sharing the lab, Frank for being a person of ready sympathy, Astrid for care and kindness, and Anke for enormous help in getting over the difficulties in foreign country. I am also grateful to Carmen, Astrid, Simone and Petra for their valuable technical assistance.

I am obliged to my diploma supervisor Anna Georgievna Lapko for giving me the opportunity to start my way in science.

My deepest thanks go my parents and sister for all kinds of support whenever I needed it.

Most of all I am thankful to Andrey for being in my life.